ISBN 978-82-471-1739-2 (printed ver.)
ISBN 978-82-471-1740-8 (electronic ver.)
ISSN 1503-8181

Doctoral theses at NTNU, 2009:173

Erland Løken Nordgård

Model Compounds for Heavy Crude Oil Components and Tetrameric Acids

Characterization and Interfacial Behaviour

Doctoral Thesis

Erland Løken Nordgård

Doctoral theses at NTNU, 2009:173

NTNU

NTNU
Norwegian University of
Science and Technology
Thesis for the degree of
philosophiae doctor
Faculty of Natural Sciences and Technology
Department of Chemical Engineering

NTNU

Norwegian University of
Science and Technology

NTNU

Norwegian University of
Science and Technology

Erland Løken Nordgård

Model Compounds for Heavy Crude Oil Components and Tetrameric Acids

Characterization and Interfacial Behaviour

Thesis for the degree of philosophiae doctor

Trondheim, September 2009

Norwegian University of
Science and Technology
Faculty of Natural Sciences and Technology
Department of Chemical Engineering

NTNU
Norwegian University of
Science and Technology

NTNU
Norwegian University of Science and Technology

Thesis for the degree of philosophiae doctor

Faculty of Natural Sciences and Technology
Department of Chemical Engineering

ISBN 978-82-471-1739-2 (printed ver.)
ISBN 978-82-471-1740-8 (electronic ver.)
ISSN 1503-8181

Doctoral Theses at NTNU, 2009:173

Printed by Tapir Uttrykk

Preface

This thesis is submitted in partial fulfilment of the PhD degree at the Norwegian University of Science and Technology and consists of 6 papers or manuscripts all completely or partially carried out at Ugelstad Laboratory from October 2006 to June 2009 under the supervision of Prof. Johan Sjöblom.

I received my "sivilingeniør"/MSc in organic chemistry in June 2006 working on the synthesis of new, optically active surfactants and dye molecules. After a couple of months with a temporarily position as a synthetic chemist for Ugelstad Laboratory, I started my PhD work 25th September 2006. The PhD has been coordinated to the project "An Integrated Approach to Interfacial/Surface Processes in Crude Oil Systems". The project is fully funded by the PETROMAKS programme. (Research Council of Norway) The work has been central in two *Joint Industrial Programmes* (JIPs); JIP1 ("Heavy Crude Oils/Particle-Stabilized Emulsions") and JIP2-3 ("A Mechanistic Approach towards Naphthenate Precipitation). The progress and results obtained have been presented in the JIP consortium twice a year to all our industrial partners and sponsors, both domestic and abroad.

The author's role in the scientific work presented is dominant in paper 1-4, the main deviation being DSC measurements in paper 4. In paper 5, the author has contributed with syntheses of all compounds, CMC determinations and Langmuir experiments. The experimental work in paper 6 has mainly been carried out by other students under the author's supervision.

Figures are numbered consecutively within each main chapter, while tables, footnotes and references are numbered consecutively throughout the entire thesis.

Acknowledgements

First of all, I would like to acknowledge my supervisor, Professor Johan Sjöblom, for kindly accepting me as a PhD student at Ugelstad Laboratory, despite my enthusiasm for organic chemistry. The introduction to the world of colloidal chemistry related to crude oil has been highly interesting and your enthusiasm for colloidal science, sprinkled with sarcastic humour, has given me much input and motivation.

All the master- and PhD students, post.doc's, technicians and engineers at Ugelstad Laboratory are greatly acknowledged for giving me a good time at the lab's, both professionally as well as socially. I hope my singing and dancing have not annoyed you too much!

Especially, I would like to thank Dr. Sébastien Simon for collaboration in all projects and all his valuable help. Thanks to Dr. Sondre Volden for fruitful coffee breaks, to Eva Landsem and Sigrid V. Slungård for synthesis work, Dr. Geir Sørland for being the world's greatest NMR expert, Dr. Heléne Magnusson for carrying out DSC experiments, PhD Anne Silset and PhD Ann-Mari D. Hanneseth for good laughs, and all my office mates throughout the PhD period. Associate Prof. Wilhelm R. Glomm is highly acknowledged for proof-reading.

A great thank you to PhD Ola Sundman at Umeå University for carrying out titration experiments and our good collaboration.

The Research Council of Norway is acknowledged for funding, and I thank the JIP consortium for discussions and help during the JIP meetings.

Finally, none of this would have been possible without the love and support from my girlfriend Anna Synnøve – meeting you is the greatest thing that has ever happened to me!

Abstract

The tendency during the past decades in the quality of oil reserves shows that conventional crude oil is gradually being depleted and the demand being replaced by heavy crude oils. These oils contain more of a class high-molecular weight components termed asphaltenes. This class is mainly responsible for stable water-in-crude oil emulsions. Both heavy and lighter crude oils in addition contain substantial amounts of naphthenic acids creating naphthenate deposits in topside facilities.

The asphaltene class is defined by solubility and consists of several thousand different structures which may behave differently in oil-water systems. The nature of possible subfractions of the asphaltene has been received more attention lately, but still the properties and composition of such is not completely understood. In this work, the problem has been addressed by synthesizing model compounds for the asphaltenes, on the basis that an acidic function incorporated could be crucial. Such acidic, polyaromatic surfactants turned out to be highly interfacially active as studied by the pendant drop technique. Langmuir monolayer compressions combined with fluorescence of deposited films indicated that the interfacial activity was a result of an efficient packing of the aromatic cores in the molecules, giving stabilizing interactions at the o/w interface. Droplet size distributions of emulsions studied by PFG NMR and adsorption onto hydrophilic silica particles demonstrated the high affinity to o/w interfaces and that the efficient packing gave higher emulsion stability. Comparing to a model compound lacking the acidic group, it was obvious that subfractions of asphaltenes that contain an acidic, or maybe similar hydrogen bonding functions, could be responsible for stable w/o emulsions.

Indigenous tetrameric acids are the main constituent of calcium naphthenate deposits. Several synthetic model tetraacids have been prepared and their properties have been compared to the indigenous analogue. The model compounds display the same high interfacial activity and film behaviour. One of the model compounds, BP10, forms a cross-linked network with Ca^{2+}, crucial for naphthenate deposit formation. On the other hand, no glass transition was found for BP10. Reactions with Ca^{2+} under emulsified conditions demonstrated the extreme influence of the available interfacial area. Finally, the acid-base properties of several tetraacids were investigated by potentiometric titrations. A high apparent pKa with hysteresis depending on the titration direction was observed for BP10, and could be explained and modelled based on the tetraacid being present as a micellar solution.

List of Papers

PAPER 1

Nordgård, E. L.; Sjöblom, J.: Model Compounds for Asphaltenes and C_{80} Isoprenoid Tetraacids. Part I: Synthesis and Interfacial Activities. *J. Dispersion Sci. Technol.*, **2008**, *29(8)*, 1114-1122.

PAPER 2

Nordgård, E. L.; Landsem, E.; Sjöblom, J.: Langmuir Films of Asphaltene Model Compounds and Their Fluorescent Properties. *Langmuir,* **2008**, *24*, 8742-8751.

PAPER 3

Nordgård, E. L.; Sørland, G.; Sjöblom, J.: Behaviour of Asphaltene Model Compounds at W/O Interfaces. Submitted to Langmuir.

PAPER 4

Nordgård, E. L.; Magnusson, H.; Hanneseth, A-M. D.; Sjöblom, J.: Model Compounds for C_{80} Isoprenoid Tetraacids. Part II: Interfacial Reactions, Physicochemical Properties and Comparison with Indigenous Tetraacids. *Colloids Surf., A,* **2009**, *340*, 99-108.

PAPER 5

Sundman, O.; Nordgård, E. L.; Grimes, B.; Sjöblom, J.: Potentiometric Titrations of Five Synthetic Tetraacids as Models for Indigenous C_{80} Tetraacids. Submitted to Langmuir.

PAPER 6

Knudsen, A.; Nordgård, E. L.; Diou, O.; Sjöblom, J.: Methods to Study Naphthenate Formation in W/O Emulsions by the use of a Tetraacid Model Compound. Submitted to J. Dispersion Sci. Technol.

ADDITIONAL PUBLICATIONS

Simon, S.; Nordgård, E.; Bruheim, P.; Sjöblom, J.: Determination of C_{80} tetraacid content in calcium naphthenate deposits. *J. Chromatgr. A*. **2008**, *1200(2)*, 136-143.

Nordgård, E. L.; Hanneseth, A-M. D.; Sjöblom, J.: Inhibition of Calcium Naphthenate. Experimental Methods to Study the Effect of Commercially Available Naphthenate Inhibitors. *J. Dispersion Sci. Technol.* **2010.** Accepted.

CONFERENCE CONTRIBUTIONS

Sjöblom, J.; Hanneseth, A-M. D.; Nordgård, E. L.; Simon, S.: Setting the scene: The current understanding and role of different naphthenates (Ca, Na, Ba, Sr), *SPE Applied Technology Workshop Managing Naphthenates and Soap Emulsions*, Pau, March 10 – 13th, 2008 (Oral pres. by J. S.)

Nordgård, E. L.; Landsem, E.; Sjöblom, J.: Model compounds for indigenous crude oil components. Synthesis, characterization and comparison. *24th Organic Chemistry Winter Meeting,* Skeikampen, January 8 – 11th, 2009. (Poster.)

Contents

Preface I
Acknowledgements II
Abstract III
List of Papers IV
1. Introduction 1
1.1 Petroleum – The Black Gold 1
1.2. Oil recovery rate – in the past and the way forward 2
1.3. Oil price fluctuations 3
2. Petroleum 4
2.1. Origin of petroleum 4
2.1.1. The abiogenic theory 4
2.1.2. The biogenic theory 4
2.2. Formation of an oil reservoir 5
2.3. Recovery of crude oil 6
2.4. Conventional and heavy oil 10
3. Composition of crude oil 12
3.1. SARA fractionation. 12
3.2. Asphaltenes 14
3.2.1 Elemental composition of asphaltenes. 14
3.2.2 The molecular weight controversy 15
3.2.2. Precipitation of asphaltenes 16
3.2.3. Fractionation of asphaltenes 17
3.2.4. Film properties. 19
3.2.5. Model molecules for the asphaltenes. 20
4. Naphthenic acids 22
4.1. Dissociation of naphthenic acids and formation of metal naphthenates. 24
4.2. The discovery of the tetrameric acids. 25
4.3. Oilfields with ARN and deposition problems 28
5. Surfactants and emulsions 30
5.1. Surfactant chemistry and micellization 30
5.2. Emulsions and emulsion stability. 34
6. Experimental techniques. 37
6.1. Methods for surface/interfacial activity – pendant drop technique and tensiometer 37
6.2. Langmuir trough technique. 40
6.3. Fluorescence 44
6.4. Nuclear Magnetic Resonance (NMR) 47
7. Main results. 50
7.1. Paper 1 50
7.2. Paper 2 52
7.3. Paper 3 54
7.4. Paper 4 56
7.5. Paper 5 58
7.6. Paper 6 60
7.7. General conclusions and future work 62

1. Introduction

1.1 Petroleum – The Black Gold

Everywhere in our daily life, we encounter products which are the results of petroleum refining. Examples are fuel and gas, plastics, paints, synthetic fibres in clothing, and synthetic soaps among others.[1] The petroleum products have become so important, that humanity for the moment is dependent on its existence. Crude oil, or "The Black Gold", is a non-renewable energy source, and it is commonly accepted that the precious oil eventually will run out. Both academia and industry are constantly developing the technology needed to make use of renewable energy sources which can supplement the oil when the oil reserves are exhausted. However, this might take several decades, and with the oil reserves and production already peaking in several countries[1] it is of great importance to make use of as much oil already existing in reservoirs as possible. As discussed later, this is not always a triviality. Depending on the properties of the oil, like in a heavy crude oil, new technology and solutions have to be put into use in order to recover as much of oil from the reservoir as possible.

Looking back in history, petroleum has been used for thousand of years. When the Tigris-Euphrat area, now Iraq, was inhabited 4000 BC, the civilization used bitumen, or asphalt, to construct ornament works.[1] The use of petroleum has also been documented in China as early as 600 BC, and from 500 to about 40 BC asphalt was generally used by Egyptians to fill corpses and to coat the cloth wrapping. The different cultures all over the world found the use of petroleum and its fractions the next 2000 years, but the modern petroleum industry began in the middle 1850s with the commercialization of petroleum in Pennsylvania and later on the first petroleum distillation setup in 1862.[1] As technology developed during the 20th century, an increasing number of countries became suppliers of oil. Especially post World War II the oil production was found in large scale all over the world.

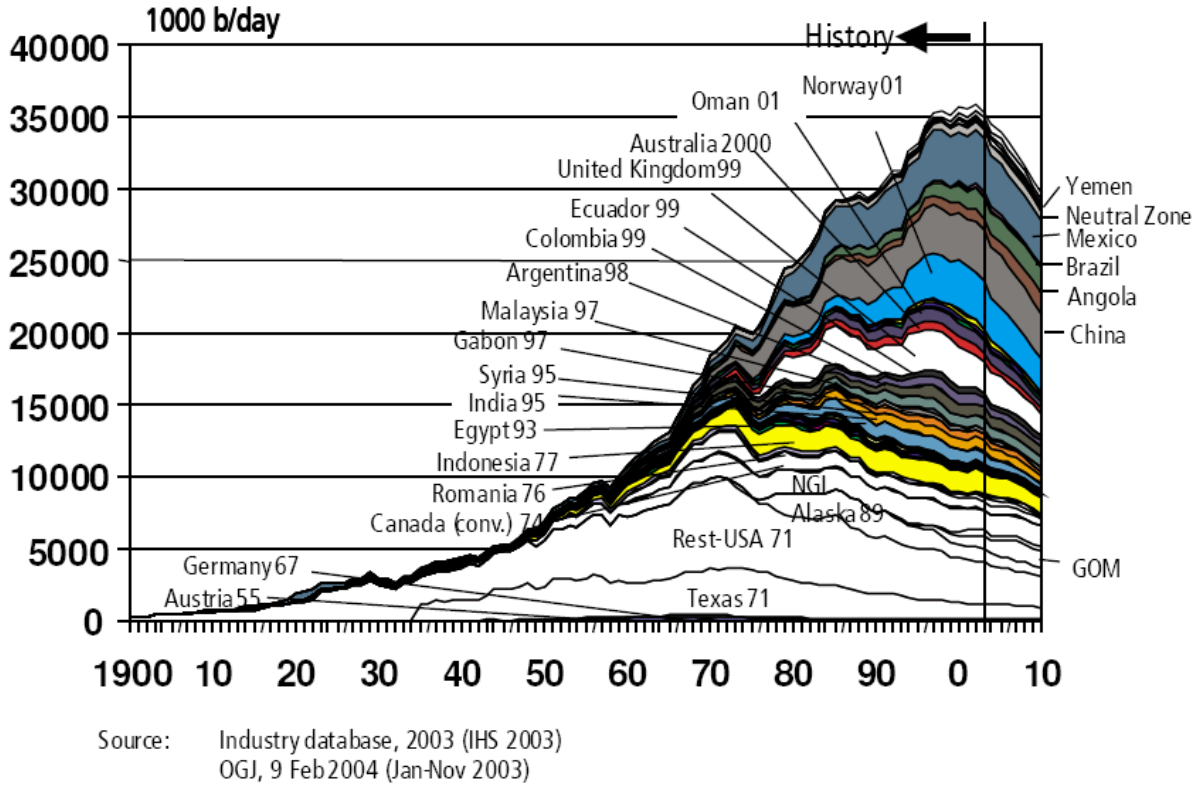

Figure 1.1. Non-OPEC countries' oil production the last century and proposed production.[2]

1.2. Oil recovery rate – in the past and the way forward

Figure 1.1 shows how the oil production has developed during the last century and shows the progressive increase after World War II both regarding the total amount produced and the increased disparity of oil-producing countries. It also illustrates the peak of oil production after year 2000, which is an issue of ongoing debate and concern. Already in 1956 Dr. M. King Hubbert did propose his theory about the oil production reaching a maximum level, the "Hubbert-peak". He predicted that the US oil production would peak in the early 1970s,[3] and as seen from figure 1.1 – he was quite right. Even though the peak prediction was correct, the oil production after the peak was higher than he had foreseen. This is due to the increase of technology development as a function of time, and hence it is possible to recover more oil from each oilfield than previously predicted. The expected recovery estimates for operating oilfields often grow with time. The total estimate of recoverable oil from the North Slope of Alaska, for instance, used to be 9.6 billion barrels; today it is 13.7 billion barrels.[3] Even if a prediction at present date shows an emptying of the oil in 20 years, we will most likely discover new oil fields and recover more oil from existing fields at a reasonable rate in comparison with oilfields being shut down. Reservoirs may also contain more oil than first

expected based on geological mapping. The degree of underestimation will hence depend on the skills of the oil companies and economical efforts. Globally, about 35% of the oil present in established fields is actually produced.[3] Traditional drilling recovers the light oil, and when this step is finished the oil companies have to use secondary extraction methods, such as water injection or carbon dioxide to push more oil out by increasing pressure. In addition, tertiary methods are in use at many oilfields. This can be by the use of steam[3] or by surfactant flooding[4] to lower the viscosity and interfacial tension of the oil. (Chapter 2.3)

1.3. Oil price fluctuations

Another factor which influences the oil production and recovery is the price of oil. After being in the range of 2 -15 USD per barrel until 1990s, the price of oil has gradually increased over the last a few decades.[1] The fluctuations of the oil price have been especially noticeable the last years; July 4th 2008 the price of Brent Oil reached its all-time high with 146 USD pr. Barrel,[i] an increase of almost 100 USD during one year! And suddenly, we saw a dramatic drop of the same 100 USD in 5 months resulting from the global financial crisis. These fluctuations in the oil price give extreme challenges for the oil companies because it is difficult to know if the oil field will in the end yield a profit or not. Nevertheless, the fluctuations also give an opportunity for the oil industry to close and re-open oilfields which are in the state of secondary or tertiary oil recovery. When the prices are high, the fields can be re-opened and costly methods to recover more oil can be utilized, still keeping profit margins high.

Clearly, the debate of the amount of recoverable oil will linger for decades, and an analysis from 2000 estimated that any world-wide peak in oil production would not happen until 2030 at the earliest.[3,5] To satisfy the world's need for energy until new sources can be produced at a satisfying rate, the best way to approach the existing oil fields is to keep on developing new technology and gain more knowledge about the oil and its behaviour to be able to extract even more oil and heavy oil by other than conventional methods. This poses in most cases great challenges, e.g. when it comes to separation of highly stable water-in-heavy crude oil emulsions, transportation of highly viscous fluids as encountered in the Athabasca tar sand fields, and precipitation of unstable constituents from heavy, immature biodegraded crude oil.

[i] Graphical representations at Oslo Børs stock market May 6th 2009 of Brent Oil the past 5 years.

2. Petroleum

2.1. Origin of petroleum

There are two main theories about the origin of petroleum; the abiogenic and the biogenic theory.[1] Since the start of the modern petroleum recovery in 1860, these theories have been already under debate. The main difference is that in the abiogenic theory the petroleum origins from inorganic material, while organic material as in animals and plants is the source for petroleum according to the biogenic theory.

2.1.1. The abiogenic theory

In 1866, Berthelot proposed that acetylene, HC≡CH, was the precursor for petroleum.[1] The considered pathway to acetylene was that calcium carbonate reacted with alkali metals to form calcium carbide (CaC_2). Upon hydrolysis of CaC_2, acetylene was formed. Mendelejeff considered the action of dilute acids or hot water on mixed iron and manganese carbides to produce mixtures of hydrocarbons from which petroleum evolved. However, if the abiogenic theory would have been correct, this would indicate that we have large amounts of carbon existing naturally on the planet. If this is the case, we may not reach the point where we run out of oil. Even if it has become more accepted that petroleum originates from organic matter, the abiogenic theory is interesting from a historical point of view.[1]

2.1.2. The biogenic theory

The biogenic theory is based on the decay of organic matter over time under conditions of high pressure and temperature. Prehistoric marine animals and terrestrial plants remains are believed to be the origin of this organic matter. Indications of the biogenic theory is that geological and chemical methods have demonstrated the optical activity of petroleum constituents, the presence of thermally labile organic compounds and the almost exclusive occurrence of oil in sedimentary rock formations.[1]

The hydrocarbons synthesized by living organisms usually accounts for less than 20% of the crude oil. The pathway in which the remaining hydrocarbons are produced is by several processes. To convert organic material to hydrocarbons, the organic matter goes through diagenesis, catagenesis and metagenesis. Dia-, cata- and metagenesis is the alteration of the

matter to form petroleum that may involve temperatures up to 50°C, between 50 and 200°C, and above 200°C, respectively.[6] In the first stage, animals and plants settled at lake bottoms. Bacteria decomposed the matter to water (carbohydrates, proteins) – and oil soluble (fat, cholesterol, etc.) matter, called kerogen. Over centuries, the organic material was buried under sedimentary layers and experienced heat and high pressure, causing evolution of carbon dioxide from carboxyl groups in the fat-soluble matter. Further light cracking gave a liquid product with high olefin content, called protopetroleum. Cyclization and polymerization of the unsaturated organic mixture formed paraffins and naphthenes. Through migration in the porous rocks, the hydrocarbons became trapped in reservoirs.[1] From this it is easily understood why each oilfield is unique in composition. Differences in climate, local flora and fauna favor different plants and marine animals, which in turn is reflected in the structural composition of an oilfield.

2.2. Formation of an oil reservoir

A reservoir can not form everywhere. There are certain conditions which need to be fulfilled in order to have a high probability of reservoir formation. Reservoir rocks must posses fluid-holding capacity (porosity) and fluid-transmitting capacity (permeability).[1] The porosity is caused by openings and cavities from fossils, solutions and fractures, and the most effective porosity for reservoir formation is a network of continuously connected pores. However, the hydrocarbons must be transported via migration inside the pores and hence the rocks must have certain permeability for the oil. There is a higher diversity in the permeability than the porosity between different oil reservoirs.[1] The migration probably starts by expelling water from the pores because of the increasing load of sediment material, and very large pores will then act as pools for the migrated oil. The oil migrates due to two main mechanisms, primary and secondary migration. The primary migration is the movement of hydrocarbons from source rocks to a point where oil and gas is collected in droplets, and secondary migration is often attributed to various aspects of buoyancy and hydrodynamics. In order for a pool to become a reservoir, the most important is that it must act as a trap sealed by a cap rock. This cap rock has low permeability, even impermeable towards oil, and hence counteracts the tendency of migration. When this reservoir with a cap is at a geological high, it is called an anticlinical trap. This situation is illustrated in figure 2.1.

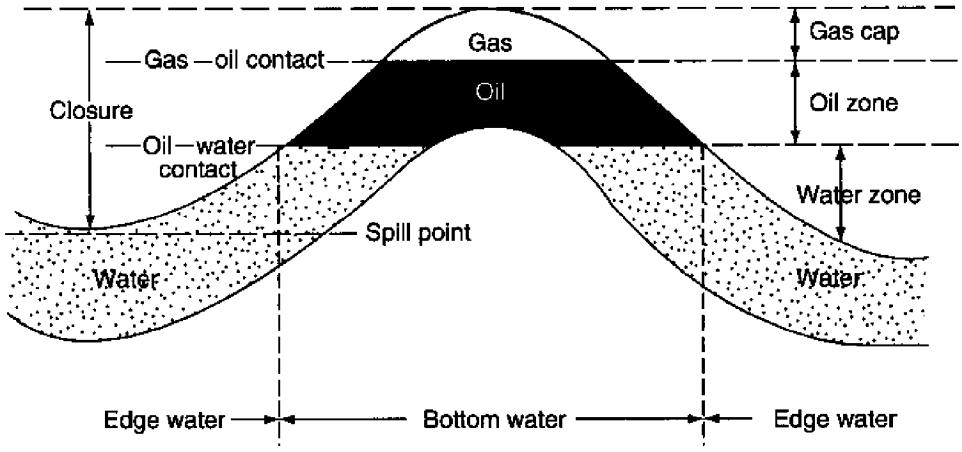

Figure 2.1. Typical anticlinical petroleum trap.[1]

Because of the need for porosity and permeability, the most common reservoir rocks are porous or fractured limestone, and examples of other typical reservoir rocks are the coarser grained sedimentary rocks; sand, sandstone and dolomite. Typical rocks acting as caps are clay and shale which have much finer pores than reservoir rocks. Another difference between the cap and the reservoir rocks is that the cap has a higher capillary pressure than the reservoir rocks.

2.3. Recovery of crude oil

Obviously, the differences between crude oils put challenges to the way the oil is recovered from the reservoirs. It is common to differentiate between *primary, secondary* and *tertiary/enhanced oil recovery*, and this section gives an introduction to different methods and in what situations they may be applied.

A reservoir is roughly built up of three phases – a gas phase, an oil phase and a water phase. Due to the differences in density the gas phase will lie on top of the oil with the water, or more correctly the brine, below the oil phase. As described earlier, the reservoir is normally trapped in porous sandstone, with a folded layer of some nonporous rock. This gas cap is then important for keeping all phases within the reservoir and keeping the pressure inside the reservoir high. The reservoir pressure is indeed the driving force for recovery of oil in *primary recovery* methods. The underground pressure is a complex function of the gases present, either as a separated gas phase or as dissolved gases, and influx of natural water,

gravity or combinations of these effects. There are three main driving forces for primary recovery:

- Dissolved gas drive – when the well gets penetrated, this will cause escape of gas, and lowered underground pressure. The system will counteract this change by releasing the gases dissolved in the oil phase to maintain the pressure. However, this is the least efficient driving force, and may be responsible for recovery of only 20% of the reservoir.

- Gas drive – if there is a gas cap overlying the oil, it is compressed and can be utilized. By producing oil only from below the gas cap, a high gas-oil ratio is maintained almost to the end of life for the pool. A typical recovery from a gas drive field is from 40 to 50%. If the gas in the gas cap is compressed to such degree that it separates from the oil phase it is possible to recycle this gas after the reservoir fluid is brought to the surface and flush it back to the gas phase, thus retaining the underground pressure.

- Water drive – is the most efficient mechanism. The pressure of the water forces the lighter recoverable oil out of the reservoir into the producing wells. Then the water-oil interface moves upwards in the reservoir until only the wells on the top still produce oil. In such fields, it is essential that the rate of removal is adjusted to the rate of incoming water. This will then be dependent on the permeability for water transportation.

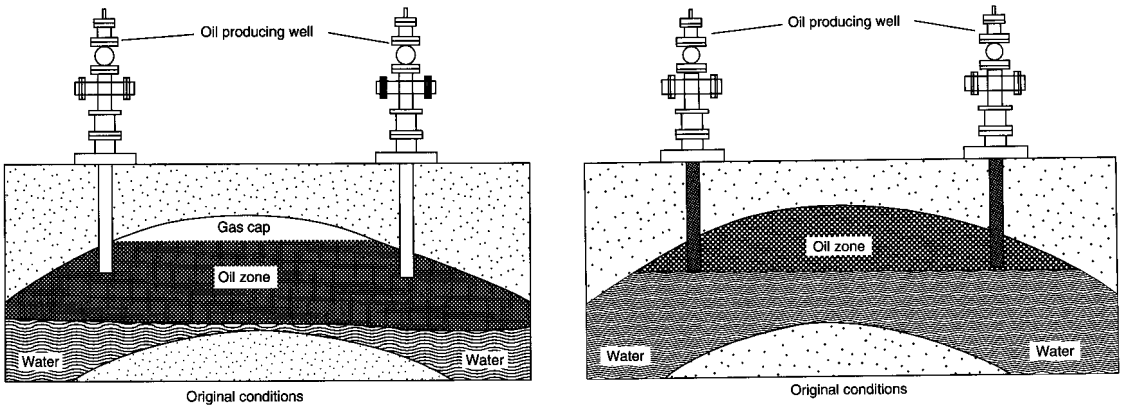

Figure 2.2. The gas drive (left) and the water drive (right) mechanism.[1]

Schematic figures of the gas drive and the water drive is shown in figure 2.2. One can see that the location of the wells is important, especially in a water drive field, to be at the highest point of the reservoir and thus able to produce oil as long as possible.

Hence, primary oil recovery is dependent on an intrinsic underground pressure which is often the case in new, conventional oilfields. No pumping is required, and the oil flows into the well by itself. However, as the reservoir is being depleted, the pressure will go down to a level where the energy is not sufficient to force the oil to the surface. Then, an external pressure has to be introduced to the reservoir to recover more oil than what is possible with primary methods. Increasing the underground pressure is an example of a *secondary recovery method.* The motivation for using secondary methods is that, as previously mentioned, conventional methods in some cases only recover 20-30% of the total reservoir. It is thus beneficial to recover more of the reservoir, with the wells and the oilfield already in place. The most common secondary method is the use of pumps to provide mechanical lift of the fluid in the reservoir. Other methods are injection of fluids. Both gases and water is used as injection fluids. Another important behaviour of the injected fluid is to *sweep* the crude oil from the injection well to the producing well. The success of secondary methods depends on the mechanism by which the injected fluid displaces the oil (displacement efficiency) and the volume the fluid enters (sweep efficiency). Water does both these things more efficiently than gases. It should be kept in mind that secondary recovery methods do not change the properties of the oil, as opposed to tertiary methods. These methods are also referred to as *enhanced oil recovery (EOR)*. EOR is an important issue for heavy oils with high viscosity and low API gravity. (Chapter 2.4) The reservoir rocks can also influence EOR because low-permeable carbonate responds poorly to secondary recovery methods.

Reduction of the viscosity of the crude is the target in most cases of EOR. One much used method is thermal flooding using steam, and the viscosity decreases with increasing temperature, thus increasing the sweep efficiency. In addition, there might be significant amounts of oil remaining in pore space, either as small droplets or films wetting the pore walls. This is due to capillary and surface forces, and to pore geometry. Residual oil in pores is difficult to obtain with primary and secondary methods. Chemical methods are then used to change the interfacial properties, wettability and physicochemical properties of the crude oil. Hence, chemical methods are typically EOR methods. Additions of polymers, surfactants or alkaline flooding are typical chemical EOR methods. In polymer flooding, polymers in water

are added to improve horizontal and vertical sweep efficiency, and are simple and inexpensive. Surfactant flooding is then, the use of surfactants. This requires more laboratory testing and is more expensive, and is mostly efficient for low- to moderate viscous crude oils.[1] Depending on the concentration of the surfactant and the reservoir conditions, micellar or microemulsion flooding is utilized. Oil and water are displaced ahead of the microemulsion slug, and a stabilized oil-water 'bank' develops. In microemulsion flooding, the slug must be designed for specific reservoir conditions, e.g. temperature, salinity and crude oil type, and mobility control for the microemulsions is also important for this process. Surfactants and polymers can be used in combination where the polymer follows the surfactant slug to preserve the integrity of the more costly surfactant and to improve sweep efficiency.

The last main EOR method is alkaline flooding, where alkaline chemicals such as NaOH is added to the water. As will be described in more detail in chapter 4, the base will dissociate indigenous acids which cause a drop in the interfacial tension, and/or change wettability of solid surfaces. Alkaline flooding can also be used in combination with polymers as an ancillary mobility control chemical, because the alkaline flooding itself may not provide adequate sweep efficiency.

Other EOR methods are miscible fluid displacement, where a fluid (alcohol, hydrocarbon, CO_2) displaces the oil, or *in situ* combustion. Especially the latter is popular with high-viscous oils, like the tar sand oilfields in Canada. Heat is generated by injecting air and the combustible part of the crude oil, which greatly reduces the oil viscosity and partially vaporizes the oil in place. Then hot water, steam and gas drive will drive the oil out of the reservoir.

2.4. Conventional and heavy oil

The properties and composition of crude oils are reflected by their origin, climate and the age of the reservoir. At the early age of modern petroleum history, it was desired to recover the oil which was, with the current technology, easy to recover by conventional methods. These oils were low in density, containing small amounts of acids and/or high molecular weight components, making the flow in oil recovery sufficient with respect to primary recovery. However, many of these ”high quality” oil reservoirs have been deprived and it is difficult to find new oil fields with conventional crude oil. Many new oilfields contain so-called heavy oil, or in some cases extra heavy oil (bitumen, tar sand). As the terminology indicates, these are heavier with a higher density and contain substantially more of the high-molecular weight components. These properties yield the need for recovery by secondary and tertiary methods. One of several definitions to distinguish the different classes of oils is the API gravity, given in equation I:

$$^{\circ}API = \left(\frac{141.5}{SpGr\,@\,60^{\circ}F}\right) - 131.5 \qquad \text{(I)}$$

The API gravity is a measure of the lightness or heaviness of petroleum which is related to density or specific gravity.[1] The classification of crude oils as a function of API gravity, density and viscosity is sketched in figure 2.3:

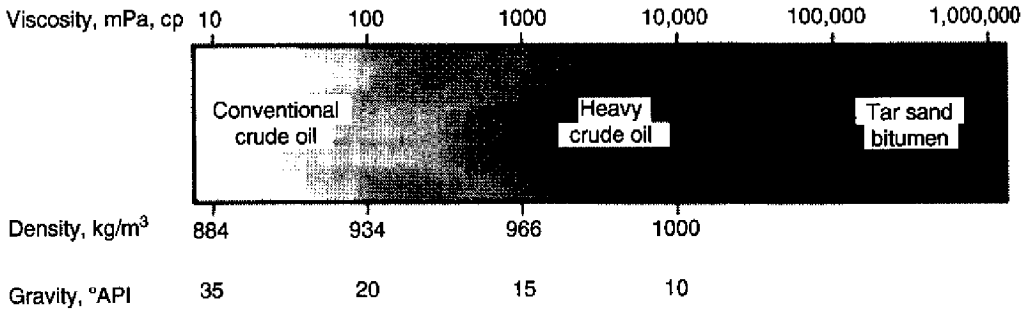

Figure 2.3. Division of crude oil with respect to viscosity, density and °API.[1]

The illustration shows that heavy crude oils are roughly between 20 - 10 °API with the extra heavy crude oils, e.g. tar sand bitumen have a °API below 10 and high viscosity and density. The increase in viscosity and density is related to their composition.

Table 1: Comparison of tar sand bitumen (Athabascha) and crude oil properties.[1]

Property	*Bitumen (Athabasca)*	*Crude Oil*
Specific gravity	**1.03**	**0.85 – 0.90**
Viscosity (cp) @ 38°C	**750,000**	**<200**
Elemental analysis (wt%)		
Carbon	**83.0**	**86.0**
Hydrogen	**10.6**	**13.5**
Nitrogen	**0.5**	**0.2**
Oxygen	**0.9**	**<0.5**
Sulphur	**4.9**	**<2.0**
Nickel (ppm)	**250**	**<10.0**
Vanadium (ppm)	**100**	**<10.0**
Fractional composition (wt%)		
Asphaltenes (C5)	**17.0**	**<10.0**
Resins	**34.0**	**<20.0**
Aromatics	**34.0**	**>30.0**
Saturates	**15**	**>30.0**

Table 1 shows a comparison between a tar sand oil, from the Athabasca field, and conventional crude oils. In chapter 3 the details of the crude oil fractions and composition will be given, but Table 1 shows that the bitumen contains much more of the high-molecular weight asphaltenes and resins, than the light saturates. In addition, more heteroatoms are found, and both factors contribute to the physicochemical properties of the crude oils.

3. Composition of crude oil

The following sections will give a description of the current status of the knowledge of crude oil composition. The emphasis is focused on the fractions of crude oil relevant for this thesis with only brief descriptions of other crude oil fractions and components.

3.1. SARA fractionation.

Crude oil consist of thousands or millions of different structures and compounds, and a separation of all these is impossible. A dividing of the crude oil into smaller fractions depending on size, polarity and aromaticity is a beneficial approach. The most common fractionation of the crude oil is the SARA fractionation.[7-13] This method divides the crude into Saturates (S), Aromatics (A), Resins (R) and Asphaltenes (A). These four fractions differ in their polarity, aromaticity and solubility in a hydrocarbon medium. Jewell et al. presented in 1972 separation of heavy-end petroleum distillates into acid, base, neutral-nitrogen, saturate and aromatic fractions.[7] The study was the first to divide the crude into these fractions by chromatographic separation. The technique included both anion – and cation exchange chromatography, coordination chromatography and adsorption chromatography. The separation technique has later been modified to include separation of the polar constituents into resins and asphaltenes, and more sophisticated preparative HPLC methods have made the separation automatic and less time-consuming.[8,9] A typical separation is shown schematically in figure 3.1.

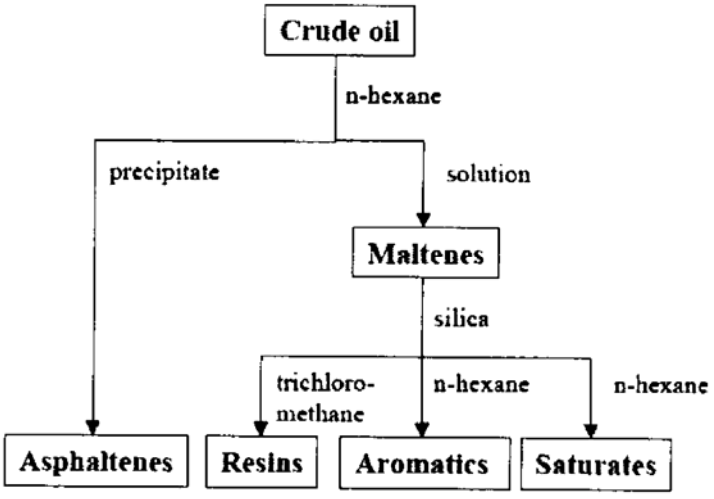

Figure 3.1. A typical scheme for SARA separation. [14]

The first step in the SARA fractionation is precipitation of the most polar and aromatic part of crude oil – the asphaltenes. Upon addition of a light hydrocarbon, such as *n*-pentane or *n*-heptane, the asphaltenes will precipitate as a brown to black solid material. In some cases, an additional pre-precipitation with an aromatic solvent like toluene (which solubilises all SARA fractions) might be feasible, if necessary to remove solid, inorganic particles from the solution.[10,15] The three remaining fractions are separated by HPLC, using a combined system composed of an amino precolumn and silica column. Saturates are easily eluted with hexane as mobile phase through both columns, and the aromatics are subsequently collected by using a back-flushing mechanism. Resins are adsorbed to the amino column, but desorbed with dichloromethane and back-flushing. The amount of each fraction is finally determined gravimetrically. SARA fractionation has been used on numerous crude oils from all over the world.[8] However, several SARA fractionation methods has been used. First of all, the asphaltenes may be precipitated by different hydrocarbons, e.g. pentane and heptane. In a comparison study, Kharrat et al. showed that the choice of precipitation medium could be highly crucial for some crude oils regarding the amount of asphaltene precipitated.[12] For one of the crude oils, the solvent effect of asphaltene precipitation gave a ratio of precipitated asphaltenes depending on the medium, % asphaltenes C5/C7, as high as 263. For all 5 crude oils tested, the lowest ratio was higher than 1.5. And, the asphaltene C5/C7 ratio will thus influence the amounts of the other fractions. In addition, volatile compounds give a low total recovery. Sample topping, that is evaporation of volatile compounds, should always be included in the SARA fractionation to give a high total recovery (~100%) and correct amounts of the four fractions.

Another SARA fractionation method is by use of thin layer chromatography, TLC, in combination with an automated flame ionization detector (FID).[16] The separation of the fractions is carried out with much the same eluents as for the HPLC method, but at a smaller scale. The TLC-FID detection can be a good alternative to the HPLC method, but lacks accuracy because of underestimating the saturate fraction due to evaporation from the TLC rod. Thus, TLC-FID have mostly been applied to determine hydrocarbon types in various high-boiling materials with initial boiling points at or above 260°C,[13] and less suitable for crude oils with high amounts of volatiles.[16]

3.2. Asphaltenes

The asphaltenes are defined based on solubility. *Asphaltenes is the fraction of crude oil that is soluble in toluene, but insoluble in alkanes such as pentane and heptane.*[1] Asphaltenes adsorb irreversibly to an oil/water interface and sterically stabilize water-in-crude oil emulsions and adsorb to solid surfaces[17-19] influencing the wettability, for example in reservoir rocks. The emulsion and adsorption behaviour of asphaltenes will be described in chapter 5.2.

3.2.1 Elemental composition of asphaltenes.

The amounts of carbon and hydrogen in asphaltenes usually vary over a narrow range, corresponding to a hydrogen-to-carbon ratio of 1.15 ± 0.5%.[1] It is in the heteroatom content the asphaltenes differ significantly from the crude oil. They contain substantial amounts of nitrogen, oxygen and sulphur, in addition to trace amounts of nickel and vandadium.[20,21] Table 2 shows an example of asphaltene characterization based on chemical composition, with two American asphaltene samples.

Table 2: Chemical composition of West Texas and Louisiana Asphaltene Samples. The data are taken from Wattana et al.[20]

Parameter	*West Texas Asphaltene*	*Louisiana Asphaltene*
Elemental analysis (wt%)		
Carbon	**85.78**	**86.24**
Hydrogen	**7.16**	**6.78**
Nitrogen	**1.19**	**1.23**
Sulphur	**2.71**	**0.65**
Oxygen	**1.34**	**3.19**
Metal content (ICP) (ppm)		
Vanadium	**190**	**13**
Nickel	**266**	**63**
Iron	**178**	**526**

It should be emphasised that Table 2 only gives examples of asphaltene samples. As previously discussed, crude oil composition can vary from field to field, and this will be reflected in the asphaltene fractions as well. Only between these two samples, the amount of several heteroatoms differs significantly. The amount of for instance oxygen and sulphur can vary from 0.3 to 4.9% and 0.3 to 10.3%, respectively.[1]

The nitrogen can give an asphaltene molecule both basic and neutral behaviour, depending on if the nitrogen is a part of a quinolines or a carbazole moiety.[22] Oxygen atoms are believed to mainly originate from phenolic, hydroxylic or carboxylic functionalities.[22] Sulphur can be both a part of the aromatic core as thiophenes or in the aliphatic chains as sulphide derivates,[22] or in some cases as sulphur bridges.[23] Transition metals as vanadium and nickel are believed to be an element of porphyrin structures in the asphaltenes.[24]

3.2.2 The molecular weight controversy

The molecular weight of asphaltene has been an issue of debate and has annoyed many researchers throughout the years. The reason behind the troublesome analysis and determination of asphaltene molecular weight is that asphaltene tend to self-associate, even at low concentrations (~0.1 g/L in toluene).[25] Thus, when first starting to analyze asphaltene samples one typically measured the size of the aggregates and not the monomeric asphaltenes. Standard methods such as Vapor Pressure Osmometry (VPO) and Size Exclusion Chromatography (SEC) have yielded molecular weights of 4 000 and ~ 10 000 g/mol, respectively.[26] The most promising techniques today are the laser desorption ionization – mass spectrometry[27] (LDI-MS) and fluorescence correlation[28] and depolarization spectroscopy.[26] These highly sensitive techniques show average asphaltene molecular weights smaller than the values obtained with VPO and SEC, and the currently accepted value of asphaltene average molecular weight now seems to range from 500 to 1000 g/mol, with an average of 750 g/mol. The number of aromatic rings in each molecule is estimated to be in the range from 4 to 10 fused aromatic rings.[26] It should be emphasized that, due to the polydisperse nature of asphaltenes, the asphaltene molecular weight is always given as an *average* molecular weight of the whole distribution.

In addition to the controversy regarding molecular weight, there has also been a debate on if the asphaltenes are comprised of only one fused, aromatic core, surrounded by aliphatic chains or that more than one fused, aromatic core can exist in one asphaltene molecule where the fused cores are interconnected through aliphatic chains.[29] These models are attributed to the “continental” and the “archipelago” model, respectively. (Figure 3.2)

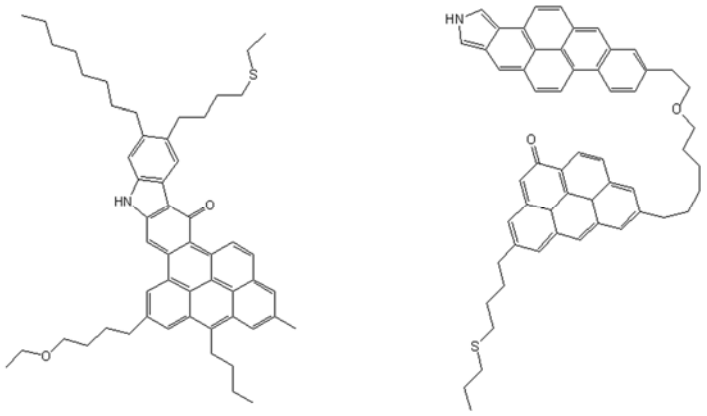

Figure 3.2. Examples of the two possible models for the asphaltene structures. Shown on the left is the continental structure, and on the right is the corresponding archipelago model.[29]

Studies support both the continental[30] and the archipelago[31,32] model. No general conclusion regarding this controversy has yet been globally accepted. The reason could be that asphaltenes can be represented with both models, thus it is mixtures of both continental and archipelago structures.

3.2.2. Precipitation of asphaltenes

As described in the SARA section, asphaltenes precipitate in a fluid of low aromatic character, due to the condensed aromatic rings and heteroatoms present. The precipitation onset, that is the vol% of hydrocarbon in toluene where the asphaltenes start to precipitate, can easily be found by titration and detection by Near-Infrared Spectroscopy (NIR). An example of such experiment is shown in figure 3.3 a.

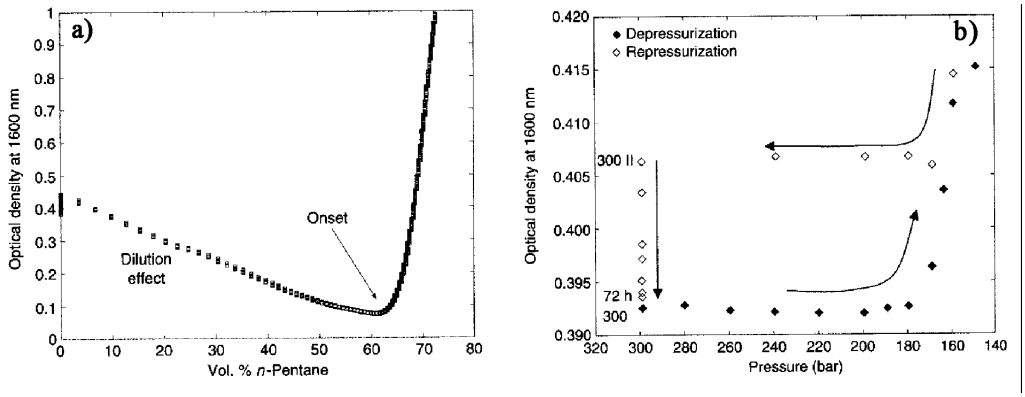

Figure 3.3. (a): Determination of asphaltene precipitation onset. (b): Influence of pressure on crude oil precipitation. From "*Emulsions and Emulsion Stability*".[16]

The increase in optical density is due to light scattering from particles formed in the solution. NIR can also be used under high pressure,[33] and it verifies observation from fields that pressure drops cause precipitation of asphaltenes. Hence, instability of asphaltenes can occur both due to dilution to a lower aromatic fluid and due to pressure drops, for instance in oil recovery. In addition a reversible effect of the pressure drop has been found for the whole crude oil. [33] This is illustrated in figure 3.3 b. The aggregation was however partially reversible for a model system containing asphaltenes (1.2 wt%) in heptane/toluene (35/65). The difference was explained by lack of dispersing resins in the model systems during repressurization.[33]

3.2.3. Fractionation of asphaltenes

It has been proposed that asphaltenes contain different fractions and these subfractions will behave differently in water – crude oil systems.[20,21,31,34] Fractionation of the asphaltenes based on solubility and polarity with subsequent characterization could thus give information on which subfractions of the asphaltenes are responsible for processing problems. One standard method for asphaltene precipitation uses a 40:1 ratio of hydrocarbon (HC)-to-toluene[8,35] and will recover the whole polydisperse asphaltene fraction. However, it is expected that there is also a high degree of dispersity in aromaticity and polarity throughout the asphaltene sample, which will be reflected in the solubility in a HC medium. Most fractionation studies use precipitation in a range of HC-to-toluene ratios giving subfractions with different solubility character.[20,24,31,36,37] Generally, the first fractions obtained at a low HC-to-toluene ratio have the highest degree of polar functionalities, average molecular size and aromaticity.

One proposed mechanism behind asphaltene problems such as stable water-in-oil emulsions is that the strong interfacial films are composed of aggregates (or particles) of asphaltenes, and when they start to aggregate in the bulk phase, these play a vital role in the stabilization mechanism.[30] This is then correlated to the critical concentration of asphaltenes in *e.g.* toluene when they start to aggregate, Critical Nanoaggregate Concentration, CNAC.[25] Values for aggregation vary between reports[38], and higher levels of aggregation are also suggested.[25] The aggregation is influenced by the resin fraction, and by removing this fraction the asphaltenes have shown to be even more prone to stabilize emulsion.[16] This has been explained by a stabilization of the asphaltene aggregates by the polar groups in the resins, dispersing the aggregates into the bulk oil phase.[39]

Even if most fractionation studies compare the different fractions with respect to aggregation, size and polarity and assuming the aggregation will reflect the emulsion behaviour, recent studies of interfacial activity of fractions show another mechanism behind the interfacial behaviour of asphaltenes. Fossen et al. have fractioned asphaltene samples into both two and four subfractions depending on the pentane-to-crude oil ratio.[36,37] The interfacial tension between toluene and water for each fraction was measured. Surprisingly, the studies show that it was not the first precipitated fraction showing the highest interfacial activity, as illustrated in figure 3.4. Characterization of the fractions showed that the first fraction was the most polar and aromatic, and with the highest average molecular weight, without having significant interfacial activity.[40] In contrast, the intermediate fraction was found to have more hydrogen bonding groups such as –OH and –COOH, as indicated from FT-IR. In contrast to the first fraction, the intermediate fraction displayed more branching in the aliphatic parts of the molecules. The studies showed that the asphaltenes could be divided into non-surface active and surface active fractions.

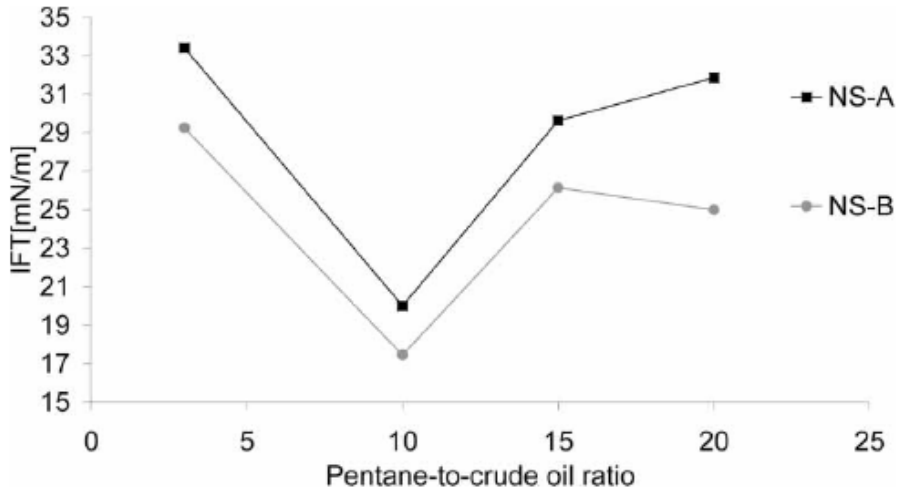

Figure 3.4. Plot of interfacial tension between toluene and brine for asphaltene fraction from crude oil with fractionation depending on the pentane-to-crude oil ratio. Clearly, the fraction obtained at 10:1 ratio have a higher interfacial activity. NS-A and NS-B are two North Sea crude oil samples.[37]

Such terminology of (non)surface active asphaltenes has also been proposed by others.[41-44] Yarranton et al. also concluded that only the surface active asphaltenes that were still soluble, that is present in monomeric state and not as aggregates, were able to stabilize emulsions.[42] This contradicts the general assumption that it is when the asphaltenes become aggregated they can stabilize emulsions. Czarnecki et al. proposed a similar model with a competitive adsorption between small, surfactant-like molecules with fast diffusion to the interface in a reversible process, while larger, less surface active compounds adsorbed slow and irreversibly, shown in figure 3.5.[43] Still, from the literature there seems not to be a general accepted conclusion regarding if the aggregates or the monomeric surfactants stabilize emulsions, and current studies involve both assumptions.

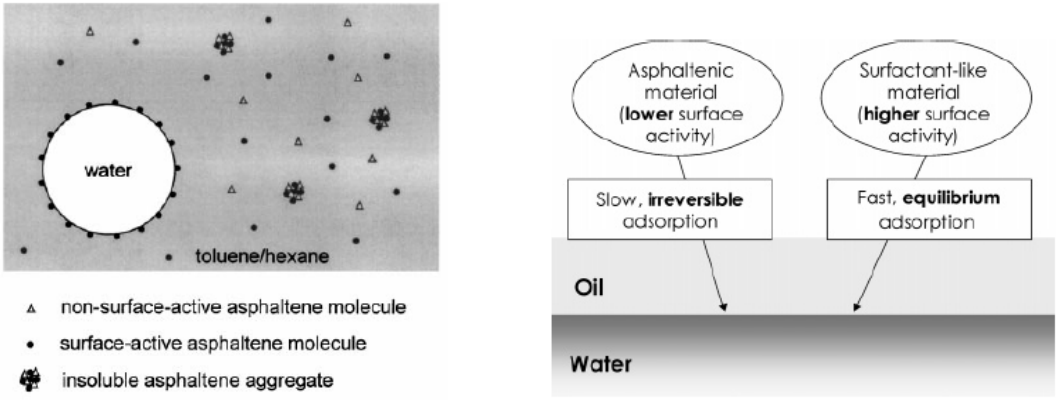

Figure 3.5. Interfacial adsorption model of asphaltenes proposed by Yarranton[42] (left) and Czarnecki[43] (right).

3.2.4. Film properties.

The properties of asphaltene films can be studied by means of the Langmuir technique (Chapter 6.2).[45-52] In general, Langmuir films prepared with asphaltenes display low compressibility and high surface collapse pressures, indicative of the formation of a strong film.[39,45,53] Addition of resins or demulsifiers affect the asphaltene films by rendering the films more compressible, both concerning air/water and oil/water films.[39,46] The compressibility of an interfacial film will have strong influence on the coalescence of water droplets in emulsion. Langmuir films comprised of asphaltenes can be studied both as a monolayer[45] or as multilayers.[48] The irreversible adsorption of asphaltenes onto an oil/water interface has been shown by washing a preformed film with fresh solvent. When the film was

comprised of multilayers, the asphaltenes were desorbed, except for the first layer.[48] This has also been confirmed when washing an asphaltene monolayer, where the monolayer did not desorb upon addition of fresh solvent.[47] In addition, 2-propanol did not solubilise the asphaltenes but rendered the monolayer more flexible. Bonding between the adsorbed monolayer with water molecules may be one explanation for the irreversible nature of the asphaltene films.[47] The composition of the oil phase has been shown to affect the films of asphaltenes. Ese et al. studied air/water films of asphaltenes from different origins and illustrated that the asphaltenes adsorbed as aggregates when solubilised in a solvent of low aromatic character.[54] Interfacial asphaltene films have also been shown to become more stable, that is highest attainable interfacial pressure, at increasing ratios,[46] indicating an increased affinity for the interface when the aromaticity of the solvent is low. The rigidity of an asphaltene film prevents droplet coalescence and is due to strong intermolecular interactions by both hydrogen bonding as well as π-bond interaction between fused rings.[55] These interactions give a viscoelastic network of asphaltene molecules in a film. Recent work with neutron scattering techniques have shown that the structure of the interfacial layer is a monolayer of asphaltene aggregates, and the size was correlated to the aggregate size in the bulk phase.[56,57] It is also suggested that the strong interfacial films of asphaltene display anisotropy with defined molecular arrangements, like a liquid crystalline phase.[58] The arrangement of the asphaltene molecules at the aqueous surface has been discussed, showing both a configuration of the aromatic core lying flat on the aqueous surface[45,54,59] and a more tilted geometry of the aromatic core with respect to the surface plane.[52] It has also been suggested that both configurations occur, depending on if the interface is relaxed or compressed.[42]

3.2.5. Model molecules for the asphaltenes.

Chapter 3.2.3 clearly demonstrates that the knowledge of what compounds of asphaltenes causing problems is limited due to the high polydispersity of this class. One approach towards this problem is the use of model compounds resembling the asphaltenes. Investigating model compounds creates an easier system due to the known composition, molecular weight and facile characterization by for instance UV or fluorescence. However, usage of model compounds has mainly been introduced as a way to investigate the molecular weight issue and self-association. Mullins and co-workers have in several studies used for instance perylene and porphyrine dyes in combination with fluorescence techniques.[26,28] Fluorescence

is a highly sensitive technique which enables the probe to be studied at very low concentrations. Thus, experiments can be carried out well under the CNAC of the asphaltenes, thus avoiding the pitfall of measuring the aggregate size. The fluorescence data for the model compounds, with known structure and size, could then be used to estimate the size for indigenous asphaltenes, resulting in the nowadays accepted molecular weight in the 500 – 1000 g/mol range. Synthetically made hexabenzocoronene derivates have also been used as model compounds for asphaltenes to approach the self-association behaviour of bitumen fractions,[60] and the association behaviour has also been the focus of a study using pyrene compounds with both aromatic and polar character.[61] However, in all previous studies these model compounds have been used to address the aggregation and size debate. Based on the findings by Fossen et al.,[36,37] the way to find mechanisms behind interfacial activity and emulsion stabilization may instead include characterization of the interfacial behaviour of model compounds. Limited information is found regarding use of model molecules with respect to these physicochemical properties. There is obviously a need for such studies and knowledge about the functionalities of asphaltene causing the actual problems.

4. Naphthenic acids

There are many crude oils which have shown to have a highly acidic character, and so being referred to as acidic crude oils. Oilfields with acidic character are found all over the world, from Africa to South America and the North Sea.[62] One way to characterize an acidic crude oil is by its total acid number, TAN. The TAN is defined as the number of mg of KOH required to neutralize the acidity of 1 g oil.[63] Oils with a TAN > 0.5 are generally classified as acidic.[63,64] Biodegradation of the oil is the dominant process that produces high acidity.[64,65] Table 3 lists the TAN number of acidic crude oils from oilfields worldwide.

Table 3: TANs of crudes from different fields.[62]

Crude	*Country*	*TAN [mg KOH/g]*
Camelia	Angola	1.90
Dalia 2	Angola	2.37
Orquidea	Angola	3.73
Moho	Congo	0.87
Bilondo	Congo	1.80
Ukot	Nigeria	1.01
Ime	Nigeria	2.08
Alba	North Sea	1.83
Heidrun	North Sea	2.60
Lagotreco	Venezuela	1.18
Laguna	Venezuela	4.10

Acidic crudes also have a low paraffin content and have higher densities than non-acidic crudes.[62] The acidity is probably due to the alteration of petroleum by living organisms, which cause biodegradation of the paraffinic structures to oxidized structures, e.g. carboxylic acids. The acidic character cause problems related to corrosion[66] and flow assurance problems, and the latter will be discussed more later.

These acidic species in crude oil are generally termed naphthenic acids. Naphthenic acids include structures with single and multiple fused cyclopentane and cyclohexane rings, where the carboxyl group is attached to the aliphatic side chain or to the cycloaliphatic ring.[67] The

definition has however become more loosely used to describe the range of organic acids found in crude oil.[66]

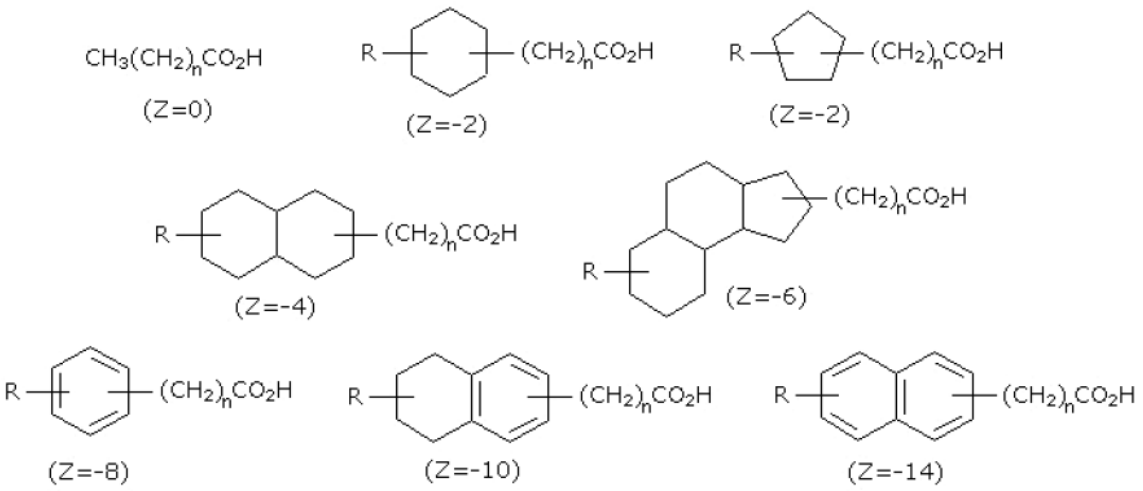

Figure 4.1. Examples of naphthenic acid structures with a general formula $C_nH_{2n+Z}O_2$.

Examples of naphthenic acid structures can be seen in figure 4.1. They have a general chemical formula $C_nH_{2n+Z}O_2$, where *n* indicates the carbon number and Z specifies a homologous series and the saturation and cyclic character of the naphthenic acid.[68]

The role of naphthenic acids in crude oil fluids is highly dependent on pH, pressure and the dissociation of carbonic acid, H_2CO_3.[62] An overview over these equilibria is shown in equations II – V. Produced water from the reservoirs contains dissolved carbon dioxide, which is in equilibrium with its hydrated form, carbonic acid. (II) Carbonic acid can in turn dissociate to its bicarbonate and carbonate forms. (III and IV) The carbon dioxide – carbonic acid equilibrium is highly dependent on the pressure in the system. As described in Chapter 2, reservoirs generally have a high underground pressure. However, when water is drained to the surface the fluid will undergo a pressure drop,[62] thus shifting equation II to the left according to Le Chatelier's principle. The effect of equations III and IV is then that more H^+ is consumed to form carbonic acid, and the influence of the system is that the pH increases. From equation V it is seen that when the pH increases solid calcium carbonate can form as well.

$$CO_2(g) + H_2O \rightleftarrows H_2CO_3(aq) \quad \text{(II)}$$

$$H_2CO_3(aq) \rightleftarrows H^+ + HCO_3^-(aq) \quad \text{(III)}$$

$$HCO_3^-(aq) \rightleftarrows H^+ + CO_3^{2-}(aq) \quad \text{(IV)}$$

$$CO_3^{2-}(aq) + Ca^{2+} \rightleftarrows CaCO_3(s) \quad \text{(V)}$$

4.1. Dissociation of naphthenic acids and formation of metal naphthenates.

The pH of the produced water will greatly affect the role of the naphthenic acids in the oil. Medium to long straight-chained carboxylic acids have apparent dissociation constants, p*K*a's, in the range of 4.8 to 8, where the increase in apparent p*K*a above the C6 acid (p*K*a ~ 4.8) is probably due to micellization.[69] When the pH of the produced water increases above the apparent p*K*a of the naphthenic acid, the acid deprotonates to form a *naphthenate*. (eq.VI) The naphthenate formation greatly enhances the interfacial activity.[70] The negatively charged naphthenate is then prone to react over an oil-water interface with cations naturally present in the produced water, forming a *metal naphthenate*, which in most cases for divalent cations is a solid. (eq. VII)

$$RCOOH + OH^- \rightleftarrows RCOO^- + H_2O \qquad \text{(VI)}$$

$$\left(RCOO^-\right)_n + M^{n+} \rightleftarrows M\left(RCOO\right)_n\left(s\right) \qquad \text{(VII)}$$

The solid precipitated upon formation of metal naphthenates is the basis for a naphthenate deposit. In cases where the counterion is sodium, the interfacial reaction causes interfacially active complexes which are prone to stabilize water-in-oil emulsions.

Most naphthenic acids found in crude oil are monocarboxylic naphthenic acids, or monoacids, with molecular weights in the range of 200 - 500 g/mol.[62,66] The oil/water-partitioning of model and indigenous naphthenic acids have been studied by Havre, who found the p*K*a of crude oil acids to be ~4.9, and that the logarithm of the partition coefficients varied linearly vs. the number of carbons in the naphthenic acid in the molecule.[70] Reactions of divalent cations with a model monoacid, *p*-(*n*-dodecyl)benzoic acid, have been studied with the pendant drop technique by Brandal et al.[71,72] The results indicated a two-stage process with initial formation of a 1:1 charged interfacially active complex and then subsequently binding of a second naphthenate to form the neutral 2:1 metal naphthenate. Mg^{2+} formed the most stable 1:1 complex due to its hydration state, while the neutral Ba^{2+} salt reacted quickly and to be dispersed in the oil phase. The interfacial films were later studied in a Langmuir trough

showing the different behaviour of the cations upon interfacial reactions with a monoacid.[73] The different behaviour could be explained by the hydration degree of the cation.
In general, the monoacids react with cations across o/w interfaces, and the reaction and interfacial behaviour depend on the pH, type of cation and structure of the acid, and the solubility of the formed product.

4.2. The discovery of the tetrameric acids.

When the reaction products as described in section 4.1 are insoluble in both oil and aqueous phase, the products tend to accumulate at the interface, causing naphthenate deposits. In the oilfield processing, calcium is the most common divalent cation found in such deposits, and a common name for such a deposit is calcium naphthenate. An example is a case study of the Heidrun field on the Norwegian Continental Shelf observing naphthenate deposits in process equipment in 1996.[74] The problem seemed to accelerate, and the first short-term solutions were to add organic acids and scale inhibitors, without success. On long term basis, much effort was put on formulating naphthenate inhibitors with varying success. With the extreme polydispersity of different naphthenic acids present in crude oil, an explanation of the naphthenate problem based on structural analysis of crude oil was a tremendous task. Instead, the R&D group at Statoil in collaboration with ConocoPhilips shifted the focus to the deposit itself, carrying out a thorough analysis of the deposit. The acids in the deposit were recovered and isolated by an Acid-IER method.[75] Through a combination of techniques, among them potentiometric titrations, Liquid Chromatography – Mass Spectrometry (LC/MS) , NMR and VPO they found that the acids responsible for deposition at Heidrun was a narrow group of high molecular weight naphthenic acids in the range of 1227 – 1235 g/mol.[76] These acids turned out to be 4-protic carboxylic acids, that is, tetrameric 'ARN' acids.[ii] Until this point, it was assumed that the composition of the acids in the crude also reflected the deposited acids composition which normally has a broad distribution centered at 200-500 g/mol. The findings by Statoil and ConocoPhilips indicated a selective reactivity for the tetraacids on behalf of other acids present even if their concentration in crude oil was much lower.

[ii] In many industrial environments, these indigenous tetraacids are called 'ARN' acids, after an old Norwegian word for 'eagle'. The reason apparently, is that eagles fly high in the sky; you need to look higher than normal to see it. Since eagles are quite large birds, there are many similarities to the ARN acids, as depicted by Baugh.

The exact structure of the tetrameric acids was solved by Lutnaes and co-workers by extensive NMR characterization,[67] and the structure for the most abundant 6-ring isomer (M_w=1231 g/mol)[iii] is given in figure 4.2.

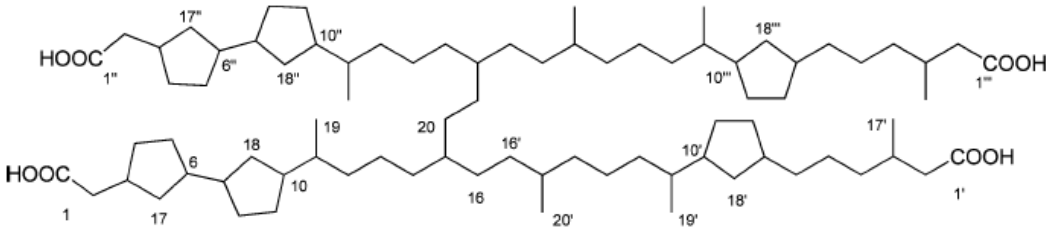

Figure 4.2. Structure of the most abundant tetrameric acid found in deposits. The term 'isoprenoid', used in the papers, originates from the isoprene unit, a branched C_5 building block. Oils and plants are mostly based on these units, also referred to as isopentenyl units.[77]

HPLC separation and structural analysis were later presented for the whole C_{80} tetrameric acid family together with C_{81} and C_{82} analogues.[78] It is believed that it is the molecular structure with four terminal carboxylic acids which enables the molecule to direct all the acid groups to the interface, acting as an efficient surfactant. This was confirmed by Brandal when studying the interfacial activity and film behaviour of the tetraacids.[79] Already at 0.005 mM, corresponding to about 5 ppm, the interfacial tension between C16:toluene (9:1) and pH 9 was lowered to 12 mN/m. 5 ppm is several orders of magnitude lower than required monoacid concentrations to reach the same interfacial activity. Addition of Ca^{2+} in the subphase when compressing an air-water film caused higher stability of the film. Due to its structure, it has been proposed that the tetrameric acids can cross-link with calcium and form an extended polymeric network.[67,80] This would prevent viscous relaxation on deformation, and the calcium film was in fact shown to be an elastic, solid-like film. Such an elastic, cross-linked film supports the observation that calcium naphthenate accumulates over o/w interfaces as a sticky film, which acts like a glue to which sand and particles can adsorb. It has been shown that the tetraacid displays a glass transition, T_g, in thermal solid state properties, similar to that of amorphous polymer systems.[80,81] These transitions were observed both for the isolated acid and its calcium salt form,[80] in addition to measurements directly on deposits.[80] Field and

[iii] Surprisingly, reports of the accurate M_w of the most abundant 6-ring isomer differ between 1230 and 1231 g/mol. Both industrial and academic papers have been incorrectly using the weight 1230 g/mol for the most abundant tetraacid. The reason might be that detection with MS use the negative mode, and thus gets out the molecule after a proton loss. Hence, the weight measured is for the anionic form, correctly stated by Baugh. Practically however, this difference does not influence the results because the ARN is isolated as an impure isomer mixture. Nevertheless, from the author's point of view the issue should be mentioned.

laboratory observations have shown the gel-like deposit comprised of calcium naphthenate to be liquid-like under process conditions, which solidifies when exposed to ambient pressure and temperatures.[74,81,82] This hardening is causing great difficulties in the removal of naphthenate deposits from topside facilities,[74] and it is suggested that the hardening of the gel can be a function of the glass transition.[81] Another interesting feature of the ARN acids is their film properties. Under compression at an air/water interface, the molecule is in the gaseous state aligned with all acid groups towards the aqueous phase, but can be lifted to an upright position, leading to tightly packed molecules in a bilayer-like arrangement.[80,83] This is illustrated in figure 4.3.

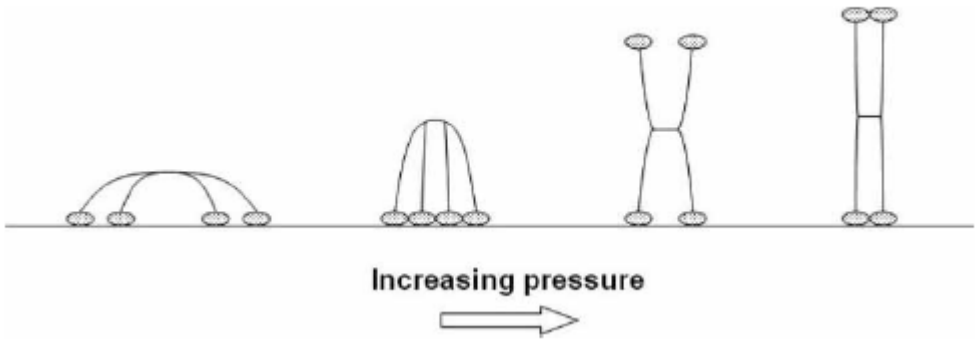

Figure 4.3. Transition between different conformations upon monolayer compression of the ARN acid.

The p*K*a value(s) of the tetrameric acids has shown to be difficult to obtain. Potentiometric titrations in organic medium have indicated only one dissociation step for the ARN molecule,[76] and field observations estimate the occurrence of calcium naphthenate deposits around pH 6.[76,81] Brocart et al. discussed if one could distinguish the apparent p*K*a for ARN acids and pKa for shorter naphthenic acids occurring in crude oil.[81] If there are different apparent p*K*a's, either way, this could explain the observation that some fields have trouble with deposits while others display emulsion problems. No final conclusion concerning the p*K*a of ARN has been found, and authors state how essential it is to gain more knowledge of the acid-base properties of both ARN and other naphthenic acids to correlate to mechanistic explanations behind the deposition.[81]

4.3. Oilfields with ARN and deposition problems

Naphthenate deposition problems have been found in a selection of oilfields, but spread all over the world. Prior to the ARN discovery, it was assumed that fields with a high TAN were prone to have a deposition issue. However, the introduction of ARN theory totally circumvented this proposition. Table 4 lists a selection of oilfields where ARN has been detected in the crude oil and compared to TAN, API, and whether they have experienced deposition problems.

Table 4: Characteristics of some selected crudes compared to deposition problems.[74,81]

Crude	*TAN [mg KOH/g]*	*°API*	*Field deposit*
Afia	1	25	Yes
Blake	0.09	30	Yes
Girassol	0.38	30.5	No
Heidrun	2.6	28	Yes
Kuito	2.15	20	Yes
Ofon	0.4	41	No
Tchibelli	0.66	36.5	No

Table 4 shows that crude of high TAN (> 0.5) does give a deposition problem, However, crude oils of low TAN may also cause deposition problem as shown in the case of Blake crude. Deposition problems are generally experienced with conventional crude oils. Acidic crude oils, not necessarily containing ARN, can display a high propensity to stabilize water-in-crude oil emulsions. These can be very tight emulsions, and in the worst case behave like a sludge.[84] These tight emulsions are formed by the sodium salts of different naphthenic acids in the crude (other than ARN) with molecular weights in the range of 200-400 g/mol. Another consequence of these emulsions is high amounts of oil in the produced water.[84]

With the recent discovery of tetrameric acids, the research on such is in its infancy, and there is clearly a need for more knowledge on the behaviour of tetraacids and the mechanism behind formation of calcium naphthenate deposits. In the meantime, chemical vendors are constantly developing new inhibitor blends as down – and upstream additions to prevent naphthenate deposition. Such inhibitor blends have become increasingly efficient, and per date the most promising inhibitor blends for use in acidic crude oils consist of a combination of a demulsifier and a naphthenate inhibitor.[84,85] The addition of a demulsifier component is

due to the possible formation of tight emulsions, and possibly that naphthenate deposition can be a function of the available interfacial area. A naphthenate inhibitor can act through different mechanisms, among them is interfacial crowding, dispersing either calcium or naphthenate or to suppress the increase in pH. Much effort has been directed towards development of test protocols for inhibition efficiency towards naphthenate deposition by the chemical companies. [84-86]

5. Surfactants and emulsions

In this chapter theory about colloidal systems relevant for this thesis will be presented. Chapter 5.1 is an introduction to the concept of surfactant chemistry, relevant for the aqueous phase behaviour of tetrameric acids. Chapter 5.2 presents emulsions and emulsion stability with the main focus directed towards emulsions formed within the crude oil processing chain stabilized by both asphaltenes and naphthenic acids.

5.1. Surfactant chemistry and micellization

Surface active agents, usually referred to as surfactants, are amphiphilic molecules that consist of a polar hydrophilic region and a nonpolar hydrophobic region.[87] A schematic view of a surfactant is shown in figure 5.1.

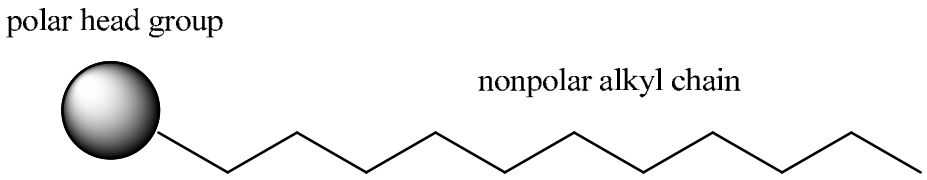

Figure 5.1. Schematic view of a surfactant.

Surfactants are different from non-amphiphilic compounds in that they can self-assemble in solution and create certain aggregates. One example of such aggregates is the *micelle*. Taking an aqueous solution as an example, the hydrocarbon region of the molecules will escape from the polar environment and concentrate in the middle of a spherical aggregate, where the polar functionalities are pointing outwards to the aqueous phase. A schematic structure of an anionic micelle is shown in figure 5.2.

The surface of the micelle consists of the surfactant head groups and adsorbed counterions. This layer is called the Stern layer, and can be up to a few Å thick. Around the micelle structure, a mobile and diffuse layer of counterions is found. This electrical double layer is called the Gouy - Chapman layer. Hydrophobic alkyl chains are located in the core of the micelle, and the radius of the micelle can not exceed the length of the fully extended hydrophobic tail. About the first four methylene groups in the tail are more immobile than the

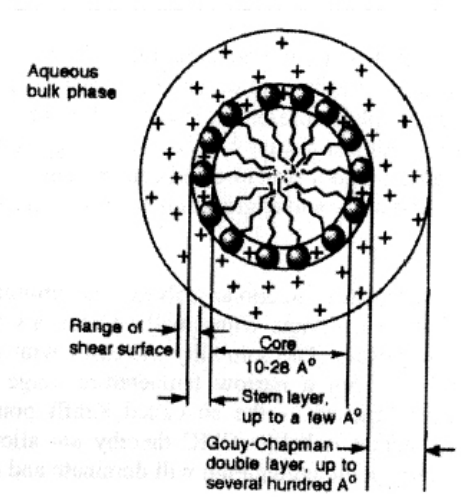

Figure 5.2. Schematic structure of an anionic micelle in water.

rest of the tail. This outer core and the headgroup is called the Palisade layer.

The nature of surfactants provides several physical properties which differ from non-amphiphilic compounds. Among these, the abrupt change in physical properties when exceeding a certain concentration is the main property of a surfactant. This concentration is called the Critical Micelle Concentration (CMC),[87,88] and the value is also related to the stability of the micelles.[89] Figure 5.3 shows physical properties of a surfactant solution with increasing surfactant concentration. The sudden change in properties is clear at the CMC.

Each surfactant molecule has a characteristic CMC at a given temperature and electrolyte concentration.[87] The CMC for an ionic surfactant decreases with increasing salinity due to less electrostatic repulsion, and there is a linear log-log relationship between the CMC and total salinity, referred to as a Corrin-Harkins plot.[90-92] Structural variations in the surfactant give rise to large disparity in the CMC value, both concerning the structure of the alkyl chain and the properties of the head group. The tendency is that the CMC decreases with increasing chain length and increases with increasing polarity of the head group. Ionic surfactants have typical CMC values of 10^{-1} to 10^{-4} M depending on the chain length.[87] To a first approximation, the CMC of an ionic surfactant is independent of temperature. Sodium dodecyl sulphate (SDS) varies by 10 - 20% over a wide temperature range, when above its Krafft point. In a narrow temperature range the solubility of a surfactant may increase by orders of magnitude, and this is called the Krafft temperature, or Krafft point. An example of

a technique for measuring CMC will be given in chapter 6.1, in this thesis by the use of surface tension measurements.

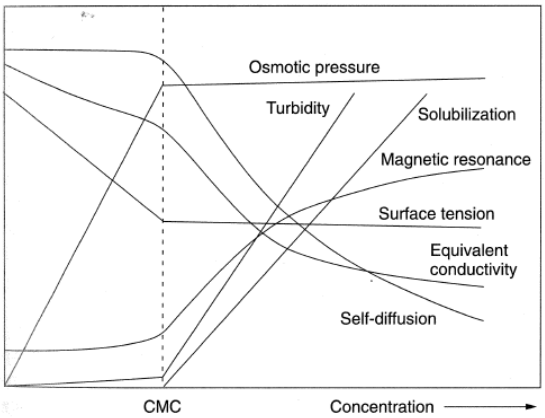

Figure 5.3. Changes in the physical properties if surfactant solutions depending on surfactant concentration.[93]

There must be some energetic driving force behind micellization. Like most other chemical processes, formation of micelles is a result of changes in the Gibbs free energy of the system. In the micelle situation, it is the delicate balance of molecular interactions which determines the Gibbs energy of the aggregates.[94] Micelle formation involves only a small change in enthalpy. The main contribution to the free energy comes from the entropy term. Micellization results in a large positive entropy change for the solvent and hence a lowering of the free energy. The clearly entropy driven process has two reasons. When the surfactant is unassociated, the hydrocarbon chain is surrounded by water molecules, forming structured water around the chain. Transfer of the monomer into a micelle where the hydrocarbon chain will be in a liquid hydrocarbon-like environment, releases these water molecules and they have a higher entropy.[87] This is called *the hydrophobic effect*. The other possible reason is that the chain in the aqueous media will have more restricted degree of orientation and bending, which is opposite to the organic environment in the micelle.[87]

Especially for ionic surfactants, the main opposing force against micellization is head group repulsion. Taking an anionic surfactant as example, the negative head groups will repel each other. Even though cations are present in between the head groups, the overall charge of the surface of the micelle is negative.

The type of assembly formed by a surfactant system can be discussed in terms of the critical packing parameter, CPP:

$$CPP = \frac{v}{l \cdot a} \qquad \text{(VIII)}$$

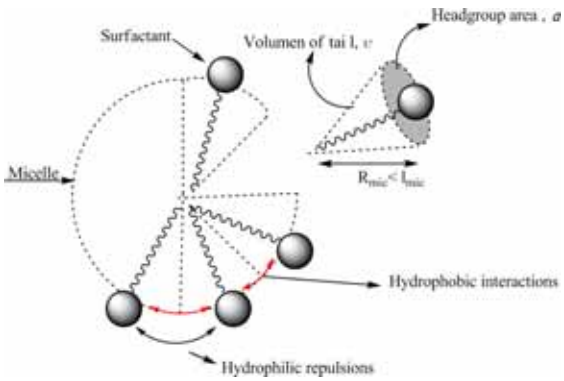

Figure 5.4. Determination of CPP based on the geometry of the surfactant.

where v is the volume occupied by the hydrocarbon chain, l is the length of the fully extended chain and a is the cross-sectional area occupied by the head group.[93] At CPP < 1/3 micelles are formed due to the preferred aggregate structure for geometrical packing reasons. Upon increasing concentration or salinity, the micelles might grow to form other surfactants assemblies like rods, which are elongated micelles. When rods are arranged in a hexagonal pattern (and 1/3 < CPP < 1/2), the system displays a *liquid crystalline phase*. Another LC phase is the lamellar phase (CPP $\approx$ 1) where the surfactants are arranged as sheets in bilayers. LC phases display anisotropy, which have the feature of scattering polarized light.[65] Such LC phases have shown to give high stability of w/o and o/w emulsions[95,96] and a high steric stabilization of w/o emulsions has been observed by Havre regarding combined systems of naphthenic acids and asphaltene particles due to formation of liquid crystalline phases.[97]

5.2. Emulsions and emulsion stability.

An emulsion is defined as the dispersion of a liquid into another immiscible liquid.[95] In contrast to a microemulsion which is thermodynamically stable, emulsions only have kinetic stability. Therefore, one often discusses the *stability* and *separation* of an emulsion. Because an emulsion is not thermodynamically but kinetically stable, the two immiscible phases will eventually separate as two phases. Droplet sizes are in the order of micrometers (μm) and a typical average droplet diameter in a crude oil emulsion is in the range from 1 to 100 μm.[42,98]

Both oil-in water (o/w) and water-in-oil (w/o) emulsions can be formed, but in crude oil emulsions, more than 95% is of the w/o type.[99] Generally, one of the phases is water or brine and the non-polar phase is a hydrocarbon medium. To form an emulsion, energy has to be put into the system. In a laboratory this can be obtained with a mechanical stirrer or a high shear mixing device. At oil processing fields turbulent flows, pressure drops and choke valves cause emulsification of the water in the crude oil. In order for the water-in-oil (w/o) emulsion to have kinetic stability, either of the phases must contain surfactants, which lower the interfacial tension and the free energy of the system. A rule of thumb is that an oil-soluble surfactant tends to give an oil-continuous emulsion (w/o), while a more hydrophilic, water-soluble surfactants tend to form a water-continuous emulsion (o/w). This is also known as the Bancroft rule. Considering the crude oil emulsions, the indigenous surfactants are soluble in the oil phase. Hence, crude oil emulsions are generally of the water-in-oil type.

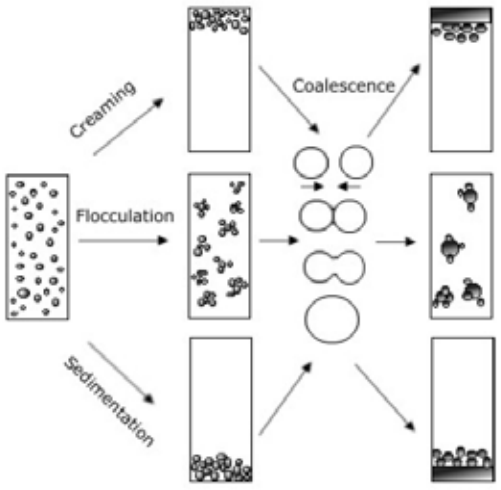

Figure 5.5. Processes taking place in an emulsion leading to emulsion breakdown and separation.

Figure 5.5 shows the different mechanisms leading to separation of emulsions. In order for droplets to coalesce, they have to be in close proximity and in contact. The mechanisms that enhance the probability of collision are flocculation and sedimentation (creaming). Sedimentation (creaming) creates a droplet concentration gradient and is a function of the density difference and viscosity of the continuous phase. Flocculation is the formation of clusters, or flocs, which may or may not be stable towards coalescence. Coalescence of droplets eventually gives separation of the two phases and is a function of the rheological properties of the interfacial film. When two droplets approach each other the contact area between the droplets is deformed, and the liquid between the two interfacial films flows out until a critical film thickness is reached.[100] Coalescence occurs when the film ruptures. Thus, the properties of the interfacial film, like stability, intermolecular interactions and rheological properties are crucial for the stability of an emulsion. The rheological character of the film can be either viscous, elastic or viscoelastic. An elastic character of the interfacial film will prevent drop coalescence. When an interface is stressed, like during drop coalescence, the uneven distribution of interfacially active components will create tension gradients on the interface that will oppose the strain. This is called the Gibbs-Marangoni effect.[16]

Water-in-crude oil emulsions are stabilized by indigenous surfactants in the crude. As briefly described in sections 3 and 4, asphaltenes and naphthenic acids may act as surfactants. These two fractions are the main stabilizers of w/o emulsion within crude oil. Naphthenic acids can roughly be regarded as part of the resin fraction. The mechanism of emulsion stability of crude oil systems can be regarded as a delicate interplay between the asphaltenes and the resins.[55,101] Researchers during several decades have shown that asphaltenes play an important role in the emulsion stability. As described in chapter 3.2.4, asphaltenes adsorbs irreversibly to the interface, causing a rigid, cross-linked elastic film which prevents coalescence of water droplets through steric stabilization.[49,55] Studies with emulsions formed with isolated asphaltenes and resins compared to emulsion with the whole crude oil strongly suggested that these fractions were responsible for crude oil emulsions, especially the most polar and condensed components.[55] The solubility state of the asphaltenes is important and their emulsifying power is highest close to their incipient precipitation onset in the context of the aromatic character of the solvent.

Resins cause less stable emulsions than the asphaltene fractions, and also act by dispersing asphaltene aggregates into the hydrocarbon phase.[16,33] By removing the most polar resin fractions, the asphaltenes display an earlier precipitation onset and higher emulsion stability as measured using the critical electric field method.[16] Sodium naphthenates can compete with the slow-adsorbing asphaltene fraction at the interface and hinder the formation of a rigid skin, allowing more fluidity and viscous behaviour of the interface.[101] Such naphthenates of size from 200 to 700 g/mol containing both mono – and diacids cause the "soap emulsions" and can also build up a 2D gel.[102] When combined, the co-precipitation of the sodium naphthenates together with asphaltenes can build up a very cohesive interface hindering coalescence.[102]

Particles, resulting from wax precipitation and minerals, can also be present in the oil and can contribute to emulsion stability. Their stabilizing ability is dependent upon the particle surface wettability, and an adsorbed layer of asphaltenes can alter their wettability from hydrophilic to hydrophobic character thus enabling them to stabilize w/o emulsions.[17,99]

6. Experimental techniques.

The following chapter will present the most relevant experimental techniques used in this thesis. Techniques where the author has not participated in the practical work will not be included, nor techniques which have only been utilized to a small degree or is too fundamental to be considered necessary to elaborate in this thesis.

6.1. Methods for surface/interfacial activity – pendant drop technique and tensiometer

Interfacial tension is a measurement of the cohesive energy present at an interface between two phases.[16] In a bulk phase, the molecules will be symmetrically surrounded by other equal molecules so that molecular interactions are equal in all directions. At an interface however, the molecules in one phase will come in contact with molecules in the other phase with, for two immiscible liquids, very different properties regarding polarity and intermolecular forces. The molecules at the interface will no longer be symmetrically surrounded by equal molecules causing a net drag force towards the bulk phase.[16] Interactions to the other phase is undesired due to creation of the net force, causing the system to decrease the interfacial area. This fact is the basis for the pendant drop technique used in the work. It utilizes a high-speed camera with a resolution of 512 x 512 pixels and a LED-based background. The setup enables to take images of a small droplet (5 – 10 μL) of one phase dispersed in another (immiscible) phase, with a high accuracy (± 0.15 mN/m or less). The drop is formed upside-down using a U-shaped needle connected to a Hamilton syringe when an oil droplet is formed in an aqueous environment. Where the oil phase is heavier than water or for measurements of the air-water interface (*surface tension*) a straight needle is utilized. A typical setup for the pendant drop technique is shown in figure 6.1.[100]

There is a relationship between the capillary pressure difference sustained across the interface between two static fluids and the interfacial tension given by the Young-Laplace equation:

$$\Delta P = \gamma \left(\frac{1}{R_1} + \frac{1}{R_2} \right) \qquad \text{(IX)}$$

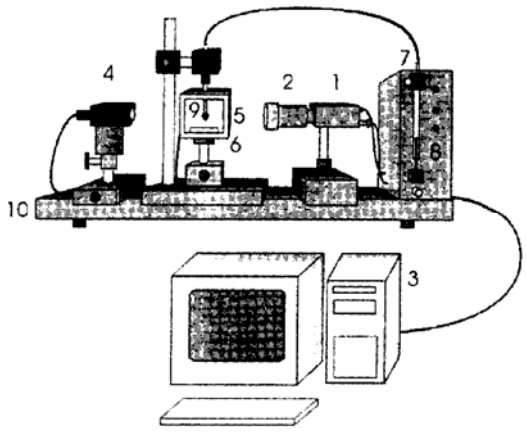

Figure 6.1. Schematic of a pendant drop apparatus, 1 – CCD, 2 – objective, 3 – PC with frame grabber, 4 - light, 5 – measuring cell, 6 – holder, 7 – dosing system, 8 – syringe, 9 – capillary with drop, 10 – optical bench. In this work the automatic dosing system was not installed and the drop was pushed out through a Hamilton syringe.

where ΔP is the pressure difference across the interface, γ is the interfacial tension (IFT) and R_1 and R_2 are the radii of curvature. In the case where gravity is the only force exerted on the system, ΔP is given by

$$\Delta P = \Delta P_0 + (\Delta\rho)gz \qquad \text{(X)}$$

where Δρ is the density difference between the immiscible phases, g is the gravity constant, ΔP_0 is the pressure difference at a selected datum plane and z is the vertical distance between the datum plane and a given point. From equation X one can see that the only information an analyst needs is the densities of the two phases, showing the simplicity of the method to determine the IFT. By combining equation IX and X, introducing dimensionless coordinates and a drop shape factor, the IFT (γ) can be calculated from an image of a droplet. The derivation can *e.g.* be found in the book "Emulsions and emulsion stability".[16]

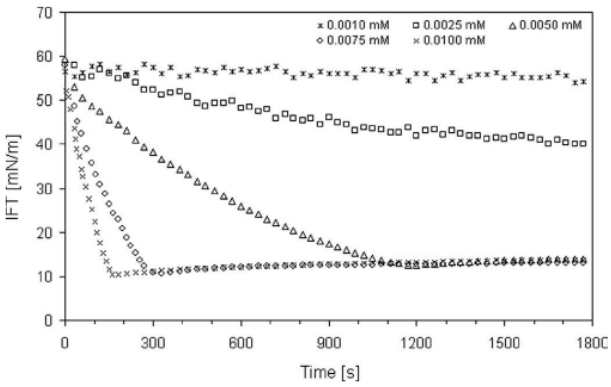

Figure 6.2: Dynamic IFT of indigenous tetraacids at different concentrations.[79]

The pendant drop technique is a *dynamic* interfacial tension technique. Thanks to the high-speed CCD camera, images in the ms range can be obtained, if necessary. Thus, in addition to obtaining equilibrium IFT values, the adsorption or diffusion to the interface can be elucidated to give more information. An example of the IFT as a function of time is given in figure 6.2, where experiments with indigenous tetraacids has been carried out. The lowering of the interfacial tension is due to the tetraacid adsorbing at the interface and thus reducing the Gibbs free energy.

The second method used for determination of surface and interfacial tensions is with the use of a tensiometer and the De Nouy ring probe. The force of the surface is measured, yielding the surface tension, by pulling the ring up from the surface. This is illustrated in figure 6.3.

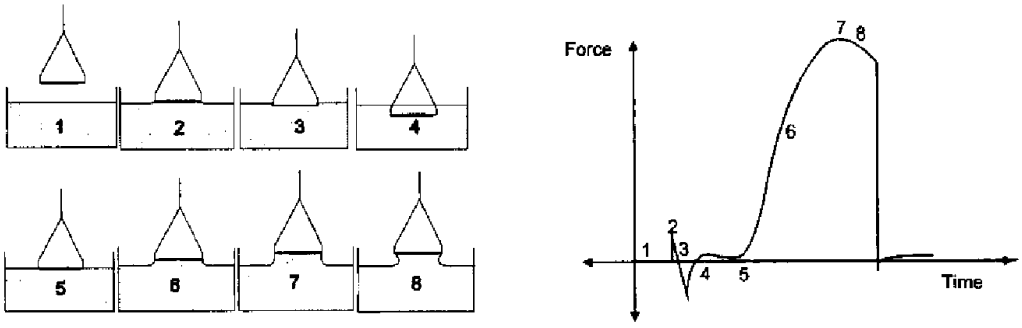

Figure 6.3: Principles of surface tension measurements using the De Nouy ring probe and the obtained force at different stages.

The interfacial tension can be measured correspondly. However, the ring has to be immersed in the aqueous phase before carefully adding the oil phase on top. The tensiometer technique yields more or less the same information as the pendant drop technique, but with a slightly higher resolution, to about 0.01 mN/m. An advantage is that it directly measures the surface force, not indirectly through the image of a droplet. In a pendant drop experiment, the results will depend on the quality of the image and image calibration which occasionally can be challenging. A tensiometer can be coupled to one or more titrators which can be controlled by the tensiometer software. The concentration of the solution can be constantly changed to obtain surface tension as a function of concentration. This is most convenient in determination of a critical micelle concentration, CMC, of an aqueous solution where the aqueous solution is constantly diluted from a starting point above the CMC.

6.2. Langmuir trough technique.

The principle of the Langmuir film balance is much in correspondence with the tensiometer technique in chapter 6.1. In the Langmuir trough technique, the term surface (interfacial) *pressure* (π) is introduced, which is the tension difference towards a *clean* surface. This is given in equation XI.

$$\Pi = \gamma_0 - \gamma \qquad \text{(XI)}$$

where γ_0 is the surface tension in absence of a film and γ the tension of the film-covered surface.[16] A Langmuir film is an insoluble monolayer of a surfactant covering an aqueous solution. The solution is poured in a trough of fixed area and the surfactant is spread on the surface via a small amount of organic solvent, which evaporates. To fully characterize the properties of such films and their phase behaviour, the monolayer film is compressed using motor – controlled barriers moving at a given speed. The surface pressure is constantly monitored with a Wilhelmy plate or a paper probe, acting roughly as the De Nouy ring method. The pressure is plotted as a function of the trough area. If the molecular weight of the surfactant is known, the *mean molecular area (Mma)* is used on the x-axis. Initially, the amount of surfactant spread is adjusted so that they are far away from each other (area > Mma) and do not lower the surface tension to a significant degree. The film is in the *gaseous* phase. During compression however, the surfactants will start to feel each other and form a *liquid* phase which cause the surface *pressure* to increase. Depending on the compressibility of the film the monolayer can behave as liquid expanded or a liquid condensed state, sometimes both phases can be observed. A horizontal break in the curve, or a range where the increase in pressure is low, is indicative of a *phase transition*. These are transitions originating from conformational change of the molecules in the film causing a denser packing of the surface active molecules in the film. At the point where the molecules in the film have reached their optimal packing (the solid state) and no more compression is possible, the monolayer film will break or collapse. A collapse from the solid state can be found as a sudden drop in pressure and collapse from a liquid condensed phase is observed as a horizontal break.

Figure 6.4 (left) shows the setup of Wilhelmy plate, film and barriers and 6.4 (right) give an example of a surface pressure – area isotherm with different phases and phase transitions.

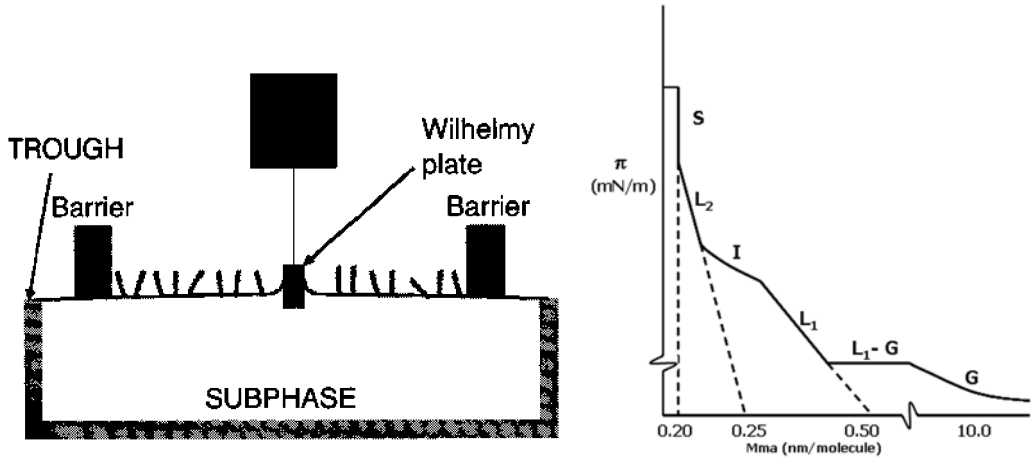

Figure 6.4: Schematic view of the Langmuir technique (left) and an example of a SP – area isotherm including the different phases and phase transitions.

Comparing transitions and phases to the mean molecular area, and correlating to the structure of a surfactant, it is possible to gain information of the conformation or arrangement of a surfactant in a given phase. This has been an issue of focus in papers 2 and 4. Knowing the arrangement of molecules at an interface is very important to explain interfacial behaviour such as emulsion stabilization mechanisms or interactions with both oil – and water soluble components.

Acceptance of high surface pressure (40 – 70 mN/m) before a film collapse is in most cases indicative of a stable film. Another way to investigate the stability of a film is to compress the film to a certain fixed surface pressure, normally in the liquid state, and maintain that pressure over time. A non-stable film, where the instability is due to dissolution into the aqueous phase, conformational changes or formation of multilayers, will cause the barriers to move to smaller trough areas to maintain the fixed pressure. Plotting the loss of area as a function of time provides good indication about the stability of a film.

The Langmuir technique can be combined with a dipper arm to deposit a film onto a solid substrate. This is generally referred to as Langmuir-Blodgett (LB) deposition. The substrate, which can be glass, silica or a hydrophobically modified surface, is placed vertically in the solution. In a common experiment for deposition of one layer, the substrate is immersed in the aqueous phase before spreading the surfactant. At a fixed pressure, the substrate moves upwards so the film is deposited. This is illustrated in figure 6.5. The barriers move inwards to keep the pressure constant. If not, the pressure would drop due to film material lost from the surface. The success of an LB deposition can be illustrated by comparing the loss of

trough area to the dimensions of the substrate, the area of the substrate covered by the film. This comparison is the Transfer ratio, and is equal to 1 for a perfectly transferred monolayer.

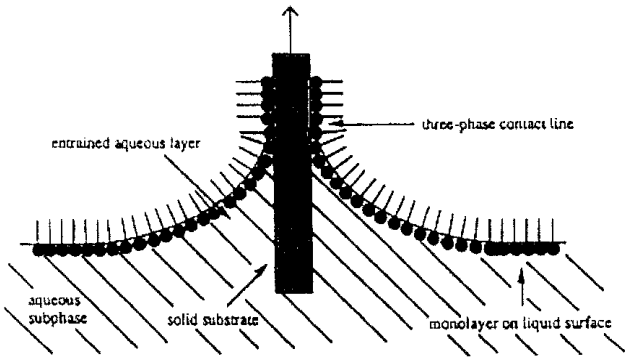

Figure 6.5: Deposition of a monolayer onto a solid substrate. Dipping in the upward direction with a hydrophilic substrate shown as example.

Multilayers can be obtained by consecutive dipping both in the up – and downward direction, and deposition onto a hydrophobic surface requires the substrate to start in the upper position so that the hydrocarbon chains interact with the non-polar substrate. Deposition onto a substrate in the horizontal direction is possible, and this technique is called the Langmuir-Schaeffer (LS) technique. However, hydrophobic or LS deposition has not been carried out in this work. Deposited films can subsequently be investigated spectroscopically or by sensitive microscopy methods such as Scanning Electron Microscopy (SEM) or Atomic Force Microscopy (AFM).

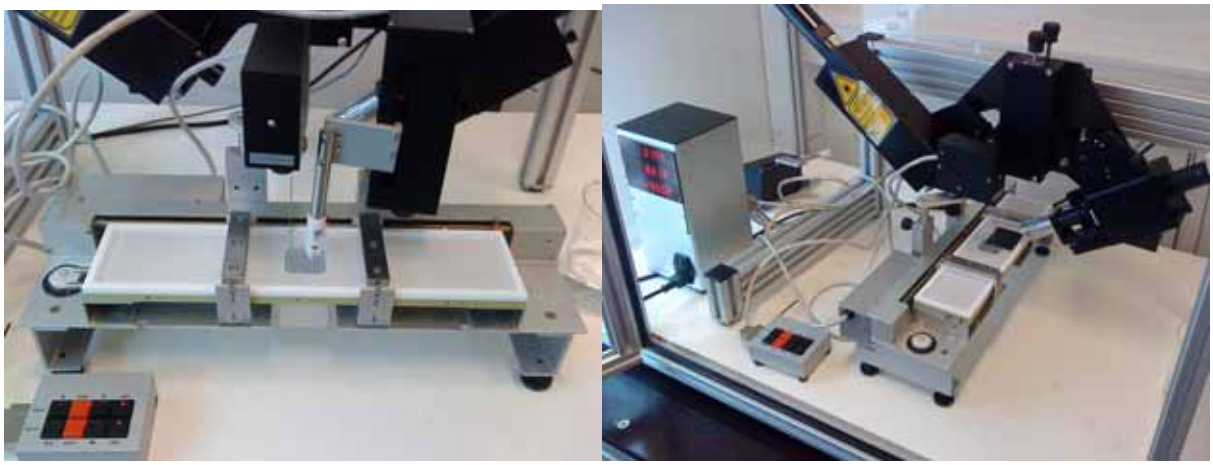

Figure 6.6: Images of the Langmuir trough in use. Shown on the left is the setup with the dipper arm, on the right the instrument is used in combination with BAM.

At Ugelstad Laboratory, the Langmuir trough is combined with a Brewster Angle Microscope. (BAM). BAM is used to visualize the morphology and heterogeneity of the film. This instrument is placed above the trough with a laser directed normal to the trough direction and at the so-called Brewster angle in the z-direction. A standard 10 mW He-Ne laser with a Glan-Thomson polarizer emits *p*-polarized light. To avoid stray light from the surface, a black wedge-shaped plate was placed at the bottom were the laser was pointed. (Figure 6.6, right) A 768 x 494 pixels CCD camera takes images through a 10x magnification and a spatial resolution of ~2 μm. The gaseous phase has a low density in the film and appears dark. At increase surface pressure to the liquid or solid state, the film density increases due to denser packing of the surfactant molecules. Territories of such phases will appear brighter due to more scattering from the film of the incoming light. A picture of the whole setup with trough, dipper arm and BAM is shown in Figure 6.6.

6.3. Fluorescence

Luminescence is the emission of light from any substance and occurs from electronically excited states.[103] This can be divided into two categories – fluorescence and phosphorescence. Fluorescence is the emission from the singlet excited state, where the electron is paired (opposite spin) to the electron in the ground state. Due to intersystem crossing, the spin of the excited state can be changed so that the two electrons have the same spin orientation. When they have the same spin, they are in the triplet excited state.(T_1) Emission from the triplet state is phosphorescence. (Figure 6.7, left) Transitions to the ground state with the same spin are "forbidden" and cause the lifetime of phosphorescence to be orders of magnitude higher than normal fluorescence.

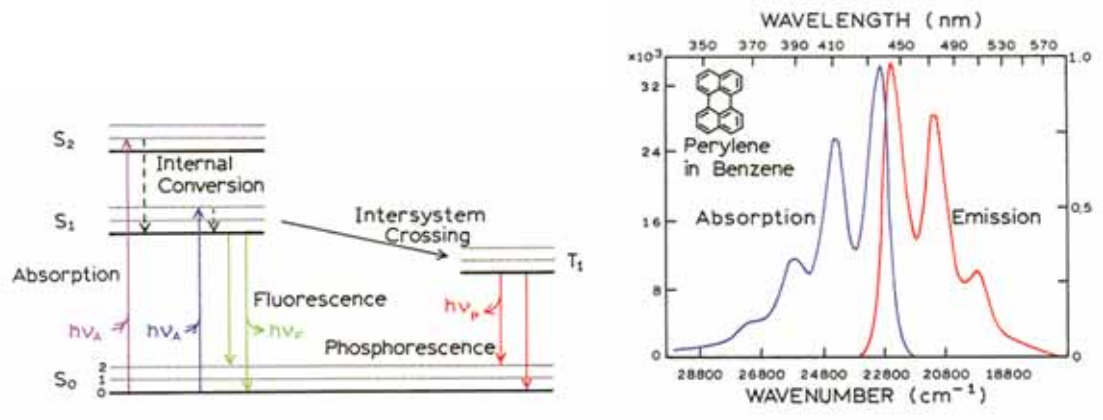

Figure 6.7, left: One type of Jablonski diagram showing the excitation and emission process. Right: Absorption and emission spectra of perylene showing the "mirror" image due to no alteration of the nuclear geometry during excitation.

The emission process can be discussed in terms of a Jablonski diagram, named after Professor Alexander Jablonski.[103] (Figure 6.7, left) The probe is excited by a photon to the excited states; S1-S_n, where n is the number of possible electronic energy state. Molecules in condensed phase rapidly relax to the lowest energy level by internal conversion, to the thermally equilibrated excited state. This process occurs within 10^{-12} s or less. Return to the ground state occurs generally to a higher excited vibrational ground state to further on reach thermal equilibrium. The possibility of emission to different vibrational state is the basis for structured emission spectra, like in perylene. When the electronic excitation does not greatly alter the nuclear geometry, the emission spectrum is a mirror image of the adsorption spectrum. (Figure 6.7, right) For more detailed description of the concept of fluorescence and the electronic behaviour, the author kindly refers to the well-written book by Lakowitch.[103]

Fluorescence typically occurs from aromatic molecules, and there exist thousands of different fluorescence probes (fluorophores) both synthetically and in nature. The excitation and emission properties of a fluorophore are perhaps the most important characteristic. In addition, fluorophores are commonly characterized according to their quantum yield, QY. This is the number of emitted photons relative to the number of adsorbed photons, and is a number between 0 and 1.[103] Processes which lower a fluorophore's QY is termed quenching or non-radiative decays. These processes are transfer of energy to a quencher or a solvent molecule or formation of aggregates, complexes and excimers ("excited dimers"). The fluorescence *lifetime* (τ) is also an important characteristic, which is defined as the average time a molecule spends in the excited state prior to returning to the ground state. The lifetime for fluorescence is typically in the range of 1 – 30 nanoseconds. Quenching will lower the lifetime, but not all non-radiative decays lower the observed lifetime. For example, the lifetime of perylene bisimide excimer (8-33 ns) is longer than the monomer lifetime (4 ns).[104,105]

The instrumentation for measuring fluorescence is with a fluorimeter, and in this work a Horiba Jobin Yvon Fluorolog 3 fluorimeter has been utilized. To obtain an emission spectrum, the instrument utilizes a constant illumination which excites the sample with monochromatic light. The fluorescence is then obtained 90º to the incoming light (Right Angle, RA) or from the same side as the excitation light, but at an angle of 22° to the glass surface. (Front Face Illumination, FF) If the sample has high optical density (OD > 0.1) or display turbidity, RA will not give the actual fluorescence intensity due to self-adsorption or scattering when the fluorescence travel from the centre of the sample to the cuvette glass.[103] Thus, for samples of high OD or turbidity, FF illumination give more correctly results. Emitted photons finally reach the detector, and the intensity is enhanced in a photomultiplier tube. Since an emission spectrum is collected using constant illumination, this is generally termed *Steady-State (SS)* fluorescence.

For lifetime measurements, a different excitation source is used. A light source, either Laser Diodes, Laser Emitting Diodes (LEDs) or dye lasers can send out very short pulses of monochromatic light at a rapid rate. This is an important feature because the lifetime to measure is in the nanosecond range. The detector will also be different, and will only measure photons at one chosen emission wavelength. Lifetime measurements give a decay curve consisting of 1000 – 10000 photons with different lifetimes. By non-linear square fitting of

the intensity of photons with a given lifetime to equation XII, the average lifetime τ can be obtained.

$$I(t) = I_0 \exp^{\left(\frac{-t}{\tau}\right)} \qquad \text{(XII)}$$

Depending on the fluorophore and the environment, the decay can be single – or multiexponential. One fluorophore can display a multiexponential decay if fractions of the fluorophores are experiencing different chemical environments. The concept of two-exponential decays and quenching of SS due to excimer emission has been used in paper 2.

6.4. Nuclear Magnetic Resonance (NMR)

NMR-based techniques have become increasingly popular as a tool to characterize emulsions.[106] The techniques offer several advantages compared to other droplet-size determination techniques, e.g. microscope, Coulter-Counter and light-scattering techniques. NMR is a non-destructive method and a sample can be measured numerous times, an advantage in studies of for example droplet size distribution as a function of time. It can be used on concentrated emulsions and do not need any dilution, which is a typical source of error in microscopy investigation of droplet sizes. In a matter of minutes, all droplets are measured and the droplet size distribution is characterized based on the whole distribution and not only a statistical selection. Clearly, NMR may be the future in the concept of emulsion characterization and stabilization mechanisms.

Before presenting NMR theory used on emulsion, it is worth mentioning the basic principles of NMR. Some nuclei possess a permanent nuclear magnetic moment μ,[107] the most common nucleus for NMR study being the proton, ^{1}H. When placed in an external magnetic field $\mathbf{B_0}$, μ precesses around the direction of $\mathbf{B_0}$ at the Larmor frequency $\omega_0 = \gamma' \cdot B_0$ where γ' is the gyromagnetic ratio[iv], specific for each nuclei.[108] Nuclei with precessing μ is called spins.[106] The ensemble of spins exhibits net magnetization in the direction of $\mathbf{B_0}$. If a radio-frequency (RF) pulse of a second magnetic field $\mathbf{B_1}$, orthogonal to $\mathbf{B_0}$ is applied, the net magnetization is rotated to an extent that depends on the duration of the pulse. The relaxation back to the equilibrium state can be measured from the spins present in the emulsion represented by two relaxation times; measuring in the direction of $\mathbf{B_0}$ give the longitudinal relaxation time T_1 and transverse to it to yield the transverse relaxation time T_2.[106]

For decades, NMR has been widely used to confirm the structures of synthesized organic compounds because the resonance frequency of a nucleus is determined by its molecular properties such as the chemical shift and scalar spin-spin couplings. These are static parameters.[107] NMR as a tool in emulsion technology uses however the dynamic parameters obtained. Dynamic processes on the molecular level influence the spin system by rendering the spin Hamiltonian time dependent. The spin relaxation is characterized by combining the two relaxation times T_1 and T_2. One dynamic process is the transport of molecules due to

[iv] The gyromagnetic ratio commonly used only the symbol γ, but in this thesis is symbolized as γ' to avoid contradiction to the γ used for interfacial tension.

thermal motion, e.g. self-diffusion. In a w/o emulsion droplet, the diffusion and mobility of the water molecules are restricted by the w/o interface. The measured diffusion is dependent on the possible travelling distance and thus the droplet size. This can conveniently be followed by the *pulse field gradient* method, PFG. By using RF-pulses and magnetic field gradients in a NMR-diffusion experiment, there is a dephasing of the net magnetic moment given by

$$\varphi = \gamma' g(z_2 - z_1) \qquad \text{(XIII)}$$

(z_2-z_1) is the distance the protons have moved during the NMR-diffusion experiment. For larger values on the mobility (z_2-z_1), the NMR-signal will decrease because of the dephasing. When assuming a Gaussian distribution of diffusivities and mono-exponential attenuation of the NMR-signal due to relaxation processes, the attenuation of the NMR-signal is written

$$I = I_0 e^{-\frac{t_1}{T_2}} e^{-\frac{t_2}{T_1}} e^{-\gamma'^2 g^2 D \int_0^t (\int_0^{t'} g(t'')dt'')^2 dt'} \qquad \text{(XIV)}$$

where t_1 and t_2 is the duration the NMR signal is influenced by the transversal and longitudinal processes respectively, $g(t'')$ the total magnetic gradient, internal and external, and D the diffusion coefficient. If ξ_i is the volume fraction of the pores with surface to volume ratio $(S/V)_i$, and by assuming piecewise smooth and flat surfaces and that only a small fraction of the particles are sensing the restricting geometries, the restricted diffusion coefficient can be written as

$$\sum_i \xi_i \frac{D_i}{D_0} \approx \sum_i \xi_i \left[1 - \frac{4}{9\sqrt{\pi}} \sqrt{D_0 t} \left(\frac{S}{V}\right)_i\right] = \left(1 - \frac{4}{9\sqrt{\pi}} \sqrt{D_0 t} \overline{\left(\frac{S}{V}\right)}\right) \qquad \text{(XV)}$$

where $D(t)$ is the time dependent diffusion coefficient, D_0 is the unrestricted diffusion coefficient, in bulk fluid, and t is the observation time.[109] Measurements of the early departure from bulk diffusion combined with a linear fit of the experimental data to the square root of time will thus result in a value for the average surface-to-volume ratio $\overline{(S/V)}$. This number can be correlated to the average ($1/T_2$) found from a CPMG experiment and equation XVI can be obtained

$$\rho = \overline{\left(\frac{1}{T_2}\right)} \cdot \overline{\left(\frac{S}{V}\right)}^{-1} \qquad \text{(XVI)}$$

where ρ is the surface relaxivity and is assumed drop size independent. The surface to volume ratio is the droplet size measure and by using the relation ship $T_2 \approx \frac{V}{S\rho}$ and multiplying with the calculated surface relaxivity the distribution is normalized to a droplet size distribution in absolute length scale.

The use of NMR was highly valuable to obtain droplet size distributions in paper 3.

7. Main results.

In this section a summary of the papers will be given with their most important findings and conclusions. The published papers and manuscripts are given as appendices.

7.1. Paper 1

"Model Compounds for Asphaltenes and C_{80} Isoprenoid Tetraacids. Part I: Synthesis and Interfacial Activities."

In paper 1 model compounds for asphaltenes and tetraacids were synthesized. Their structure, molecular weights and abbreviations are given in figure 7.1.

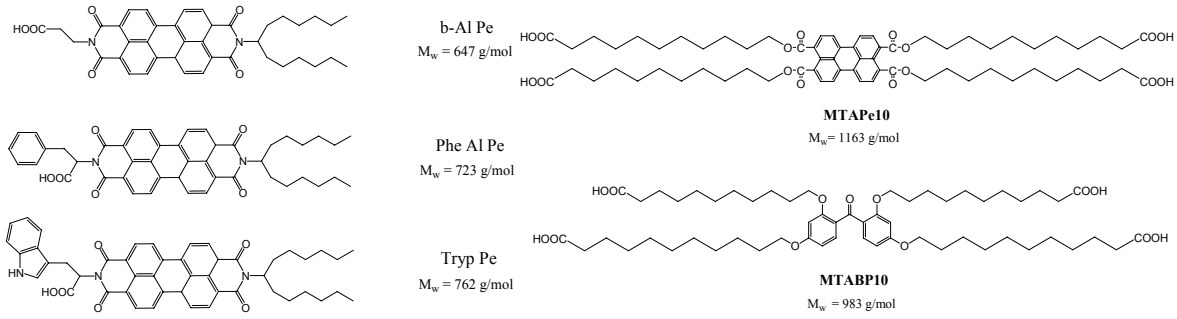

Figure 7.1: Structures and molecular weights of the asphaltene (left) and tetraacid model compounds (right) synthesized and characterized.

To investigate the model compounds resemblance to indigenous surfactants from crude oil, their interfacial behaviour was characterized in terms of interfacial tension. The asphaltene model compounds displayed an interfacial tension between toluene and a buffer pH 9 around 5 mN/m of 12.5 – 35 μM depending on the compound and were considered highly interfacially active (Figure 7.2, left). The interfacial activity increases with increasing pH, indicating that the acidic functions and dissociation of such were determining their interfacial activity.

The solubility behaviour of asphaltene model compounds was investigated by means of titration with *n*-heptane and precipitation onsets estimated by NIR spectroscopy. (Figure 7.2, right) *n*-heptane precipitated the studied model compounds. Addition of acetone (10-20 vol%) to the stock solution shifted the precipitation onset to higher vol% of *n*-heptane, indicating that the precipitation was influenced by both aromatic as well as polar interactions. Nevertheless, the asphaltene model compounds became precipitated upon addition of *n*-heptane showing similar solubility behaviour as real asphaltenes.

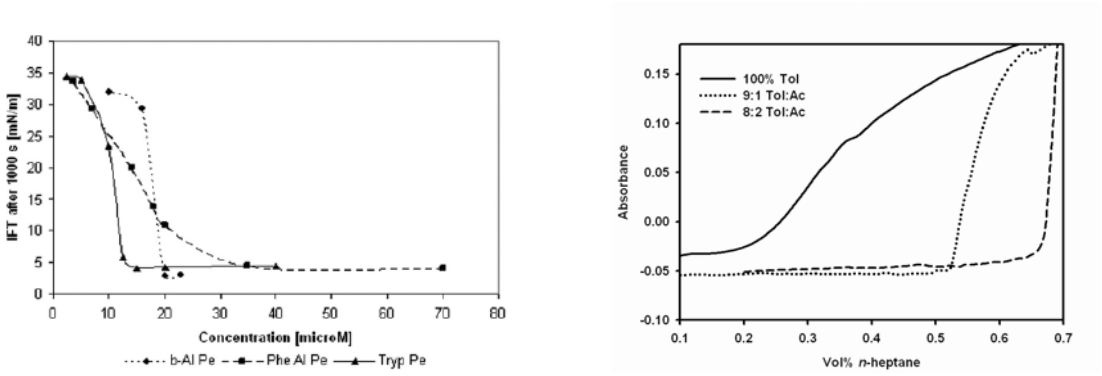

Figure 7.2, left: Plots of IFT as a function of concentration of asphaltene model compounds between toluene and pH 9. Right: Precipitation of Tryp Pe with *n*-heptane and different starting solvent conditions using NIR spectroscopy. Absorbance measured at 10000 cm^{-1}.

The two tetraacid model compounds were investigated in the same way by means of interfacial tension between chloroform and pH 9 aqueous solution because indigenous tetraacids are known to exhibit interfacial activity at ppm values. Similar interfacial behaviour as a function of concentration for both compounds (Figure 7.3) to indigenous tetraacids (Figure 6.2) suggested that the synthesized compounds were promising model compounds for the indigenous tetrameric acids. Synthesis of pure compounds with UV and fluorescence active moieties without the need for chromatographic separation was expected to ease the naphthenate research with respect to the time-consuming isolation of indigenous tetraacids still containing impurities and due to the challenging detection of such tetraacids.

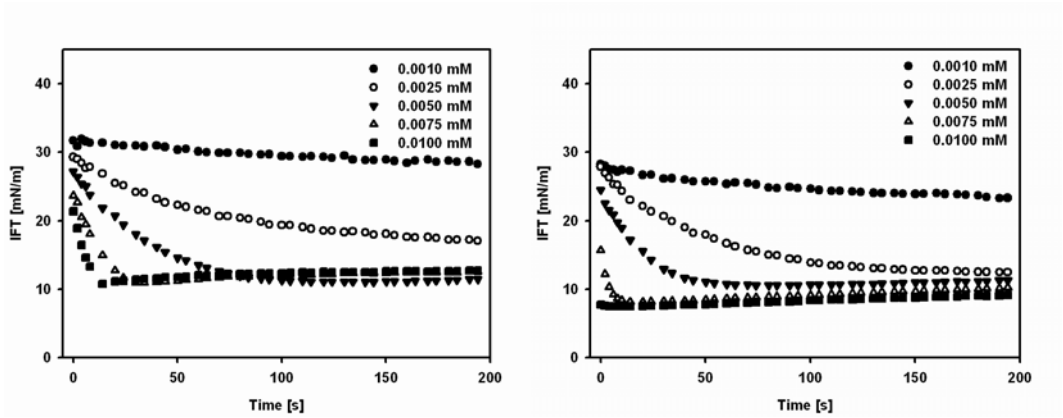

Figure 7.3. Plots of IFT as a function of time at varying concentration for two tetraacid model compounds, MTAPe10 (left) and MTABP10 (right).

Paper 2 states that there were found a non-surface active impurity in PAP (here: Phe Al Pe), yielding incorrect concentrations used in paper 1. This fact illustrates why the drop of Phe Al Pe appeared more gradual than b-Al Pe and Tryp Pe.

7.2. Paper 2

"Langmuir Films of Asphaltene Model Compounds and Their Fluorescent Properties."
The second paper is a continuation of paper 1 regarding the film properties of the asphaltene model compounds. By use of the Langmuir trough with LB deposition and subsequent fluorescence investigation of the deposited film, it was expected to give information to explain the sudden drop of interfacial tension in paper 1.

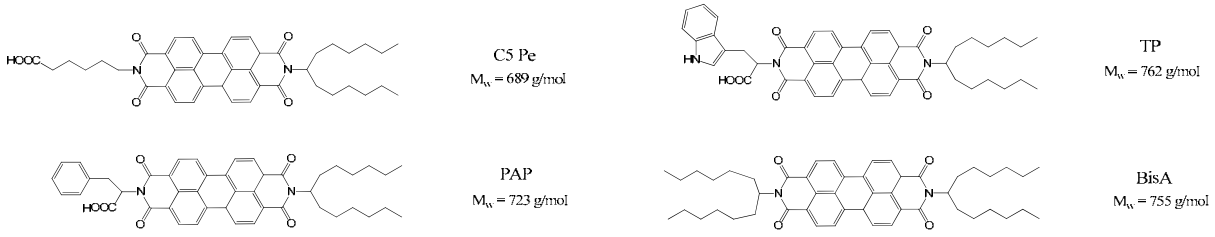

Figure 7.4: Structures, abbreviations and molecular weights of asphaltene model compounds used in paper 2.

Three acidic model compounds were investigated together with a non-acidic analogue (figure 7.4) for comparison to investigate the influence of a strong hydrogen bonding moiety, in this case a carboxylic acid, on the film and interfacial behaviour. Interfacial tension measurements showed a complete absence of interfacial activity in the corresponding concentration range when no acid group was present. Surface pressure – area isotherms and area loss measurements (figure 7.5) were obtained in a Langmuir trough indicating stable films for the acidic compounds, comparable to real asphaltene isotherms. BisA did not form a stable film as evident with a loss of 35% of the trough area after only 500 s. Investigations with BAM (figure 7.6, right) displayed formation of multilayers and crystalline behaviour already at low surface pressure. Images of C5Pe upon compression showed islands of liquid condensed phase converging to a uniform monolayer when the surface pressure increased.

Films deposited with the LB technique in the liquid condensed phase were investigated with SS fluorescence. Spectra showed only presence of the excimer emission indicating a close proximity of the aromatic cores in the films. Together with the mean molecular areas obtained in SP – area isotherms a *head-on* arrangement of the acidic model compounds was proposed. (Figure 7.6, left) This arrangement gives favourable π- π interactions between the aromatic cores yielding an extra stabilization in the 2D surface plane most likely giving highly stable films.

The bulk phase behaviour of the model compounds was investigated by fluorescence lifetime measurements. Presence of a longer average lifetime for the acidic compounds with (an)

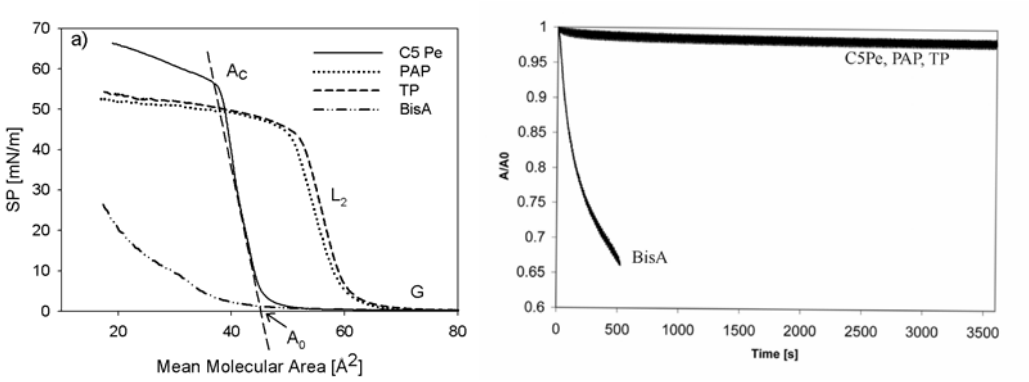

Figure 7.5: a) Surface pressure – area Langmuir isotherms of all four model compounds spread onto ultrapure water of pH 6. b) Film stability of all model compounds measured as the loss in area available in the trough over time at a constant pressure, Π = 20 mN/m.

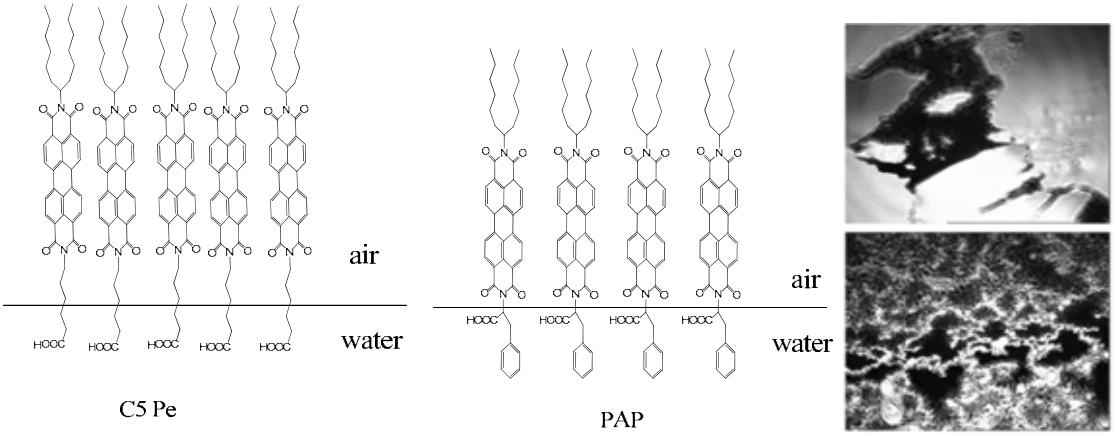

Figure 7.6: Left and middle: Proposed arrangements for acidic model compounds. Right: BAM images of C5Pe (upper) and BisA (lower) in the gaseous state upon compression.

aromatic ring(s) in the head group indicated that these aggregated in toluene at low bulk concentrations. Studying PAP, aggregation increased when the aromaticity of the bulk phase decreased. However, the study showed less interfacial activity when PAP aggregated.
In paper 1 a sudden drop of the interfacial tension was observed. Paper 2 showed that this was most likely due to an efficient packing and islands of surfactants growing until they could cover the whole droplet, causing aromatic interactions in the interface plane and a 2D stabilization. It was shown that the monomers and not aggregates gave interfacial activity. Finally, the profound impact of an acidic function in such molecules was evident, and suggested that acidic subfractions of asphaltene could be a problematic subfraction responsible for stable water-in-oil emulsions.

7.3. Paper 3

"Behaviour of Asphaltene Model Compounds at W/O Interfaces."

Studying emulsion behaviour stabilized by crude oil fraction is a challenging task due to the fact that the actual composition and concentrations are in most cases perceived. Paper 3 study the emulsion and adsorption behaviour of two asphaltene model compounds. Using single molecular systems with known characteristics opens up for investigating emulsion behaviour as a function of true, rather than perceived concentrations.

A modified PFG NMR method with a pulse-length correction was used to determine droplet size distributions of emulsions prepared with C5Pe and PAP in xylene and a pH 8 buffer. The surfactant concentration was kept constant with varying water cut (WC). The mean volumetric droplet diameter of C5Pe is given in figure 7.7 (left) and compared to values obtained with the standard microscopy method.

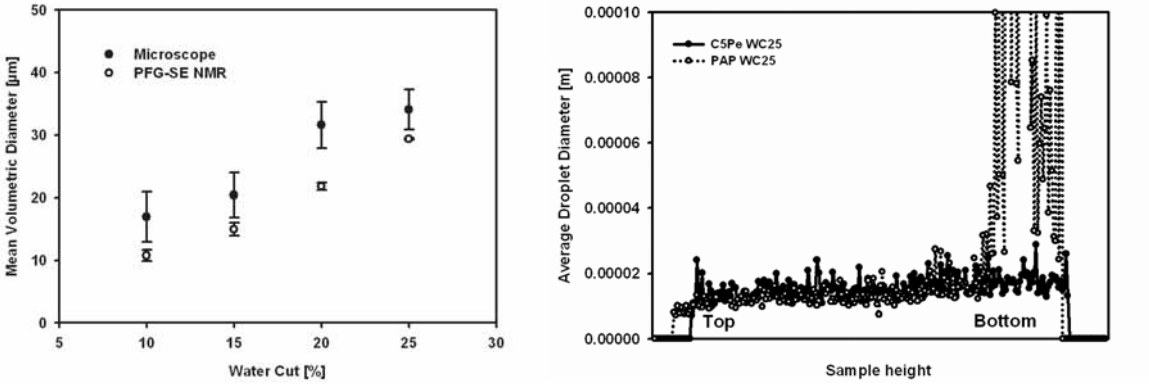

Figure 7.7, left: Mean volumetric diameter of C5Pe emulsions. Right: Mean droplet size as a function of height.

The average droplet diameter as a function of height showed that while C5Pe displayed high emulsion stability, emulsion with PAP developed free water at the highest WC. A difference in stability was also confirmed when the total mean droplet diameter of C5Pe and PAP at WC 15 and 25 was investigated over 6-10 hours. Emulsion prepared with BisA (non-acidic) separated immediately.

Adsorption of C5Pe, PAP and BisA from toluene onto hydrophilic silica was carried out as a way to model the adsorption onto a "water" surface with a known surface area. C5Pe and PAP displayed Langmuir Type I isotherms, while BisA did not adsorb. (Figure 7.8, right) C5Pe was calculated to have a significantly higher affinity for the interface and a higher adsorbed

amount. From the adsorption data the mean molecular area could be obtained. This was compared to a calculation of the Mma from the surface-to-volume ratio found by NMR combined with UV depletion. (Figure 7.8, left)

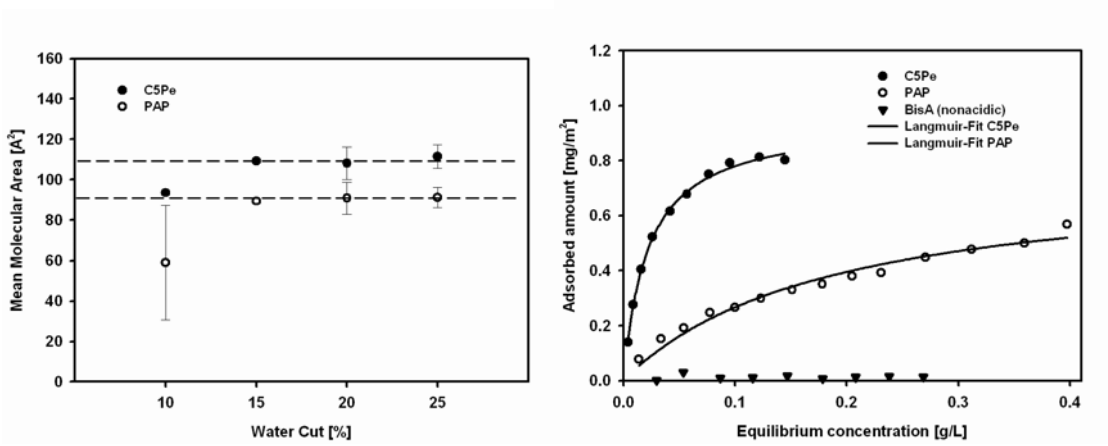

Figure 7.8, left: Mean molecular area in Å^2 calculated from the surface-to-volume datas from NMR. Right: Adsorption of asphaltene model compounds onto hydrophilic silica (Aerosil 150)

The results showed similar areas between the two techniques for C5Pe, in the range 110 – 120 Å^2, but deviations for PAP. The instability and evolution of free water was proposed as the reason behind the observation that no conclusions could be made for PAP. The mean molecular area of C5Pe suggested an arrangement much similar to the *head-on* arrangement from paper 2, but with a tilt of the aromatic core.

Compression of C5Pe and PAP in a liquid – liquid Langmuir interfacial trough showed that C5Pe displayed a phase transition enabling a closer packing and higher surface pressure before collapse. The higher emulsifying power of C5Pe compared to PAP was correlated to a more efficient packing of C5Pe with increasing intermolecular π- π interactions giving a higher stability of the interfacial film.

A model compound without the acidic function did not adsorb or stabilize emulsions at all, showing the extreme influence such a strong hydrogen bonding group can have on the behaviour at oil-water interfaces. The study shows that acidic, or similar hydrogen bonding groups, present in an asphaltene structure is greatly increasing its power to stabilize water-in-crude oil emulsions and support the conclusions from paper 2 that one such subfraction which authors have addressed as a "surface active asphaltene fraction" most likely contains acidic functions or similar strong hydrogen bonding groups.

7.4. Paper 4

"Model Compounds for C_{80} Isoprenoid Tetraacids. Part II: Interfacial Reactions, Physicochemical Properties and Comparison with Indigenous Tetraacids."

In paper 4 a screening of the physicochemical properties of the tetraacid model compounds was carried out to compare with the known properties of indigenous tetraacids. The goal was to elucidate to what extent the model compounds could reflect all aspects of the properties of indigenous tetraacids. Aqueous behaviour was studied by determining CMC of two model compounds, BP10 and Pe10 in addition to an indigenous TA sample.(Figure 7.9, left) The two model compounds had CMC values in the same order or magnitude (10^{-4} M) as the indigenous TA, somewhat lower in exact values. The lower CMC value, especially for BP10 was described as the more linear structure of the hydrocarbon chains of BP10 compared to the high degree of branching in indigenous TA.

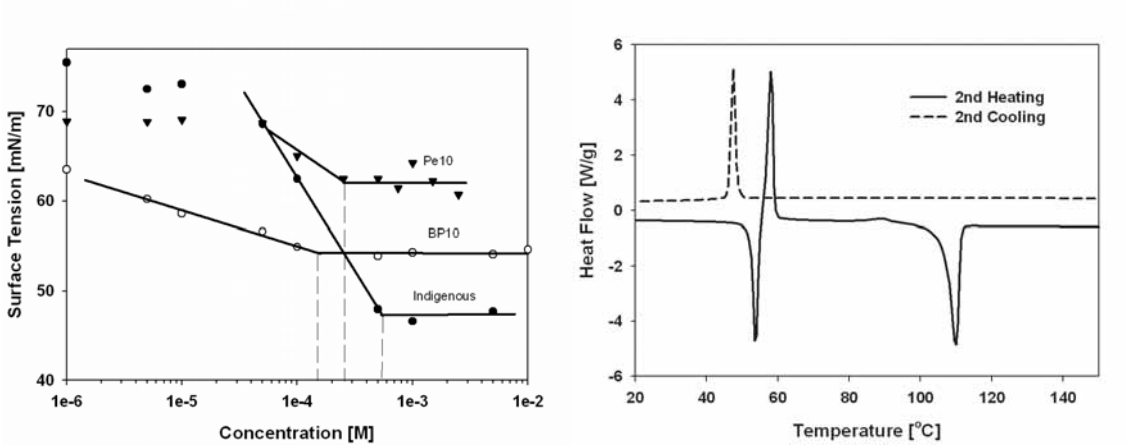

Figure 7.9, Left: Surface tension versus concentration plots obtained for model and indigenous TA with the pendant drop technique. Right: DSC thermogram of BP10 in the acid form.

Indigenous TA displays glass transitions, T_g, in thermal properties of the solid state. BP10 on the other hand, displayed only crystalline transitions, indicating the presence of a liquid crystalline mesophase at intermediate temperatures. (Figure 7.9, right) The formation of the mesophase was attributed to melting of the hydrocarbon chains, rendering the whole molecule more flexible. Surface pressure – area isotherms of both BP10 (fig. 7.10) and Pe10 showed a phase transition at low to medium pH, which is attributed to the flipping mechanism, observed for indigenous TA. At high pH with Ca^{2+} present in the subphase, the film stability increased as seen by the higher surface collapse pressure (fig. 7.10, upper right) and for BP10 with the presence of a visual gel-like film in the trough, comparable to studies on indigenous TA. Partially protonated tetraacid to form a charged 1:1 complex or influence from the

aromatic core could be reasons behind the low stability at pH 9.2. BAM images during compression of BP10 at pH 5.8 supported the flipping mechanism due to formation and growing of spherical domains in the monolayer during the phase transition. As evident from the Langmuir trough experiments, BP10 was the model compounds showing most similarities to indigenous TA and was able to form the cross-linked network with calcium, a crucial key towards formation of naphthenate deposits during crude oil processing.

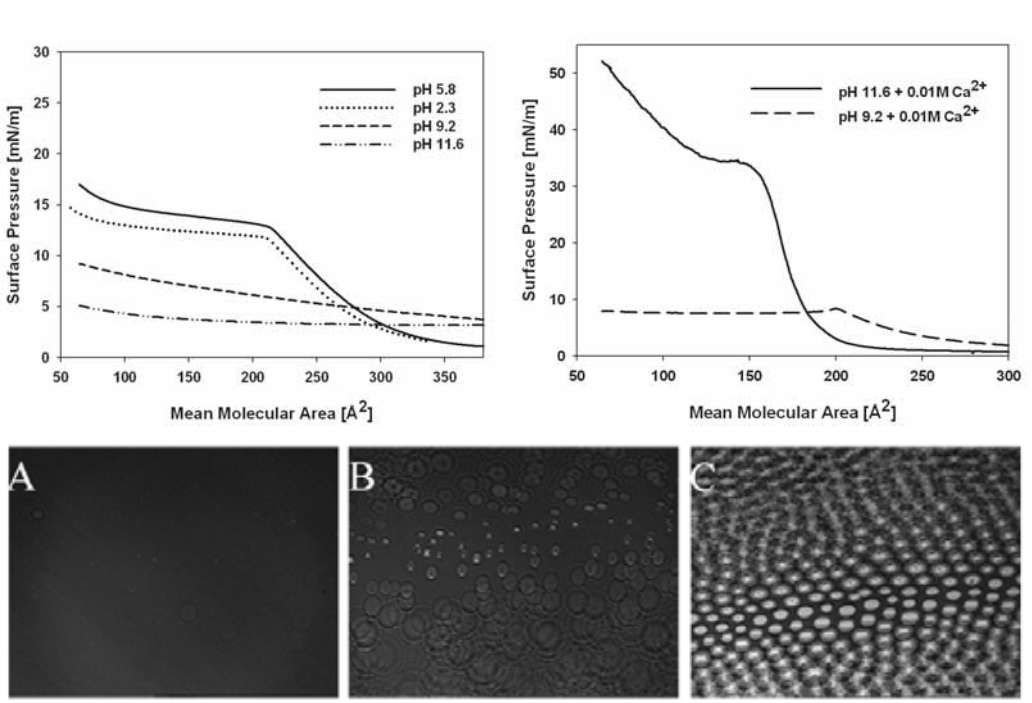

Figure 7.10, upper left: Surface pressure – area isotherm for BP10 at different pH. Upper right: Surface pressure – area isotherm for BP10 under basic conditions and Ca^{2+} in the subphase. Lower images A, B, C: BAM images of BP10 monolayer upon compression at (A) 9.2 mN/m, (B) 10.8 mN/m and (C) 12.6 mN/m.

Interfacial reactions between BP10 and different divalent cations (Ca^{2+}, Mg^{2+}, Br^{2+}, Sr^{2+}) was carried out using the pendant drop technique to investigate any evidence of selectivity upon film formation. All four divalent cations could form the interfacial film with BP10 evident from increase in IFT and images taken during manually contracting/expanding the droplets. However, the film formation was dependent upon the molar ratio M^{2+} / TA and thus the concentration of M^{2+}. More interfacially active complexes were formed at intermediate cation concentrations. Comparing the model compounds and indigenous TA, the main deviations were in the solid state, because BP10 only displayed crystalline transitions. The study however concluded that they are promising compounds, due to similarities in several physicochemical properties. Especially BP10 showed to be a promising compound to use in naphthenate research as the cross-linked gel-like film was observed.

7.5. Paper 5

"Potentiometric Titrations of Five Synthetic Tetraacids as Models for Indigenous C_{80} Tetraacids."

In paper 5 the acid/base behaviour of tetrameric acids was investigated by the use of high-precision potentiometric titration and correlated to the micellization of tetraacids. A series of tetraacids with one to ten methylene groups in the alkyl chains giving BP1 – BP10 was synthesized and studied (Figure 7.11) at different salinities, 20 – 600 mM NaCl. The results were modelled in terms of speciation, thermodynamic equilibrium models, titration of tetraacids when present in a micelle exhibiting a surface charge and monolayer acidity constants.

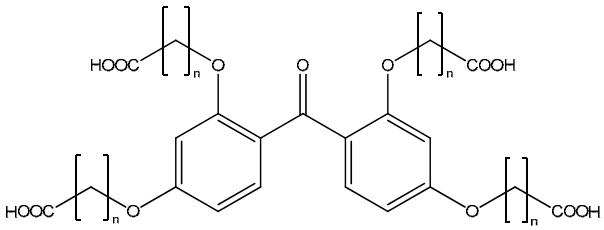

n = 1, 3, 5, 7, 10 => BP1, BP3, BP5, BP7, BP10

Figure 7.11. Structure of tetrameric acids used in the study. *n* denotes the number of methylene groups. Molecular weigths: BP1: 478 g/mol, BP3: 591 g/mol, BP5: 703 g/mol, BP7: 815 g/mol, BP10: 983 g/mol

The most hydrophilic tetraacids BP1 and BP3 displayed aqueous dissociation behaviour with separated dissociation step and was successfully modelled by common aquatic acid-base equilibriums. At medium chain length, as in BP5, only one dissociation step was observed releasing all four protons simultaneously. It was proposed that the carboxylic groups in BP1 and BP3 are in close proximity and a deprotonation of one group would affect the other through space and inductive effects. For BP5 and above however, the chain lengths became too extended for an acid group to feel the deprotonation of a neighbouring group. The titration curves for BP10 and BP7 above the CMC showed a completely different behaviour with a hysteresis effect depending on the direction of titration and more influence of the ionic strength. Titration of BP7 above the CMC and BP10 is given in figure 7.12, left.

CMC data and Corrin-Harkins plots were obtained for BP5 – BP10 (Figure 7.12, right) and showed that at the concentration range used in the titrations deprotonation of the monomeric form in the case of BP5 and on a micellar system for BP10 occurred. The "Δp*K*a" observed could be related to the surface charge density of the micelle, and thus the environment of the

acid group of BP10 caused the p*K*a to increase. All tetraacids were present as dispersed solids in the fully protonated form. Titrations from alkaline conditions with HCl, protonated BP10 present in micelles and the hysteresis effect was explained by a solubilisation of the fully or partly protonated species in the micellar environment until breakdown of the micelle.

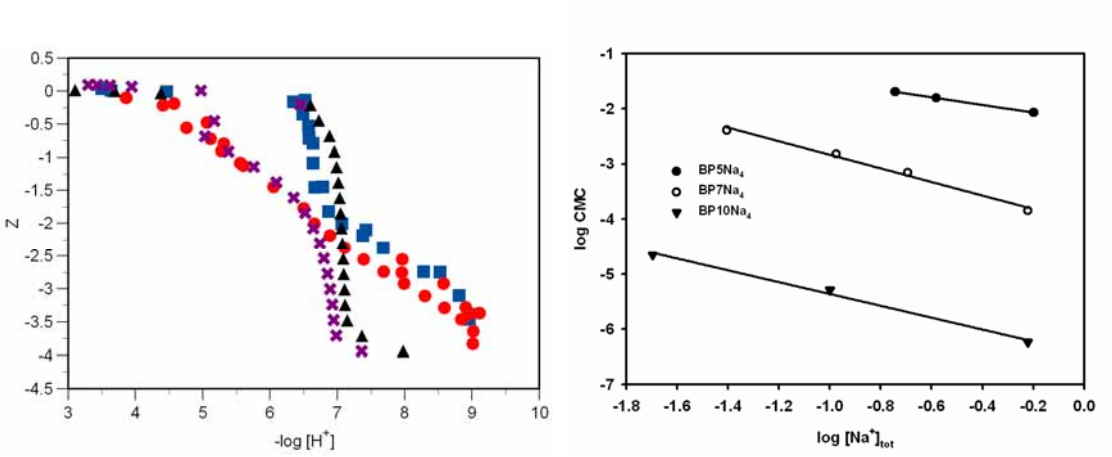

Figure 7.12. Left: Comparison between titration data recorded for, ■, dissolution and, ●, precipitation of BP10, and ▲, dissolution and, x, precipitation of BP7. Right: Corrin-Harkins plot of log CMC as a function of log total Na^+ concentration for BP5 – BP10.

Using the intrinsic p*K*a for BP5 and assuming the same intrinsic p*K*a for BP10 at infinite dilution, the titration curve for BP10 can be modelled in terms of surface charge densities and assumed micellar geometries. The modelling showed in fact an increase of the aggregation number from around 60 to 102 from $-4 \approx Z \approx -2$ to $-2 \approx Z = 0$. (Fig 7.13) However, it was emphasized that one should be careful to accept the modelling and a comparison to experimental data for aggregation number and micellar geometry is needed in the future.

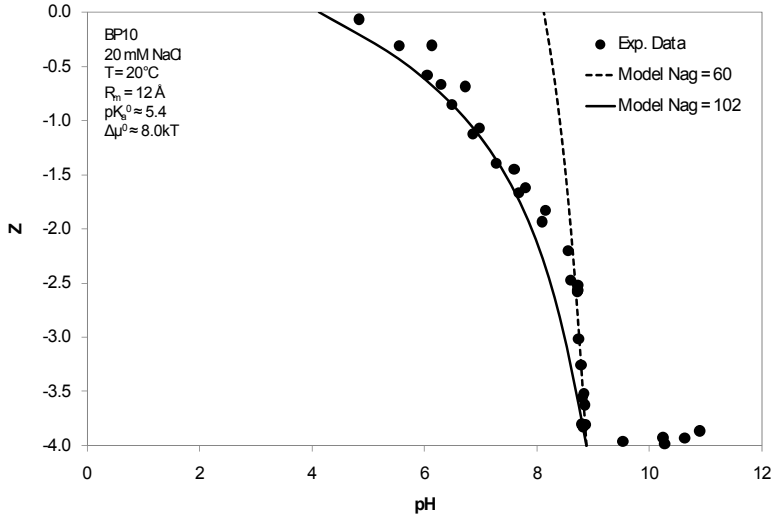

Figure 7.13. Comparison of the experimentally measured back-titration curve for BP10 to the theoretical prediction.

7.6. Paper 6

"Methods to Study Naphthenate Formation in W/O Emulsions by the use of a Tetraacid Model Compound."

The focus in paper 6 was directed towards use of BP10 to study the reaction with calcium in emulsified systems. Two systems were developed depending on the concentration range of species and stirring methodology. The goal was to find a suitable method to investigate the interfacial reaction between tetraacid and calcium under emulsified conditions and correlate to the available interfacial area. In addition, commercially available inhibitor blends were added to study their efficiency towards naphthenate precipitation of the model TA.

Tetrameric acids do not form stable water-in-oil emulsions alone due to their propensity to form oil-in-water emulsions. Thus, a co-surfactant was needed in order to invert to emulsion to w/o. In system 1, Span 60 was added as co-surfactant. Reactions with calcium were studied as depletion of the TA from the bulk phase, determined spectrometrically. The influence on the depletion by inhibitors is shown in figure 7.14. Inhibitor C lowers the depletion, thus retaining more of the TA in the oil phase. The influence of a monoacid (MA), lauric acid, was investigated in the same system, given in Table 5. At the higher concentration of the MA, a lowering of the TA was seen, indicative of a competitive adsorption at the interface. However, Table 5 also shows that during reaction with inhibitor C, the pH of the water phase displayed a significant drop. Thus, the efficiency of inhibitor C in system 1 was attributed to a lowering of the pH.

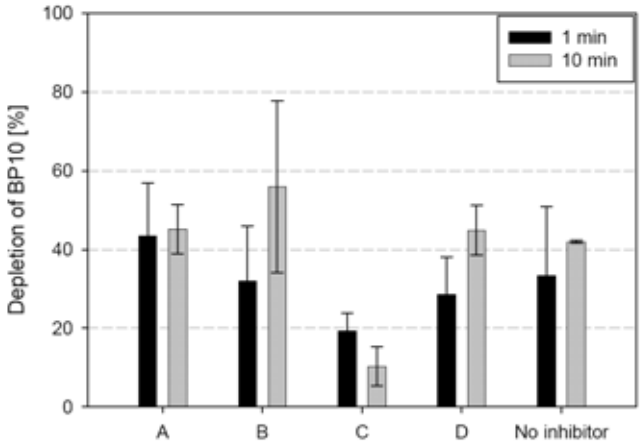

Figure 7.14: Depletion of BP10 in systems with inhibitors A-D (1.0 mM BP10, 0.5 wt% Span 60 and 1 000 ppm inhibitor in toluene, 20 mM $CaCl_2$ in buffer pH 7.5, 70 ^{0}C, WC 10, total volume 40 mL, 300 rpm magnet stirring)

To have more realistic conditions concerning the concentration of all species and to have a better pH control, system 2 was developed with a lowering of concentration of all species. The co-surfactant was C5Pe, one of the model asphaltenes. To gain higher signal-to-noise in the concentration determination, a normal phase HPLC-UV method was developed.

Table 5: % Depletion of BP10 from oil phase at varying additive conditions

Concentration MA (mM)	**0**	**8**		**40**	
Concentration inhibitor C (ppm)	1 000	250	1 000	250	1 000
After 1 min	18.8	41 ± 3	15 ± 3	27 ± 3	7 ± 2
After 10 min	16.5	39 ± 3	2 ± 1	28 ± 5	> 1
pH after 10 min	5.2	6.2 ± 0.2	4.4 ± 0.1	6.3 ± 0.1	4.8 ± 0.3

Figure 7.15 (left) show the results at a mixing speed of 600 rpm using a mechanical stirrer. To the right is shown the same concentration system but with no emulsification.

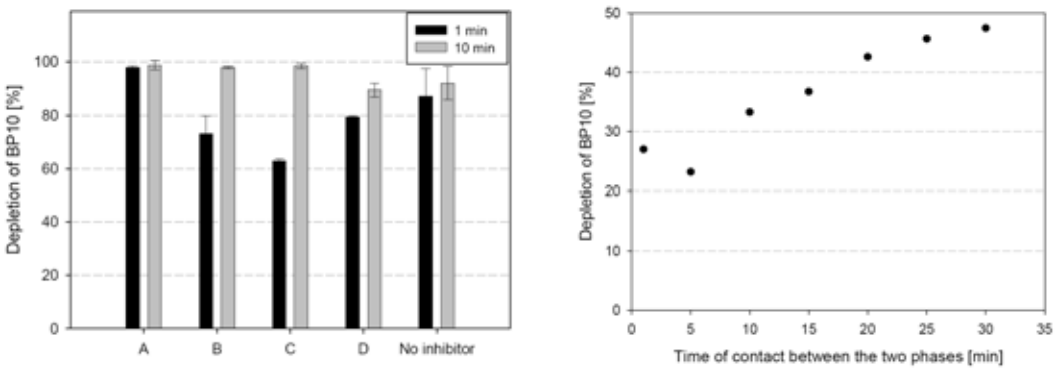

Figure 7.15, left: Depletion of BP10 in systems with inhibitor A-D (0.015 mM BP10, 0.1 mM C5Pe and 50 ppm of inhibitor in toluene, 3.5 wt% NaCl and 20 mM $CaCl_2$ in buffer pH 8, room temperature, WC 5, total volume 80 mL, 600 rpm). Right: Same system, but no emulsification. 40 mL of each phase in a beaker with gentle magnetic stirring.

No significant drop in the pH was observed during reaction in system 2. Inhibitors B and C show efficiency the first minute upon contact, with C depleting the most. Comparing to fig. 7.15 right, less than 50% depletion was observed after 30 minutes of contact. This comparison illustrates the extreme importance that available interfacial area has on such interfacial reactions. In an emulsified system the area increases by several orders of magnitude, highly accelerating the reaction. Comparing the two systems, the low concentration system 2 is closer to real conditions and is thus the most realistic one. However, great caution must be taken in the choice of energy input to the system. In both systems, inhibitor C displayed the highest efficiency towards naphthenate formation.

7.7. General conclusions and future work

The composition of crude oil and the macroscopic phase behaviour as a function of molecular interactions has been, and still is, an issue of great concern and focus. To be able to deal with potential problems and challenges in oil-water systems it is essential to understand how they arise and why they occur. Crude oils may behave differently towards each other due to compositional variations creating confusion in the aim for a general understanding of oil-water systems.

One approach to address this issue is the use of model molecules specified for problematic fractions of the crude oil. To the author's knowledge, this thesis presents the first thorough investigation of model compounds for asphaltenes and tetrameric acids directed towards interfacial behaviour and interface characterization. A long-term goal is to use these simple, defined systems to understand the problems caused by indigenous surfactants. The work presented in this thesis makes use of such model compounds throughout the whole sequence, from developing the molecules by organic syntheses to characterization and interfacial behaviour (in processes similar to those experienced in crude oil/water mixtures). Asphaltene model compounds were prepared as polyaromatic surfactants within the solubility definition of an asphaltene and were characterized and studied in papers 1, 2 and 3. Incorporating an acidic function enhanced their interfacial activity significantly and such compounds were able to form stable air-water and oil-water films resulting from an efficient molecular packing. On a macroscopic level this resulted in the formation of stable water-in-oil emulsions and adsorption onto a polar surface. Absence of such strong hydrogen bonding groups completely changed the behaviour, as no interfacial activity and no stable emulsions were observed. The results support the proposal by other research groups that only a subfraction of the asphaltenes may be responsible for flow assurance and emulsion issues. This study indicates that this fraction might contain acidic or similar hydrogen bonding groups. Regarding the aggregation behaviour, the studies show that it is the monomers of these model compounds and not the aggregates which are interfacially active.

In numerous oilfields tetrameric acids are found to form naphthenate deposits upon selective reaction with calcium. Formation of a cross-linked gel-like network causes accumulation of these calcium naphthenates in topside facilities. However, the isolation, purification and

characterization of such indigenous tetraacids is a challenging task. The need for simple, promising model compounds to represent these acids is obvious. Synthesis and characterization of such model compounds has been presented in papers 1 and 4. One of the model compounds, BP10, could mimic the cross-linked network formation with divalent cations, a crucial key towards naphthenate formation and showed several similarities in physicochemical properties. The main deviation was found in the solid state due to the more linear structure of BP10. A series of tetrameric acids was studied in paper 5 using potentiometric titrations to find the dissociation behaviour of such acids. When in a monomeric state, only one dissociation step around pH 6-7 was seen for chain length > 3. Titrations of the micellar system of BP10 caused a shift of the apparent pKa and hysteresis effects. This could be modelled in terms of surface charge densities and assumed micellar geometries. Finally, reactions in emulsified systems were carried out in paper 6 with BP10 demonstrating the great influence of available reaction area towards the amount of BP10 depleted from the oil phase. The systems investigated could be used to study inhibitor efficiency and influence of monoacid present.

In the future, the tetraacid model compounds are valuable in terms of conducting a mapping of the aqueous phase behaviour, such as aggregation number, micelle size/structure and formation of liquid crystals. The information gained could support dissociation and partitioning data and a mechanistic approach towards naphthenate precipitation is an obvious goal. This new class of long-chained tetrameric acids could act as building blocks for vesicle formation and thus for investigation of the use in gene transport. Other possibilities are cation complexation probes or as UV-active building cores in dendrimers. From an industrial point of view, the model compounds are a promising alternative to indigenous tetraacids when it comes to studying naphthenate formation, reactivity and selectivity.

An interesting approach for the asphaltene model compounds is their use in mixtures with resin fractions, or an isolated basic asphaltene fraction. The latter could indicate whether acid-base interactions at neutral pH promote interfacial activity. Assuming acids (and bases) in asphaltenes are responsible for stable emulsions, a fractionation of asphaltenes based on pH or polarity could be an alternative to the common SARA fractionation to predict if flow assurance problems of a new oilfield can occur.

References

(1) Speight, J. G. *The Chemistry and Technology of Petroleum*; 4th ed.; Taylor & Francis: Boca Raton, 2007.

(2) Johnsen, H. R.; Crawford, P. M. *Strategic Significance of America's Oil Shale Resource*, *1: Assesment of Strategic Issues*, Energy, D. o.,Bunger, James W.

(3) Witze, A. *Nature* **2007**, *445*, 14-17.

(4) Curbelo, F. D. S.; Neto, E. L. B.; Dutra, T. V.; Dantas, T. N. C.; Garnica, A. I. C. *Pet. Sci. Technol.* **2008**, *26*, 77 - 90.

(5) *US Geological Survey World Petroleum Assessment*, Interior, U. D. o. t.,2000

(6) Fossen, M. *Aggregation, Interfacial Properties and Structural Characteristics of Asphaltene Solubility Fractions* PhD, NTNU, 2007.

(7) Jewell, D. M.; Weber, J. H.; Bunger, J. W.; Plancher, H.; Latham, D. R. *Anal. Chem.* **1972**, *44*, 1391-5.

(8) Hannisdal, A.; Hemmingsen, P. V.; Sjöblom, J. *Ind. Eng. Chem. Res.* **2005**, *44*, 1349-1357.

(9) Klein, G. C.; Angstrom, A.; Rodgers, R. P.; Marshall, A. G. *Energy Fuels* **2006**, *20*, 668-672.

(10) Hannisdal, A.; Hemmingsen, P. V.; Silset, A.; Sjöblom, J. *J. Dispersion Sci. Technol.* **2007**, *28*, 639 - 652.

(11) Hannisdal, A.; Orr, R.; Sjöblom, J. *J. Dispersion Sci. Technol.* **2007**, *28*, 81 - 93.

(12) Kharrat, A. M.; Zacharia, J.; Cherian, V. J.; Anyatonwu, A. *Energy Fuels* **2007**, *21*, 3618-3621.

(13) Castro, L. V.; Vazquez, F. *Energy Fuels* **2009**, *23*, 1603-1609.

(14) Silset, A. *Emulsions (w/o and o/w) of Heavy Crude Oils. Characterization, Stabilization, Destabilization and Produced Water Quality.* PhD, NTNU, 2008.

(15) Mansoori, G. A.; Vazquez, D.; Shariaty-Niassar, M. *J. Pet. Sci. Eng.* **2007**, *58*, 375-390.

(16) Sjöblom, J.; Øye, G.; Glomm, W. R.; Hannisdal, A.; Knag, M.; Brandal, Ø.; Ese, M.-H.; Hemmingsen, P. V.; Havre, T. E.; Oschmann, H.-J.; Kallevik, H. In *Emulsions and Emulsion stability*; 2nd ed.; Sjöblom, J., Ed.; Taylor & Francis: Boca Raton, 2006; Vol. 132, p 415-471.

(17) Dudásová, D.; Simon, S.; Hemmingsen, P. V.; Sjöblom, J. *Colloids Surf., A* **2008**, *317*, 1-9.

(18) Dudasova, D.; Silset, A.; Sjöblom, J. *J. Dispersion Sci. Technol.* **2008**, *29*, 139 - 146.

(19) Dudásová, D.; Flåten, G. R.; Sjöblom, J.; Øye, G. *Colloids Surf., A* **2009**, *335*, 62-72.

(20) Wattana, P.; Fogler, H. S.; Yen, A.; Carmen Garcia, M. D.; Carbognani, L. *Energy Fuels* **2005**, *19*, 101-110.

(21) Nalwaya, V.; Tantayakom, V.; Piumsomboon, P.; Fogler, S. *Ind. Eng. Chem. Res.* **1999**, *38*, 964-972.

(22) Merdrignac, I.; Espinat, D. *Oil & Gas Science and Technology - Revue de l'IFP* **2007**, *62*, 7-32.

(23) Kirkwood, K. M.; Ebert, S.; Foght, J. M.; Fedorak, P. M.; Gray, M. R. *J. Appl. Microbiol.* **2005**, *99*, 1444-1454.

(24) Kaminski, T. J.; Fogler, H. S.; Wolf, N.; Wattana, P.; Mairal, A. *Energy Fuels* **2000**, *14*, 25-30.

(25) Andreatta, G.; Bostrom, N.; Mullins, O. C. *Langmuir* **2005**, *21*, 2728-2736.

(26) Groenzin, H.; Mullins, O. C. *Energy Fuels* **2000**, *14*, 677-684.

(27) Martínez-Haya, B.; Hortal, A. R.; Hurtado, P.; Lobato, M. D.; Pedrosa, J. M. *J. Mass Spectrom.* **2007**, *42*, 701-713.

(28) Schneider, M. H.; Andrews, A. B.; Mitra-Kirtley, S.; Mullins, O. C. *Energy Fuels* **2007**, *21*, 2875-2882.

(29) Kuznicki, T.; Masliyah, J. H.; Bhattacharjee, S. *Energy Fuels* **2008**, *22*, 2379-2389.

(30) Rogel, E. *Langmuir* **2002**, *18*, 1928-1937.

(31) Gawrys, K. L.; Spiecker, P. M.; Kilpatrick, P. K. *Pet. Sci. Technol.* **2003**, *21*, 461 - 489.

(32) Sheremata, J. M.; Gray, M. R.; Dettman, H. D.; McCaffrey, W. C. *Energy Fuels* **2004**, *18*, 1377-1384.

(33) Aske, N.; Kallevik, H.; Johnsen, E. E.; Sjöblom, J. *Energy Fuels* **2002**, *16*, 1287-1295.

(34) Trejo, F.; Centeno, G.; Ancheyta, J. *Fuel* **2004**, *83*, 2169-2175.

(35) Hannisdal, A.; Ese, M.-H.; Hemmingsen, P. V.; Sjöblom, J. *Colloids Surf., A* **2006**, *276*, 45-58.

(36) Fossen, M.; Kallevik, H.; Knudsen, K. D.; Sjöblom, J. *Energy Fuels* **2007**, *21*, 1030-1037.

(37) Fossen, M.; Sjöblom, J.; Kallevik, H.; Jakobsson, J. *J. Dispersion Sci. Technol.* **2007**, *28*, 193 - 197.

(38) Zeng, H.; Song, Y.-Q.; Johnson, D. L.; Mullins, O. C. *Energy Fuels* **2009**, *23*, 1201.

(39) Ese, M.-H.; Galet, L.; Clausse, D.; Sjöblom, J. *J. Colloid Interface Sci.* **1999**, *220*, 293-301.

(40) Fossen, M. *Aggregation, Interfacial Properties and Structural Characterization of Asphaltene Solubility Fractions.* PhD, NTNU, 2007.

(41) Wu, X. *Energy Fuels* **2003**, *17*, 179-190.

(42) Yarranton, H. W.; Hussein, H.; Masliyah, J. H. *J Colloid Interface Sci.* **2000**, *228*, 52-63.

(43) Czarnecki, J.; Moran, K. *Energy Fuels* **2005**, *19*, 2074-2079.

(44) Graham, B. F.; May, E. F.; Trengove, R. D. *Energy Fuels* **2008**, *22*, 1093-1099.

(45) Zhang, L. Y.; Lawrence, S.; Xu, Z.; Masliyah, J. H. *J. Colloid Interface Sci.* **2003**, *264*, 128-140.

(46) Zhang, L. Y.; Xu, Z.; Masliyah, J. H. *Langmuir* **2003**, *19*, 9730.

(47) Zhang, L. Y.; Lopetinsky, R.; Xu, Z.; Masliyah, J. H. *Energy Fuels* **2005**, *19*, 1330-1336.

(48) Zhang, L. Y.; Breen, P.; Xu, Z.; Masliyah, J. H. *Energy Fuels* **2007**, *21*, 274-285.

(49) Wang, S.; Liu, J.; Zhang, L.; Xu, Z.; Masliyah, J. *Energy Fuels* **2008**, *23*, 862.

(50) Chandra, M. S.; Xu, Z.; Masliyah, J. H. *Energy Fuels* **2008**, *22*, 1784.

(51) Long, J.; Zhang, L.; Xu, Z.; Masliyah, J. H. *Langmuir* **2006**, *22*, 8831.

(52) Lobato, M. D.; Pedrosa, J. M.; Hortal, A. R.; Martinez-Haya, B.; Lebron-Aguilar, R.; Lago, S. *Colloids Surf., A* **2007**, *298*, 72-79.

(53) Leblanc, R. M.; Thyrion, F. C. *Fuel* **1989**, *68*, 260-262.

(54) Ese, M.-H.; Yang, X.; Sjöblom, J. *Colloid Polym. Sci.* **1998**, *276*, 800-809.

(55) Fingas, M.; Fieldhouse, B. G. In *Encyclopedic Handbook of Emulsion Technology*; Sjöblom, J., Ed.; Marcel Dekker Inc.: New York, 2001, p 409-442.

(56) Jestin, J.; Simon, S.; Zupancic, L.; Barre, L. *Langmuir* **2007**, *23*, 10471-10478.

(57) Alvarez, G.; Jestin, J.; Argillier, J. F.; Langevin, D. *Langmuir* **2009**, *25*, 3985-3990.

(58) Czarnecki, J. *Energy Fuels* **2009**, *23*, 1253-1257.

(59) Singh, S.; McLean, J. D.; Kilpatrick, P. K. *J. Dispersion Sci. Technol.* **1999**, *20*, 279 - 293.

(60) Rakotondradany, F.; Fenniri, H.; Rahimi, P.; Gawrys, K. L.; Kilpatrick, P. K.; Gray, M. R. *Energy Fuels* **2006**, *20*, 2439-2447.

(61) Akbarzadeh, K.; Bressler, D. C.; Wang, J.; Gawrys, K. L.; Gray, M. R.; Kilpatrick, P. K.; Yarranton, H. W. *Energy Fuels* **2005**, *19*, 1268-1271.

(62) Hurtevent, C.; Rousseau, G.; Bourrel, M.; Brocart, B. In *Emulsions and Emulsion stability*; 2nd ed.; Sjöblom, J., Ed.; Taylor & Francis: Boca Raton, 2006; Vol. 132, p 477-515.

(63) Zhang, A.; Ma, Q.; Wang, K.; Liu, X.; Shuler, P.; Tang, Y. *Appl. Catal., A* **2006**, *303*, 103-109.

(64) Meredith, W.; Kelland, S. J.; Jones, D. M. *Org. Geochem.* **2000**, *31*, 1059-1073.

(65) Horváth-Szabó, G.; Czarnecki, J.; Masliyah, J. *J. Colloid Interface Sci.* **2001**, *236*, 233-241.

(66) Barrow, M. P.; McDonnell, L. A.; Feng, X.; Walker, J.; Derrick, P. J. *Anal. Chem.* **2003**, *75*, 860-866.

(67) Lutnaes, B. F.; Brandal, O.; Sjoblom, J.; Krane, J. *Org. Biomol. Chem.* **2006**, *4*, 616-620.

(68) Hanneseth, A.-M. D. *An Experimental Study of Tetrameric Acids at w/o Interfaces.* PhD, NTNU, 2009.

(69) Kanicky, J. R.; Shah, D. O. *Langmuir* **2003**, *19*, 2034-2038.

(70) Havre, T. E.; Sjöblom, J.; Vindstad, J. E. *J. Dispersion. Sci. Technol.* **2003**, *24*, 789 - 801.

(71) Brandal, Ø.; Sjöblom, J.; Øye, G. *J. Dispersion. Sci. Technol.* **2004**, *25*, 367 - 374.

(72) Brandal, Ø.; Hanneseth, A.-M. D.; Sjöblom, J. *Colloid Polym. Sci.* **2005**, *284*, 124-133.

(73) Brandal, Ø.; Sjöblom, J. *J. Dispersion Sci. Technol.* **2005**, *26*, 53 - 58.

(74) Vindstad, J. E.; Bye, A. S.; Grande, K. V.; Hustad, B. M.; Hustvedt, E.; Nergård, B. *SPE 80375 Fighting naphthenate deposition at the Statoil operated Heidrun field* In *SPE 5th International Symposium on Oilfield Scale* Aberdeen, 2002.

(75) Mediaas, H.; Grande, K. V.; Hustad, B. M.; Rasch, A.; Rueslåtten, H. G.; Vindstad, J. E. *SPE 80404 - The acid-IER method - A method for selective isolation of*

carboxylic acids from crude oil and other organic solvents In *SPE 5th International Symposium on Oilfield Scale* Aberdeen, 2003.

(76) Baugh, T. D.; Grande, K. V.; Mediaas, H.; Vindstad, J. E.; Wolf, N. O. *SPE/IADC 93011 The Discovery of High Molecular Weigth Naphthenic Acids (ARN acids) Responsible for Calcium Naphthenate Deposits.* In *SPE 7th International Symposium on Oilfield Scale* Aberdeen, 2004.

(77) Torssell, K. B. G. *Natural Product Chemistry. A mechanistic, biosynthetic and ecological approach.* ; 2nd ed.; Apotekarsocieteten: Stockholm, 1997.

(78) Lutnaes, B. F.; Krane, J.; Smith, B. E.; Rowland, S. J. *Org. Biomol. Chem.* **2007**, *5*, 1873-1877.

(79) Brandal, Ø.; Hanneseth, A.-M. D.; Hemmingsen, P. V.; Sjöblom, J.; Kim, S.; Rodgers, R. P.; Marshall, A. G. *J. Dispersion. Sci. Technol.* **2006**, *27*, 295 - 305.

(80) Magnusson, H.; Hanneseth, A.-M. D.; Sjöblom, J. *J. Dispersion. Sci. Technol.* **2008**, *29*, 464 - 473.

(81) Brocart, B.; Bourrel, M.; Hurtevent, C.; Volle, J.-L.; Escoffier, B. *J. Dispersion. Sci. Technol.* **2007**, *28*, 331 - 337.

(82) Rodrigues, A. R.; Ubbels, S. J. *World Oil* **2007**, 1-3.

(83) Brandal, Ø.; Viitala, T.; Sjöblom, J. *J. Dispersion. Sci. Technol.* **2007**, *28*, 95 - 106.

(84) Hurtevent, C.; Ubbels, S. J. *SPE 100430 Preventing naphthenate stabilised emulsions and naphthenate deposits on fields.* In *2006 SPE International Oilfield Scale Symposium* Aberdeen, 2006.

(85) Goldszal, A.; Hurtevent, C.; Rousseau, G. *SPE 74661 - Scale and Naphthenate inhibition in Deep-Offshore Fields* In *2002 SPE Oilfield Scale Symposium* Aberdeen, 2002.

(86) Dyer, S. J.; Williams, H. L.; Graham, G. M.; Cummine, C.; Melvin, K. B.; Haider, F.; Gabb, A. E. *SPE 100632 - Simulating calcium naphthenate formation and migitation under laboratory conditions.* In *2006 SPE International Oilfield Scale Symposium* Aberdeen, 2006.

(87) Tadros, T. F. *Applied Surfactants. Principles and Applications*-; 1st ed.; Wiley-VCH: Weinheim, 2005.

(88) Menger, F. M.; Galloway, A. L.; Chlebowski, M. E. *Langmuir* **2005**, *21*, 9010-9012.

(89) Robinson, B. H.; Bucak, S.; Fontana, A. *Langmuir* **2000**, *16*, 8231-8237.

(90) Corrin, M. L.; Harkins, W. D. *J. Am. Chem. Soc.* **1947**, *69*, 683-688.

(91) Jacquier, J. C.; Desbène, P. L. *J. Chromatogr. A* **1996**, *743*, 307-314.

(92) Matsuoka, K.; Suzuki, M.; Honda, C.; Endo, K.; Moroi, Y. *Chem. Phys. Lipids* **2006**, *139*, 1-10.

(93) Holmberg, K.; Jönsson, B.; Kronberg, B.; Lindman, B. *Surfactants and Polymers in Aqueous Solutions*; 2nd ed.; John Wiley & Sons: West Sussex, 2003.

(94) Bijma, K.; Blandamer, M. J.; Engberts, J. B. F. N. *Langmuir* **1998**, *14*, 79-83.

(95) Friberg, S. E. In *Encyclopedic Handbook of Emulsion Technology*; Sjöblom, J., Ed.; Marcel Dekker Inc.: New York, 2001, p 47-58.

(96) Horváth-Szabó, G.; Masliyah, J. H.; Czarnecki, J. *J. Colloid Interface Sci.* **2001**, *242*, 247-254.

(97) Havre, T. E.; Sjöblom, J. *Colloids Surf., A* **2003**, *228*, 131-142.

(98) Less, S.; Hannisdal, A.; Bjørklund, E.; Sjöblom, J. *Fuel* **2008**, *87*, 2572-2581.

(99) Ali, M. F.; Alqam, M. H. *Fuel* **2000**, *79*, 1309-1316.

(100) Miller, R.; Krägel, J.; Fainermann, V. B.; Makievski, A. V.; Grigoriev, D. O.; Ravera, F.; Liggieri, L.; Kwok, D. Y.; Neumann, A. W. In *Encyclopedic Handbook of Emulsion Technology*; Sjöblom, J., Ed.; Marcel Dekker Inc.: New York, 2001, p 1-45.

(101) Moran, K.; Czarnecki, J. *Colloids Surf., A* **2007**, *292*, 87-98.

(102) Pauchard, V.; Sjöblom, J.; Kokal, S.; Bouriat, P.; Dicharry, C.; Müller, H.; al-Hajji, A. *Energy Fuels* **2009**, *23*, 1269-1279.

(103) Lakowitch, J. R. *Principles of Fluorescence Spectroscopy*; 3rd ed.; Springer Science+Business Media, LLC: New York, 2006.

(104) Neuteboom, E. E.; Meskers, S. C. J.; Meijer, E. W.; Janssen, R. A. J. *Macromol. Chem. Phys.* **2004**, *205*, 217-222.

(105) Chen, Z.; Stepanenko, V.; Dehm, V.; Prins, P.; Siebbeles, Laurens D. A.; Seibt, J.; Marquetand, P.; Engel, V.; Würthner, F. *Chem. Eur. J.* **2007**, *13*, 436-449.

(106) Peña, A. A.; Hirasaki, G. J. In *Emulsions and Emulsion stability*; 2nd ed.; Sjöblom, J., Ed.; Taylor & Francis: Boca Raton, 2006; Vol. 132, p 283-309.

(107) Balinov, B.; Söderman, O. In *Encyclopedic Handbook of Emulsion Technology*; Sjöblom, J., Ed.; Marcel Dekker Inc.: New York, 2001, p 279-303.

(108) Friebolin, H. *Basic One- and Two Dimensional NMR spectroscopy*; 3rd ed.; Wiley-VCH: Weinheim, 1998.

(109) Mitra, P. P.; Sen, P. N.; Schwartz, L. M. *Phys. Rev., B* **1993**, *47*, 8565.

The reference list is presented based on the “ACS no title” template, used *e.g.* in Langmuir.

Journal names have been abbreviated according to
http://www.library.ubc.ca/scieng/coden.html.

Paper 1

Is not included due to copyright

Paper 2

Is not included due to copyright

Paper 3

Is not included due to copyright

Paper 4

Colloids and Surfaces A: Physicochem. Eng. Aspects 340 (2009) 99–108

Contents lists available at ScienceDirect

Colloids and Surfaces A: Physicochemical and Engineering Aspects

journal homepage: www.elsevier.com/locate/colsurfa

Model compounds for C_{80} isoprenoid tetraacids Part II. Interfacial reactions, physicochemical properties and comparison with indigenous tetraacids

Erland L. Nordgård*, Heléne Magnusson, Ann-Mari D. Hanneseth, Johan Sjöblom

Ugelstad Laboratory, Department of Chemical Engineering, Norwegian University of Science and Technology, Sem Sælandsvei 4, N-7491 Trondheim, Norway

ARTICLE INFO

Article history:
Received 12 December 2008
Received in revised form 24 February 2009
Accepted 2 March 2009
Available online 14 March 2009

Keywords:
Tetraacids
Model compounds
Interfacial reactions
Monolayer properties

ABSTRACT

Novel model compounds are desired to study properties of a narrow group of tetrameric acids from crude oil mainly responsible for naphthenate deposition. It is important to make a comparison to find to what degree the model compounds can reflect the properties of the indigenous tetraacids and where there are deviations, before using the model compounds in naphthenate research. A comparison between two synthesised model compounds and indigenous tetraacids has been carried out regarding physicochemical properties including thermal solid state properties, critical micelle concentrations, monolayer properties and interfacial reactions. Of the two studied model compounds, one was observed to form the same cross-linked network with Ca^{2+}, a typical feature of the indigenous tetraacids. Interfacial reactions using the pendant drop technique also showed that four different divalent cations could all form this network with the model tetraacid. The film formation was however dependent on the ratio M^{2+}/TA. The main deviations were in the solid state, where the model compounds showed crystalline transitions, contrary to the indigenous tetraacids. We conclude that the two different model compounds mimic the indigenous tetraacids well with respect to several of their properties and are suitable for use in naphthenate research.

1. Introduction

Naphthenate deposition in crude oil recovery and transportation is a severe problem for the oil industry. During transportation from the well, the naphthenic acids dissociate due to pressure drops leading to increased pH. The pressure drop is causing dissolved CO_2 to be released as gas which affects the bicarbonate equilibrium in the produced water to consume H^+. The formed naphthenates react with metal ions from the produced water to form metal naphthenates [1]. Depending on the type of both the acid and the cation, the metal soaps can either be dispersed in the oil bulk phase or, more seriously, accumulate over oil–water interfaces in topside separators and de-salters. Naphthenates that accumulate at the oil–water interface may contribute to the formation of highly stable emulsions [2].

The naphthenic acids in crude oil are a complex mixture of thousands of different structures. These acids are mainly monoacids which can be either cyclic or linear, in addition to containing aromatic moieties [1]. However, even though the monoacids dominate in the bulk phase, a narrow group of four-protic naphthenic acids with a molecular weight around 1230 g/mol has been shown to dominate in the deposits. These tetraacids are orders of magnitudes more interfacially active than monoacids [3]. The structure of the tetraacids was determined after extensive NMR research by Lutnaes et al. and a C_{80} tetraacid with six cyclic rings was found [4]. Later, HPLC studies showed that the deposits also contain other isomers with 4–8 cyclic rings, including traces of methyl-substituted C_{81} and C_{82} structures [5,6]. The presence of each isomer and relative amount may vary from well to well. Tetraacids are found in crudes all over the world from oilfields offshore Norway to West-Africa and China, among others. An archeal origin has been proposed to be the source of these membrane-like tetraacid structures [4]. The tetraacids from crude oil are sometimes referred to as ARN acids or C_{80} isoprenoid tetraacids. In this paper we refer these as indigenous, native or isolated tetraacids.

While common monoacids have intermediate interfacial activity, the indigenous tetraacids lower the interfacial tension between 10% toluene in hexadecane and a pH 9 aqueous phase to 12 mN/m at only 0.005 mM as determined by the pendant drop technique [3]. In the same study, the molecular area of tetraacids was determined by the Langmuir technique and found to be about 160 Å^2. This would indicate that the tetraacids are directing all four acid groups to the interface, and most likely separated by parts of the hydrocarbon chains. Depending on the conditions in the subphase, like pH and presence of divalent cations, the tetraacid molecules

* Corresponding author. Tel.: +47 73550325; fax: +47 73594080.
E-mail address: erlandn@chemeng.ntnu.no (E.L. Nordgård).

0927-7757/$ – see front matter © 2009 Elsevier B.V. All rights reserved.
doi:10.1016/j.colsurfa.2009.03.002

in the monolayer film might be able to flip from a conformation were all acid groups are pointing towards the interface, to a conformation similar to a trans-membrane structure with two of four acid groups pointing towards air [3,7,8]. Increasing pH and presence of Ca^{2+} appeared to prevent the molecules from flipping. As pointed out by Brandal et al. [8] this is analogous to the conformation of bipolar tetraether lipids in biological membranes. A future commercial use of tetraacids might be preparation of vesicles mimicking a cell membrane. This will however not be an issue in this study.

Calcium is the dominating metal ion species in tetraacid deposits. A cross-linked polymer-like structure is proposed for the calcium naphthenate film [7]. The cross-linking makes the film more elastic than viscous. In fact interfacial dilatational rheology measurements have shown that both the tetraacid and the calcium salt films were elastic in nature, and the elasticity being much larger for the calcium containing system [7]. The high interfacial activity of tetrameric acids in combination with the formation of a cross-linked network is believed to be the most essential factors for the deposition problem. Another feature of the tetrameric naphthenic acids is the presence of glass transitions in DSC measurements, similar to polymer systems, found both for the isolated acid and for the calcium salt [7].

Even though the knowledge about this interesting class of surfactants has increased during the latest years, the isolation and characterization of tetraacids remain challenging. The isolation procedure is time – and solvent consuming [9], the purity of the isolated product may vary [7] and the chemical structures of tetraacids reveal no UV active moieties, making bulk concentration characterization dependent upon chemical derivatisation [10]. In order to circumvent some of the difficulties associated with the isolation and characterization of native tetraacids, we have recently synthesised tetraacid model compounds [11]. In the model acids an aromatic core is attached to four hydrocarbon chains with terminal carboxylic groups. This allows us to study the compounds by spectroscopic methods. Two model compounds with different aromatic cores were synthesised and investigated. Synthetic model compounds also give a better control over the purity and composition. The model compounds were extensively characterized with respect to interfacial properties. They were found to have similar high interfacial activity as the native tetraacids rendering them suitable model compounds.

In this paper, we present physicochemical properties of tetraacid model compounds, both in bulk and at interfaces, and compare them to those of the indigenous tetraacids. In addition, we have studied reactions between tetraacid model compounds and different divalent cations at the oil–water interface.

2. Experimental

All chemicals and solvents used were purchased from Sigma–Aldrich and used without further purification. Tetraacid model compounds were synthesised according to previously reported literature procedure [11]. Their structures, molecular weights and abbreviations are shown in Fig. 1, together with the most common tetraacid found in deposits. Indigenous tetraacids were isolated from a deposit collected at a Norwegian offshore field according to an ion-exhange resin method described elsewhere [9].

Determination of critical micelle concentrations (CMCs) for indigenous and model tetraacids was carried out using two different techniques. First by measuring the dynamic surface tension at equilibrium of an aqueous phase as a function of concentration using a CAM 200 pendant drop equipment (KSV Instruments, Finland). The instrument is equipped with a CCD video camera with telecentric optics, a frame grabber and a LED based background light source. The diameter of the syringe was 0.7 mm for BP10 and indigenous tetraacids, and 1.6 mm for Pe10. Three tetraacids were dissolved in aqueous solutions. The pH was set to >11 in order to gain sufficient aqueous solubility and diluted to the desired concentrations and the equilibrium surface tension was recorded at each concentration. Secondly, surface tension measurements were performed using a Sigma70 Tensiometer (KSV Instruments, Finland) using a De Nuoy ring probe. The solutions were the same as used in the pendant drop experiments. A CMC could not be obtained for the indigenous tetraacids with the latter technique, however.

The pendant drop equipment was also utilized to investigate the dynamic interfacial tension during addition of different divalent cations to an aqueous solution with an oil droplet immersed. A tetraacid, BP10, was dissolved in the oil phase, 1-octanol, (99%, spectrophotometric grade) to a concentration of 1 mM and an oil droplet

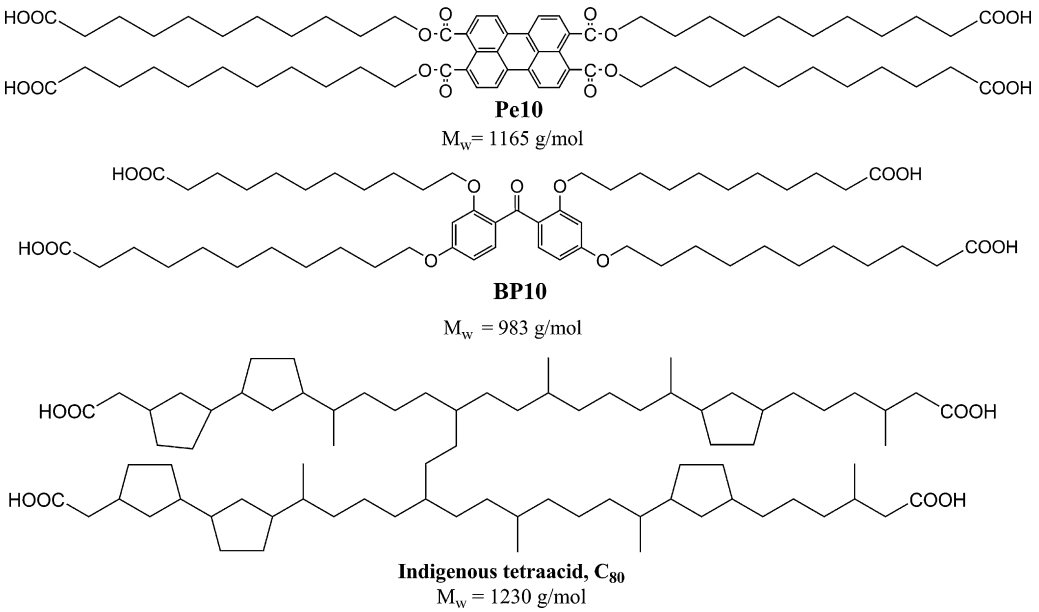

Fig. 1. Structures, molecular weights, and abbreviations of tetraacids used in the study. Pe10 and BP10 are synthesized model compounds, while the indigenous tetraacids are isolated from crude oil deposits. Only the most common C_{80} analogue is shown [4].

was formed upwards, using a U-shaped needle, in an aqueous solution of 3.2 mL in a polystyrene cuvette. After 500 s, a small amount, depending on the final cation concentration, of a 1 M M^{2+} solution was injected with a 100 μL pipette. The cations were dissolved in ultrapure water as their chloride–hydrate salts.

The thermal properties of one tetraacid, BP10, and the corresponding calcium naphthenate in bulk were analysed by differential scanning caloriometry, DSC, on a DSC300Q from TA instruments (USA). The sample was heated to 300 °C at a rate of 5 °C/min, kept at the maximum temperature for 1 min and then cooled at the same rate to −50 °C. The cycle was repeated in order to erase effects of thermal memory and the transitions were recorded on the second cycle. The experiments were run under nitrogen.

Surface pressure–area isotherms were recorded on a Langmuir minitrough (KSV Instruments, Finland) of effective film area 364 mm × 75 mm at ambient temperature. The trough was made of Teflon and the barriers of Delrin. The trough and barriers were thoroughly cleaned with acetone or ethanol, tap water and ultrapure water before use, and by aspirating the surface with a Pasteur pipette connected to a vacuum-aspirator. The surface was assumed pure when the surface pressure of subphase only did not exceed 0.5 mN/m upon full compression. Isotherms were recorded at different pH of the aqueous subphase; pH 2.3, 5.8, 9, and 11.6. The pH 2.3 subphase was adjusted with 1 M HCl, pH 5.8 using ultrapure water with a resistivity of at least 18.2 Ω, pH 9 buffer from Merck and pH 11.6 was obtained by adjusting with 1 M NaOH. When necessary, additional NaCl was added in order to obtain equal Na^+ concentrations for all buffers. In experiments where the subphase contained calcium ions, calcium chloride dihydrate was dissolved in the subphase. Tetraacid model compounds were dissolved in spectrophotometric grade chloroform at a concentration of 0.2 mM for Pe10 and 0.3 mM for BP10. The solution of Pe10 was sonicated under heating for 15 min to ensure complete dissolution. An amount of 40 μL (45 μL for Pe10) was spread on the subphase using a 50 μL Hamilton syringe to get the appropriate amount of molecules on the surface. The solvent was allowed to evaporate for at least 5 min before compression. The compression of the films was carried out at a barrier speed of 5 mm/min with a target pressure of 100 mN/m.

A Brewster angle microscope (BAM) (KSV Instruments, Finland) was utilized for visualisation of the film morphology. The microscope was placed above the trough with a laser directed normal to the trough direction and at the Brewster angle in the *z*-direction. A standard 10 mW He–Ne laser with a Glan–Thomson polarizer emitted *p*-polarized light. To avoid stray light from the surface, a black wedge-shaped plate was placed at the bottom were the laser was pointed. For imaging a 768 × 494 pixels CCD camera was used through a 10× magnification and a spatial resolution of ∼2 μm yielding images of approximately 400 μm × 300 μm in size.

Images of BP10 in the solid state were obtained with a Nikon ME600 Optical Microscope equipped with polarizers and temperature control.

3. Results and discussion

3.1. Critical micelle concentrations

The tetraacids are highly interfacially active at oil–water interfaces, and should display critical micelle concentrations (CMCs) in aqueous solutions. This is however not easily detected at neutral pH, due to the fact that the tetraacids in the undissociated form are insoluble in water. Increasing the pH will successively dissociate more acid groups, rendering the tetraacid increasingly water soluble. Hence, measurements of the CMC of this compound class must be carried out under basic conditions. Fig. 2a and b displays the obtained plots of surface tension as a function of tetraacid concentration on a logarithmic scale by using two different techniques; (a) the pendant drop technique and (b) a tensiometer. A buffered aqueous phase at pH 11 was used to ensure water solubility and complete dissociation of acid functions. The CMC is defined as the concentration where surface tension becomes independent of tetraacid concentration. (Fig. 2) Table 1 lists the CMCs for the tetraacids. It was not possible to get a CMC of the indigenous tetraacids with the tensiometer due to the surfactant absorbing onto the ring probe. Surface tension values at equilibrium could not be obtained, and experiments at different buffer pH and concentrations were unsuccessful. The pendant drop technique gave however a CMC for the indigenous tetraacids. In general, the indigenous tetraacids gave the lowest surface tension, 47.3 mN/m, but BP10 displayed the lowest CMC, independent of technique used. All CMCs were in the same order of magnitude (10^{-4} M) and fairly comparable. The CMCs of the model compounds were similar even though the aromatic cores are different and the bonds connecting the chains and the core are of different polarity. Hence, the CMC values are mainly dependent on the acid groups available and only minor influenced by the remaining molecule. In fact, the CMC for the indigenous tetraacids, which have the most hydrophobic core, was higher than both model compounds. If the CMC is solely dependent upon the presence of polar groups in the structure, indigenous tetraacids should have the lowest CMC value since the acid groups are the only polar groups in the structure. There may be two explanations for the results. First of all, the actual concentration of the indigenous tetraacids may be incorrect because, isolated from a deposit,

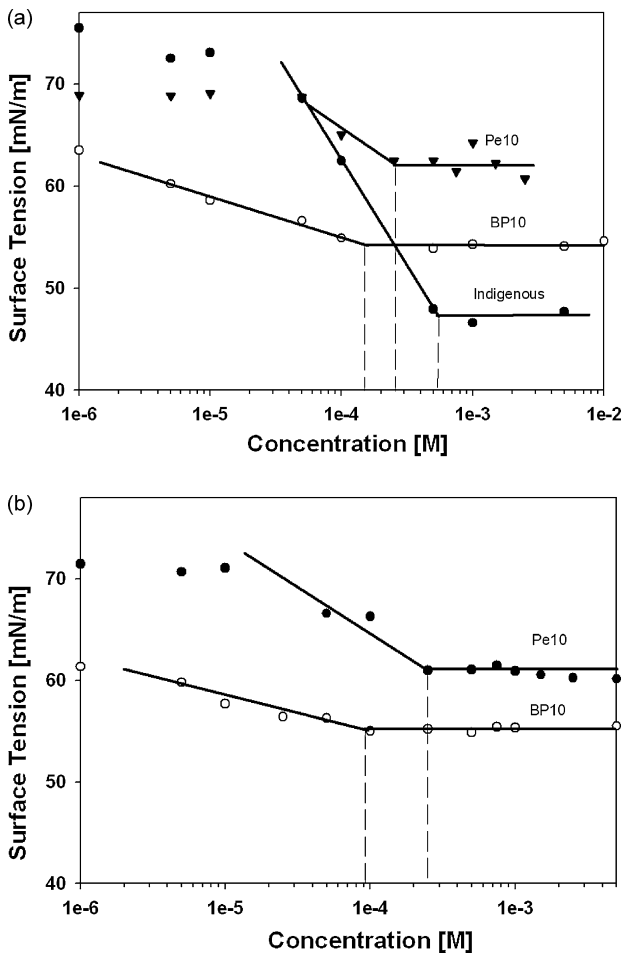

Fig. 2. Surface tension versus concentration plots obtained for the tetraacids by using (a) the pendant drop technique and (b) tensiometer. The dashed, vertical lines indicate the CMC, by visual considerations of the break point of the solid lines.

Table 1
CMC, γ_{cmc}, surface excess Γ, and surface area $A_{molecule}$ for model and indigenous tetraacids obtained by two instrumental techniques, denoted as tensiometer/pendant drop technique.

Compound	CMC (mM)	γ_{cmc} (mN/m)	Γ (μmol/m^2) $n=1$	Γ (μmol/m^2) $n=5$	$A_{molecule}$ (Å^2), $n=1$	$A_{molecule}$ (Å^2), $n=5$
BP10	0.09/0.15	55.2/54.1	0.64/0.71	0.13/0.14	261/232	1305/1162
Pe10	0.25/0.25	61.1/62.2	1.58/1.59	0.32/0.32	105/105	524/523
Indigenous TA	NA/0.55	NA/47.3	NA/3.64	NA/0.73	NA/47	NA/228

the purity may vary. A recent study by Simon et al. using HPLC and NMR to determine tetraacid content in deposits and purified tetraacid samples, found out that the purity of a batch of isolated tetraacids was 83% [10]. Normally, the isolated tetraacids appear as a brown, sticky material, with absorbance in UV and displaying fluorescence, and is most likely contaminated with similar polyacids incorporating aromatic moieties. In another study, Magnusson et al. determined the purity of the isolated tetraacid to 94% by thermogravimetric analysis, TGA [7]. Assuming contamination in the sample, the actual concentration of indigenous tetraacids in the CMC measurements may have been somewhat lower, and actually approached the value for BP10. Secondly, the indigenous tetraacids have much more branching in the hydrocarbon moieties than BP10, and branching of the hydrocarbon chains is strongly influencing the CMC [12]. An illustration of this is that the CMC of branched sodium dodecyl sulfate is twice as high as for linear sodium dodecyl sulfate [13].

Table 1 lists the surface excess and surface area per molecule obtained from Fig. 2a and b. The surface excess have been calculated using the Gibbs equation

$$\Gamma_{max} = -\frac{1}{nRT}\left(\frac{\partial\gamma}{\partial \ln C}\right) \quad (1)$$

and for the molecular area

$$A_{min} = \frac{1000}{6.023\Gamma_{max}} \quad (2)$$

Γ_{max} is given in μmol/m^2, R is the universal gas constant (8.314 J/(K mol)), T = 298 K and A_{min} is the minimum area per surfactant in Å^2. A tetraacid under basic conditions will be present in solution as its tetrasalt with a total of five species adsorbing to the surface from pure water (n = 5). This definition is analogous to work on gemini surfactants [14,15]. When extra salt is added, such as the introduction of a buffer, the extra cations can swamp out the effect of counterions in the Gibbs equation and values can be calculated with n = 1 [16]. As noted by Diamant and Andelman, discussion of the state of adsorption at the air/water interface is a complex topic for oligomeric surfactants, and neither of the two extreme scenarios seems probable [15]. Thus, we have decided to give the calculated values of surface excess and molecular area for both n = 1 and n = 5 in Table 1. The areas of the tetraacids are in the order TA < Pe10 < BP10, with an area of 47 Å^2 for indigenous TA with n = 1. This is smaller than what has been obtained using the Langmuir technique (160 Å^2) [3], but the area with n = 5 is again too large, 228 Å^2. The adsorption of these tetraacids might be too complex to be considered with one of these extreme scenarios, or the ionic strength of the buffer solutions (M^+ = 0.05 M) may not have been high enough to completely swamp out the effects of the counterions. The area of Pe10 was over half the area of BP10 even the core in Pe10 is more extended. This indicates that while BP10 is arranged with all four carboxylic groups to the interface, the molecules of Pe10 is more tilted, or even perpendicular, to the interface. Langmuir results shown in Section 3.3 support that Pe10 have a higher tendency of a perpendicular arrangement.

3.2. Thermal properties of a tetraacid model compound

One tetraacid model compound was investigated by DSC, BP10. This compound was most similar to the indigenous tetraacids regarding film properties. The calcium salt of BP10 was isolated in the same way as previously described for the indigenous tetraacids [7], except the oil phase used was chloroform and an aqueous phase of pH 11. Fig. 3a and b displays DSC thermograms of BP10 and the corresponding calcium salt. Unlike the indigenous tetraacid, the BP10 acid showed only crystalline transitions. The heating trace showed three distinct first order transitions. According to the molecular structure there may be two different origins of those transitions, inter- and intramolecular hydrogen bonds and crystallization of the aliphatic chains. We therefore attribute the first melt transition at approximately 52 °C to the melting of the aliphatic chains, rendering the system more flexible. Under the conditions of slow heating, the acid groups may approach each other and form

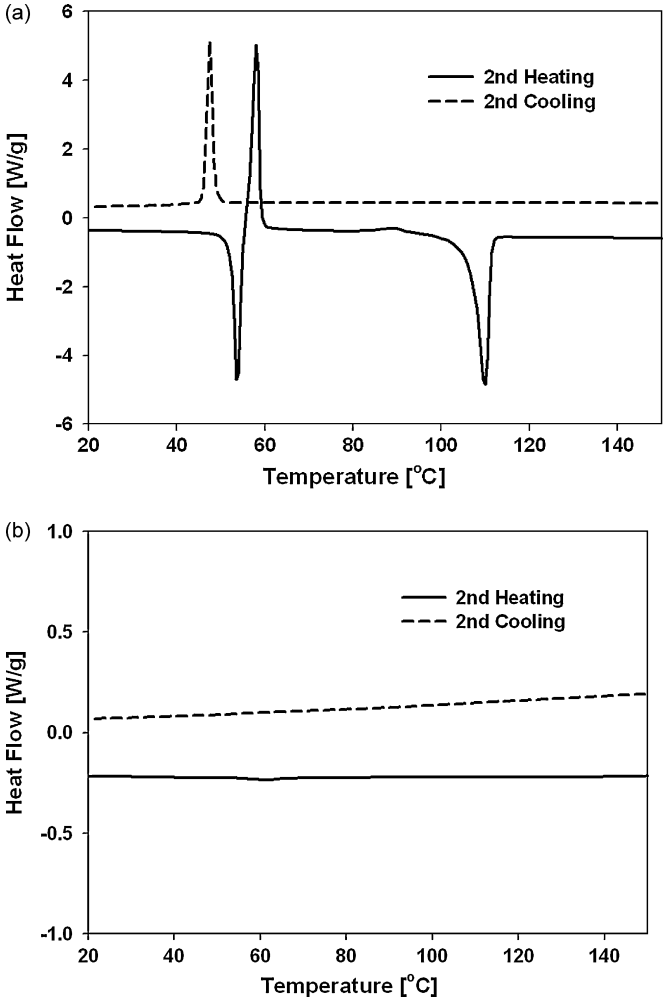

Fig. 3. DSC thermograms of BP10 in (a) acid form and (b) Ca^{2+} salt form. The second heating and cooling cycles are shown, and the temperature gradient was 5 °C/min in a nitrogen atmosphere.

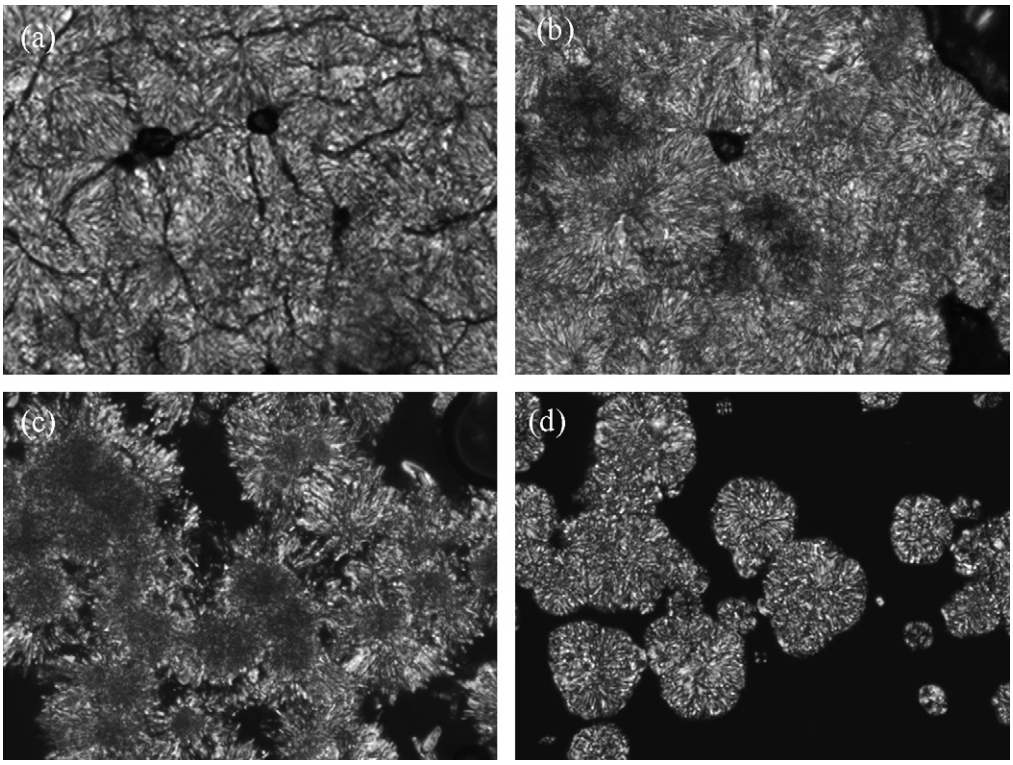

Fig. 4. Optical microscope images of BP10 during cooling and heating (a) second heating at 46.5 °C, (b) second heating at 86.5 °C, (c) during melting process at 111.5 °C and (d) during formation of birefrigerant crystals upon second cooling at 67.5 °C. The magnification was 20× and the cooling and heating rate was 5 °C/min.

strong intra- and intermolecular hydrogen bonds. We attribute the peak at 60 °C to the decrease in energy due to association of acid groups by hydrogen bonding to form a liquid crystalline phase. As temperature is increased further, the hydrogen bonds are broken and a melt is formed resulting in the third peak at 110 °C. The cooling trace shows a single peak at 46 °C. In the melt, the acid groups are randomly distributed and therefore prevented from interacting with each other. To investigate this, BP10 in the solid state was studied by a thermocontrolled, polarized, optical microscope. Birefringence was in fact observed all the way up to the second melting at 112 °C, while this could not be observed upon cooling before passing 67 °C at a speed of 5 °C/min (Fig. 4a–d) This supports the theory that a mesophase is formed. This LC phase is hence not formed upon cooling because it requires a slower cooling or a larger degree of order to make the molecules and the acid groups arrange themselves so that the LC phase can form. The transition temperature upon cooling is somewhat different than in the DSC spectrum, but the temperature gradient speed could in both cases cause a delay to what the actual sample temperature was.

The DSC thermogram of the calcium salt is shown in Fig. 3b. No thermal transitions are observed in the temperature range under investigation. The high cross-link density of the BP10 calcium naphthenate restricts the mobility of the aliphatic chains. The high regularity of the aliphatic chains promotes crystallization instead of the formation of a glassy solid under the conditions of slow cooling. The strong ionic bonds render the systems much less flexible than the corresponding acid and the melting of the solid therefore occurs at higher temperatures than for the corresponding acid and outside the range of the present experiment.

Unlike the model compounds, the indigenous tetraacid and its calcium naphthenate both show glass transitions at −15 °C and 73 °C, respectively [7]. Below the glass transition, the calcium salt remains as a rigid, glassy material and no crystalline melt temperature was observed for either acid or calcium salt. Deposits appear as a sticky material which may solidify with time.

3.3. Langmuir films and monolayer properties

Brandal et al. have studied the indigenous tetraacids by means of the Langmuir technique [3,8]. The surfactant is spread as a monolayer on an aqueous surface in a trough, and is compressed using motor-controlled barriers. At given molecular areas, the film might go through different phases and eventually the film will break. Indigenous tetraacids are believed to form a very elastic, cross-linked film which can stick to surfaces. Two important questions arise when comparing model and indigenous tetraacids; do the model compounds form the cross-linked network? Do the model compounds behave in the same way as for the indigenous tetraacids in a monolayer when it comes to molecular area and flipping? Studying the monolayer properties was expected to highlight these questions.

Fig. 5a and b shows the isotherms obtained for model tetraacids at different pH of the aqueous phase. A film collapse can be found in two ways, a sudden drop in pressure from the solid state, or as a horizontal break from the liquid state. The model compounds did not form stable monolayers at higher pH when no divalent cations were added, as can be seen from the very high compressibility and the low surface pressures. Most likely, the aqueous solubility for the model compounds in these cases was higher than for the indigenous tetraacids. Nevertheless, both for Pe10 and BP10, a horizontal break was observed in the same way at acidic conditions as what was found for indigenous tetraacids. This supports that the model compounds do in fact show the same flipping behavior. BAM images of BP10 (Fig. 6a–d) and Pe10 (Fig. 6e and f) indicate that the film thickness and density after the horizontal breaks had increased due to the higher light intensity in Fig. 6c, d, and f as opposed to the dark images obtained in the gaseous state in Fig. 6a

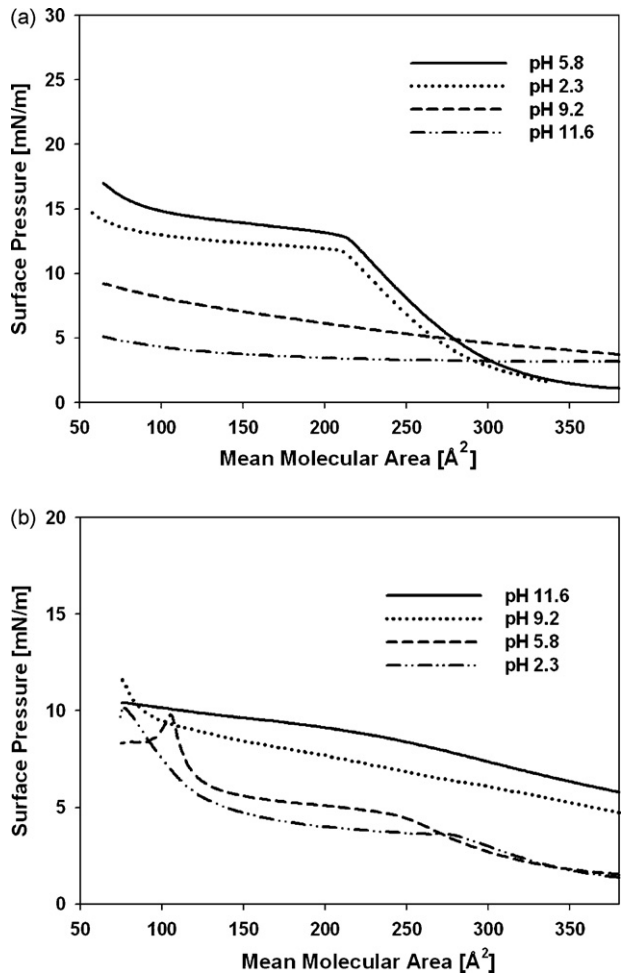

Fig. 5. Surface pressure–area isotherms of Langmuir monolayers of (a) BP10 and (b) Pe10 at different subphase pH. In cases where the pH was obtained with NaOH or HCl, NaCl was added in order to have salinity comparable to the buffers.

and e. Especially for BP10, the same islands of liquid expanded state were observed after the horizontal break as in previous studies using indigenous tetraacids [8], and supports that the flipping occurs for BP10 as well. For Pe10, the images after the horizontal break seemed to have a more "crystalline" pattern for the formed islands and higher light intensity. The film of a bilayer-type monolayer of Pe10, with two acid groups in the aqueous phase and the other remaining two towards air, might crystallize due to the strong aromatic interactions between the perylene cores. Stronger intermolecular interactions of Pe10 may be the reason why this model compound is less soluble in organic solvents than BP10. Increased brightness in Fig. 6f contrary to Fig. 6e supports that Pe10 is able to form the bilayer structure as well.

The molecular areas obtained at the horizontal break for the model compounds at pH 7 suggest that these films are arranged with the aromatic cores lying on the surface, separated by the acid groups in a "spider" – like arrangement. The hydrocarbon chains are able to fold towards air to some extent. A broad gaseous phase that is the region where the pressure increases slowly until the horizontal break was observed for both BP10 and Pe10. Due to the aromatic cores, the molecules were stretched in all directions from the beginning, and during compression in the gaseous state slowly folded to give the spider – arrangement. The indigenous tetraacids have not shown this behavior because of the lack of the aromatic moiety and already at start of compression have the nonpolar moiety more or less directed towards air. The nearly constant surface pressure after the initial break observed for indigenous tetraacids is the phase transition where the molecules flip two of the four acid groups towards air. For the model compounds, this arrangement will give further suitable interactions between each molecule, because the flipped conformation can be stabilized by aromatic interactions between adjacent molecules. A new collapse point could in some cases be observed after all molecules had flipped, around 60 $Å^2$ for BP10. A linear monoacid, like stearic acid, normally have a collapse point around 20 $Å^2$ [17], and taking into account more space occupied for BP10 due to the aromatic core, a collapse point around 60 $Å^2$ seems reasonable for two of four hydrocarbon chains directed toward the aqueous surface.

The effect of pH and addition of Ca^{2+} to the subphase on the isotherms of tetraacids has also been investigated. Fig. 7a and b shows the isotherms obtained at pH 9.2 and pH 11.6 with 0.01 M Ca^{2+}. At the lowest pH, the introduction of Ca^{2+} increased the film stability of the tetraacids and comparable to the film obtained at pH 5.8 without calcium. For Pe10 at pH 9.2 with calcium, it seemed like the bilayer, or flipped, structure was obtained directly for Pe10 without the gaseous state and the flipping region. At this subphase pH, it might be that two of four carboxylic acids have been deprotonated, leaving these two able to form a 1:1 salt with calcium, while the two undissociated acid groups easily flips to the bilayer structure. However, the strongest changes occurred when the subphase pH was raised to pH 11.6. The isotherm of BP10 showed a great increase in surface pressure between 100 and 200 $Å^2$, a collapse point between 25 and 35 mN/m and further increase in pressure. The latter increase is probably a formation of multilayers. This isotherm behavior resembles what was found for indigenous tetraacids. In fact, a gel-like film could be observed with the naked eye under compression for BP10. This film was not observed at pH 9.2. For Pe10, the isotherm at pH 11.6 does not provide any information because it is not a smooth line but rather jagged. This could be explained by defragmentating or dissolution of the film or new layers of film is gradually formed. No film was observed for Pe10. The differences observed at higher subphase pH may suggest that the typical interfacial film of tetraacids can be obtained when all the four acid groups are dissociated and is complexed with calcium in a neutral 2:1 Ca^{2+}:TA salt with no free acid groups, either dissociated or undissociated. Pe10 has a perylene core as the aromatic moiety, which upon packing in a bilayer structure forms very stabilizing aromatic interactions, and these interactions give perylene derivates their high liquid crystal ability. BP10 has a less aromatic core and will, at intermediate pH, dissolve into the aqueous phase instead of forming the bilayer structure.

Langmuir results show that BP10 is the model compound which show most similarities regarding film properties to indigenous tetraacids, but slightly less film stability due to higher water solubility and that the aromatic core occupy available space. However, it is reasonable to believe that at an oil–water interface, the nonpolar part, including the aromatic core, is directed into the oil phase. Hence, the similarities may be even larger for an oil–water system. Langmuir isotherms and interfacial pressure can be obtained in a liquid–liquid trough as well, and this would be the most realistic way to compare the film properties between model compounds and indigenous tetraacids. However, this requires that the tetraacid is solubilised in a non-polar solvent with high boiling point which is immiscible with water. We have so far only been able to dissolve the synthetic tetraacids in chloroform, or more polar solvents. Chloroform has a low boiling point and is therefore not suitable in liquid–liquid Langmuir experiments, and more polar solvents are not suitable due to solubility in water. The air–water experiments performed in this study give anyway sufficient indications of how well the model compounds can reflect the properties of indigenous tetraacids, and which model compound is the best choice in experiments where film properties are discussed.

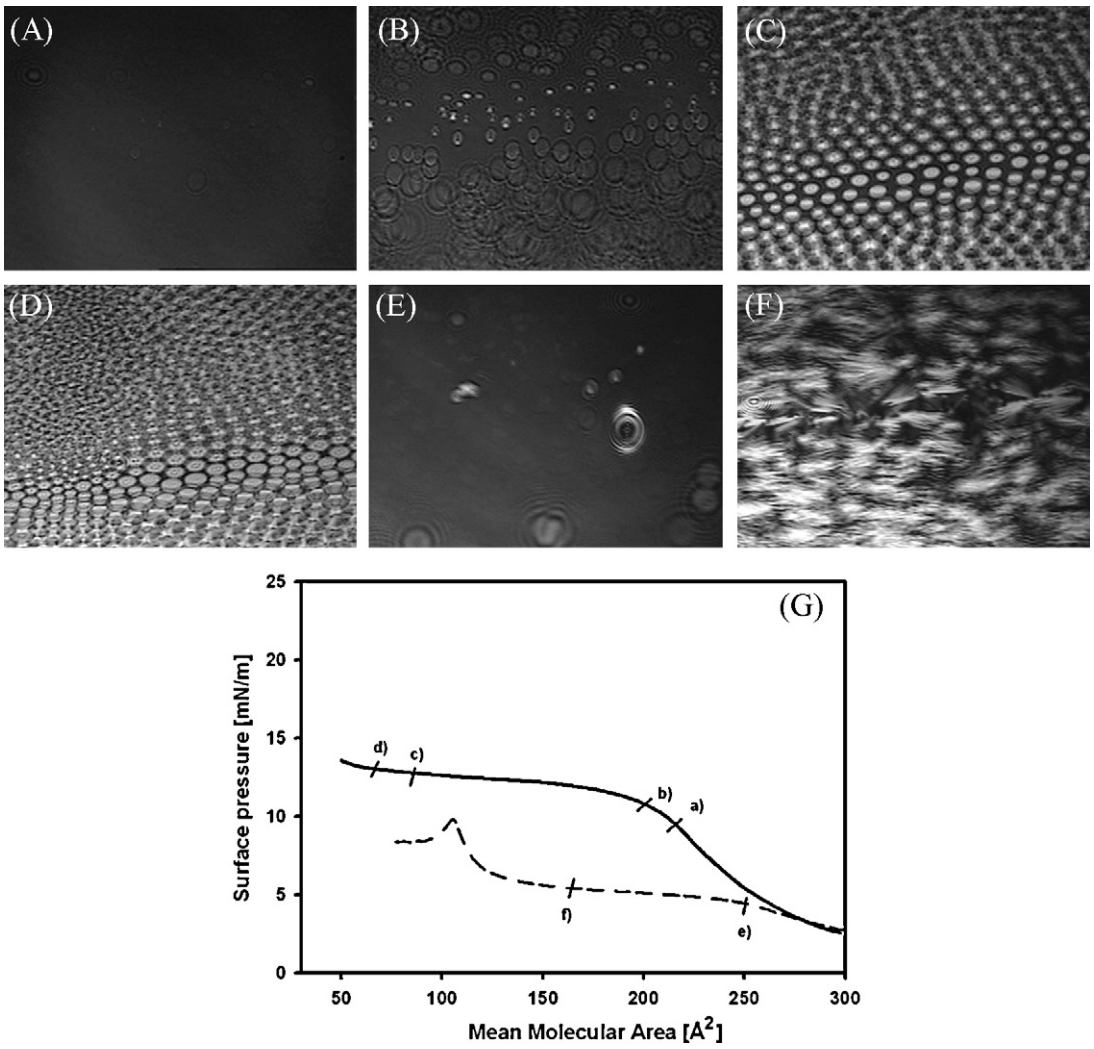

Fig. 6. BAM images of model tetraacids upon compression with ultrapure water at pH 5.8 as the subphase. Image (A–D) is of BP10 at (a) 9.2 mN/m, (b) 10.8 mN/m, (c) 12.6 mN/m of (d) 13 mN/m. Image (E and F) is of Pe10 at (e) 250 Å^2 and (f) 5 mN/m. Pressure–area isotherms under image taking of BP10 are given in (G) with markers where the images were taken. The image size is 400 μm × 300 μm.

3.4. Interfacial reactions between a model tetraacid and divalent cations

The tetraacid deposits found in oilfields are completely dominated by calcium as the counterion. Produced water also contains substantial amounts of other divalent cations like magnesium, barium and strontium. To investigate whether tetraacids have selectivity for calcium compared to other divalent cations, interfacial reactions were performed using the pendant drop technique. Changes in the dynamic interfacial tension when adding divalent cations can give information about the interactions between an acid and a cation, and what complex or salt may be formed. This has been carried out between monoacids and cations, and based on the shapes of the curves obtained the mechanism of the reactions involved in the process could be highlighted [18]. For indigenous tetraacids, the presence of a visible elastic film covering the oil droplet has been observed in such interfacial reactions.

Based on the Langmuir results, BP10 was chosen as the model tetraacid because it displayed most similarities regarding film properties, and due to solubility reasons. However, common solvents like toluene and hydrocarbons do not dissolve BP10 sufficiently at ambient temperatures. Instead, 1-octanol was chosen as the oil solvent, because it easily dissolves BP10, has sufficient viscosity and its density is lower than water. The drawback with 1-octanol is, due to the presence of terminal hydroxyl groups, it is itself surface active with an interfacial tension towards a buffer solution at 7.8 mN/m. However, it was assumed that the tetraacid would nevertheless be even more interfacially active and hence accumulate at the interface. Reactions using chloroform was tested, but did not give reproducible results, and using toluene at higher temperatures was difficult due to instability of BP10 in the oil phase and formation of air bubbles in the aqueous phase distorting the images. However, the trends obtained in these test where similar to results obtained with 1-octanol. 1-octanol was unsuccessfully used as oil phase in liquid–liquid Langmuir experiments.

The same four divalent cations previously used for monoacid studies were used in this study, namely calcium, magnesium, barium and strontium [18]. They differ in size and hydration state, which showed to be crucial in the case of monoacid reaction. The concentration of tetraacid was kept constant, while the cation concentration was increased to vary the ratio M^{2+}/TA. Fig. 8a shows the dynamic tension profiles obtained at a molar ratio M^{2+}/TA = 0.1. The interfacial tension was lower than for pure 1-octanol, because of the tetraacid present at the interface. After addition of the cation, initially a more interfacially active complex was formed for Ca^{2+} and Mg^{2+}, but the system relaxed back with time. The complexes formed may have dissolved in the aqueous phase and been replaced by more tetraacids molecules, since the pH of the aqueous phase

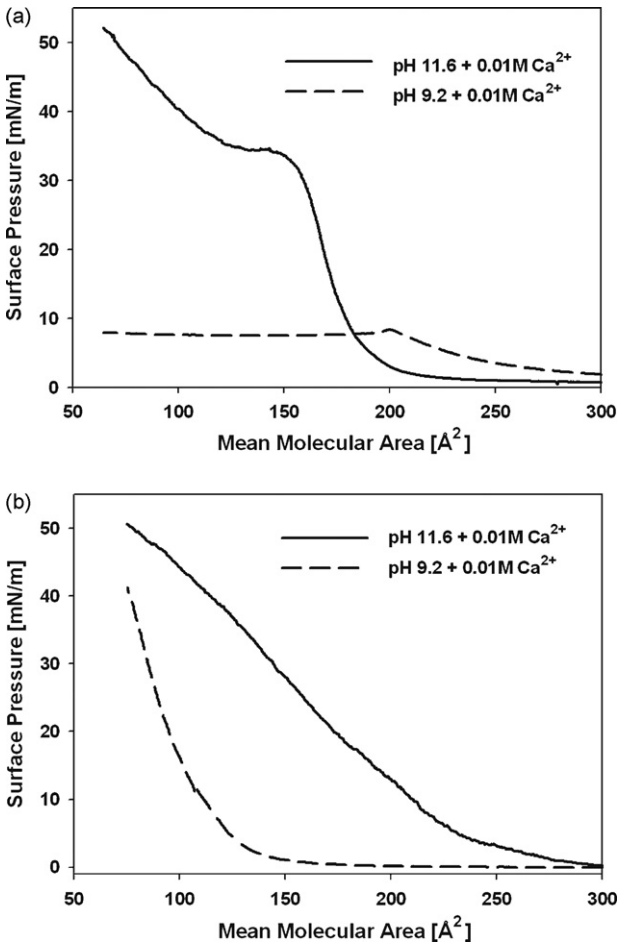

Fig. 7. Surface pressure–area isotherms of Langmuir monolayers of (a) BP10 and (b) Pe10 at pH 9.2 and 11.6 with [Ca^{2+}] = 0.01 M.

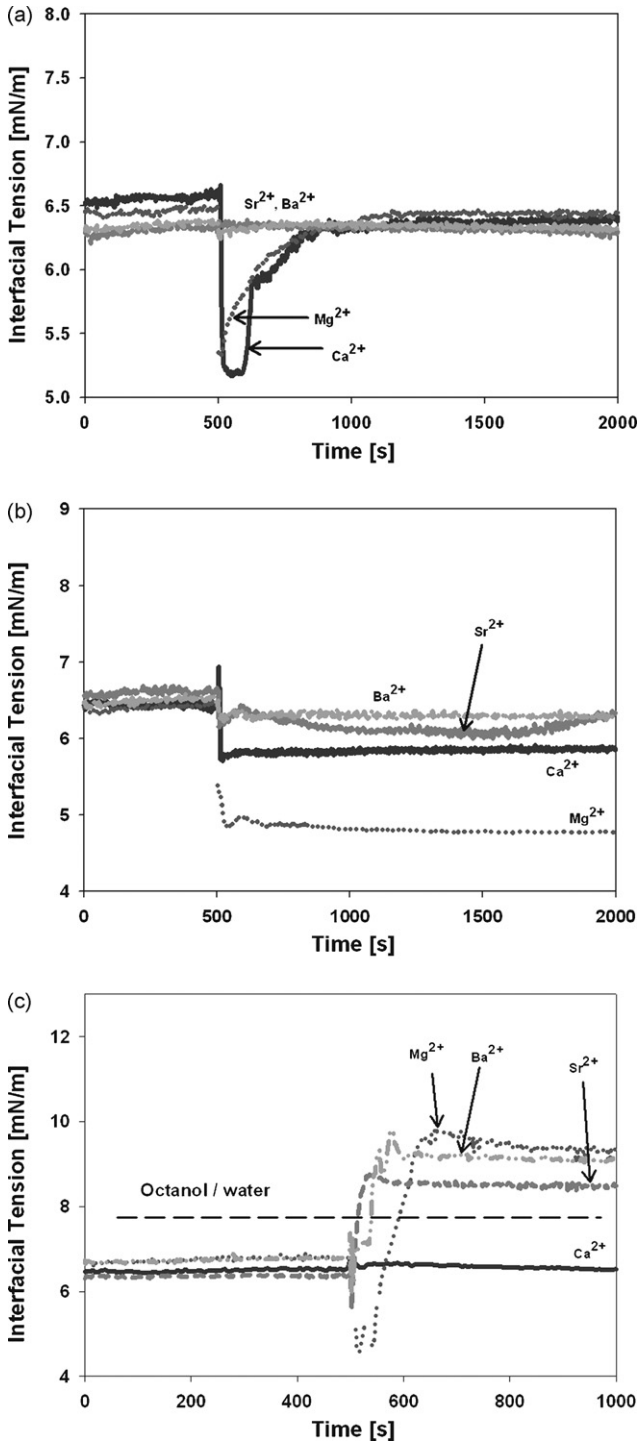

Fig. 8. Dynamic interfacial tension curves of BP10 in 1-octanol towards pH 7.4 upon addition of divalent cations after 500 s with a ratio (a) M^{2+}/TA = 0.1, (b) M^{2+}/TA = 1 and (c) M^{2+}/TA = 3.

was 7.4. Increasing the cation concentration to a ratio of 1, (Fig. 8b) gave larger differences between the different cations, and the formation of more interfacially active complexes was at equilibrium. The magnesium complex was the most interfacially active complex, due to the higher hydration state and more complexed water, and the trends in Fig. 8b is the same as what is observed with monoacids, only differing in the behavior of the Ba^{2+} complex [18]. For monoacids, the IFT increases due to dispersion of the salt into the oil phase. For the tetraacid salt, this did not occur, probably due to the tetraacid being a more hydrophilic compound than a general monoacid.

Finally, the molar ratio of M^{2+}/TA was increased to 3. A very different situation was now observed (Fig. 8c). After initially forming the more interfacially active complex, the IFT increased. In fact, the tension was higher than for pure 1-octanol/buffer. One no longer measured the interfacial tension between the oil and the water phase, but actually between the water phase and the film. This was supported by images taken of the droplet after manually compressing and decompressing a droplet after reaction (Fig. 9) which clearly showed the presence of an interfacial film, comparable to the film obtained with indigenous tetraacids. In the case of BP10, the film appeared to be slightly more solid-like, and was crumpling like a paper. It may be the linear structure of the model tetraacid causing a more solid-like film compared to the branched nature of indigenous tetraacids. Anyway, the presence of an interfacial, rigid film with BP10 showed that this model tetraacid was able to form the cross-linked network as well.

Fig. 10 shows Langmuir isotherms of the equimolar system used in Fig. 8b. Compression was carried out with an equal aqueous cation concentration and at the same pH, 7.4. During the discussion of the tension profiles at low ratio of M^{2+}/TA, possible dissolution into the aqueous phase was proposed as the reason for an increasing in the IFT back to the starting value. At a ratio of 1, a difference in equilibrium state was observed with magnesium as the most interfacially active complex. In fact, Fig. 10 shows that magnesium created the most stable film with highest collapse point, support-

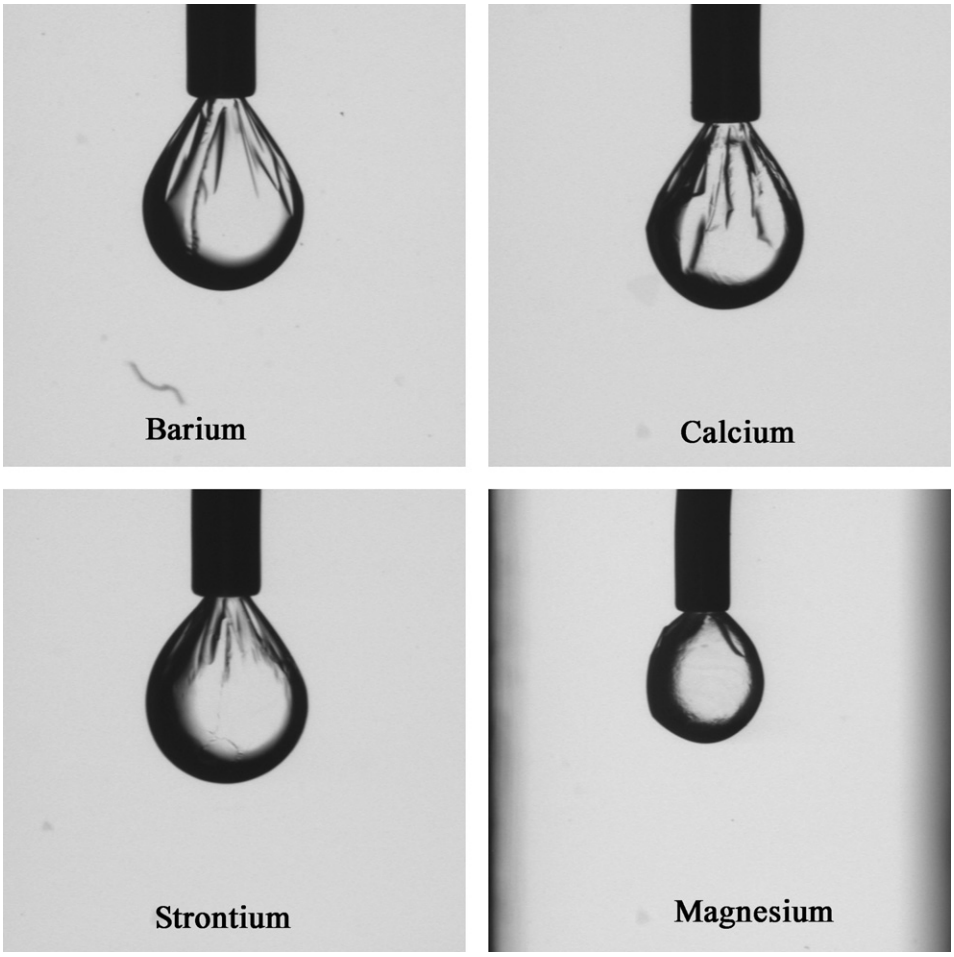

Fig. 9. Images taken of droplets after reactions and manually contracting/expanding the droplets.

ing that the other complexes were too hydrophilic. A higher film stability may have been due to the hydrated water surrounding the magnesium cation in a octahedral pattern, making the film more stable and rigid, even it will be more hydrophilic. No change in the isotherms was observed when increasing the ratio to three. (not shown) A reason why the film formation did not occur in the Langmuir experiments may be that the model tetraacid have a different arrangement at medium high pH at a surface than at an oil–water interface due to the presence of the medium polar aromatic core. At the interface, this core is directed into the bulk oil phase, and at a surface arranged like a spider.

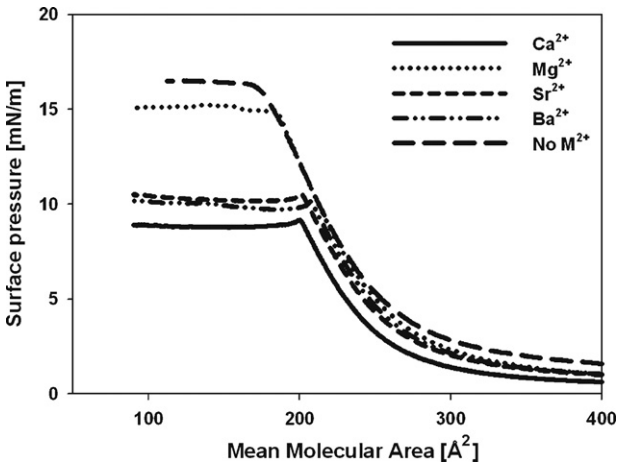

Fig. 10. Surface pressure–area isotherms of BP10 monolayers with different divalent cations.

One of the motivations behind the interfacial reaction study was to find a reason why only calcium is present in the deposits. Both dynamic interfacial tension and the images obtained show that all four cations are able to make the cross-linked network. It is also observed that the film formation was dependent upon the cation concentration. However, this does not explain why the deposits almost exclusively contain calcium, because the concentration difference between calcium and magnesium in produced water is not that large. The experiments are carried out with a single cation at a time, and perhaps studies using mixtures of divalent cations with characterization of calcium content only would be a better approach towards answering this question. This will be studied in the future in our laboratories.

In order to model the naphthenate deposition, model substances will be a great leap towards that goal. Important parameters such as partitioning coefficients and reaction kinetics are easier to obtain in a fast, reliable way with molecules possessing the tetraacid behavior and in addition possibilities for determining concentrations below ppm level by use of spectrophotometrical methods. In this paper, a comparison between model tetraacids and the known features of physicochemical properties of indigenous tetraacids have been carried out, and several important observations have been obtained. First of all, one of the model tetraacids, BP10, forms the interfacial film and the proposed cross-linked network. The inter-

facial activity of this compound both in aqueous solution and in oil–water systems is comparable to the indigenous tetraacids isolated from crude oil deposits. The synthesis of this compound can be done in three days over three steps, without any chromatographic workup. In physicochemical studies regarding reaction kinetics and film formation, BP10 is the most suitable model compound. However, one drawback is the low quantum yield in fluorescence of BP10. Pe10 on the other hand have a perylene core, and perylene systems have generally high fluorescence quantum yields. Hence, to measure the tetraacids down to, and under, ppm levels, Pe10 will be the model compound of choice. Pe10 have not shown to possess the characteristic film properties of tetraacids, so in cases where film formation is important and no need for detecting the tetraacid at low concentration levels, BP10 is the most suitable model compound.

4. Conclusion

Model compounds for tetraacids show many similarities to tetraacids isolated from crude oil, especially with respect to interfacial properties. One of the model compounds, BP10, has shown to create the typical cross-linked film at an oil–water interface which is believed to be one crucial key towards the formation of naphthenate deposits. Interfacial reactions with different divalent cations showed that all four metal ions could form a naphthenate film with the model compound, and the reaction was dependent on the ratio M^{2+}/TA. However, the results do not answer why calcium is exclusively present in naphthenate deposits. The main deviations between model and indigenous tetraacids are in the solid state and bulk oil phase. The model compounds are less soluble in common nonpolar solvents than their native counterparts. The thermal properties of the model compounds are significantly different from those of the indigenous tetraacid. While the indigenous tetraacids show the characteristics of an amorphous, cross-linked polymer, the model tetraacid show typical crystalline behavior with a liquid crystalline mesophase in the range of 60–110 °C. This is due to the more regular structure of the aliphatic chains compared to the branched and irregular structure of indigenous tetraacids. Using model compounds with appropriate design instead of the limiting and time-consuming work with isolated products, opens up for faster and easier experimental work with better control of your system.

Acknowledgements

The authors thank The Research Council of Norway for financial support through the PETROMAKS program. Acknowledgements are extended to the JIP consortium, consisting of AkzoNobel, Baker Petrolite, BP, Champion Technologies, Chevron, Clariant Oil Services, ConocoPhillips, Shell Global Solutions, StatoilHydro ASA, Talisman Energy and Total.

References

[1] C. Hurtevent, G. Rousseau, M. Bourrel, B. Brocart, in: J. Sjöblom (Ed.), Emulsion and Emulsion Stability, CRC Press, Boca Raton, 2006, pp. 477–516.
[2] M.-H. Ese, P.K. Kilpatrick, Stabilization of water-in-oil emulsions by naphthenic acids and their salts: model compounds, role of pH, and soap:acid ratio, J. Dispersion Sci. Technol. 25 (2004) 253–261.
[3] Ø. Brandal, A.-M.D. Hanneseth, P.V. Hemmingsen, J. Sjöblom, S. Kim, R.P. Rodgers, A.G. Marshall, Isolation and characterization of naphthenic acids from a metal naphthenate deposit: molecular properties at oil-water and air-water interfaces, J. Dispersion Sci. Technol. 27 (2006) 295–305.
[4] B.F. Lutnaes, O. Brandal, J. Sjoblom, J. Krane, Archaeal C80 isoprenoid tetraacids responsible for naphthenate deposition in crude oil processing, Org. Biomol. Chem. 4 (2006) 616–620.
[5] B.E. Smith, P.A. Sutton, C.A. Lewis, B. Dunsmore, G. Fowler, J. Krane, B.F. Lutnaes, Ø. Brandal, J. Sjöblom, S.J. Rowland, Analysis of "ARN" naphthenic acids by high temperature gas chromatography and high performance liquid chromatography, J. Sep. Sci. 30 (2007) 375–380.
[6] B.F. Lutnaes, J. Krane, B.E. Smith, S.J. Rowland, Structure elucidation of C80, C81 and C82 isoprenoid tetraacids responsible for naphthenate deposition in crude oil production, Org. Biomol. Chem. 5 (2007) 1873–1877.
[7] H. Magnusson, A.-M.D. Hanneseth, J. Sjöblom, Characterization of C80 naphthenic acid and its calcium naphthenate, J. Dispersion Sci. Technol. 29 (2008) 464–473.
[8] Ø. Brandal, T. Viitala, J. Sjöblom, Compression isotherms and morphological characteristics of pure and mixed langmuir monolayers of C80 isoprenoid tetraacids and a C18 monoacid, J. Dispersion Sci. Technol. 28 (2007) 95–106.
[9] H. Mediaas, K.V. Grande, B.M. Hustad, A. Rasch, H.G. Rueslåtten, J.E. Vindstad, The acid-IER method—a method for selective isolation of carboxylic acids from crude oil and other organic solvents, SPE 80404, Aberdeen, United Kingdom, January 29–30, 2003.
[10] S. Simon, E. Nordgård, P. Bruheim, J. Sjöblom, Determination of C80 tetraacid content in calcium naphthenate deposits, J. Chromatogr. A 1200 (2008) 136–143.
[11] E.L. Nordgård, J. Sjöblom, Model Compounds for Asphaltenes and C80 Isoprenoid Tetraacids. Part I: Synthesis and interfacial activities, J. Dispersion Sci. Technol. 29 (2008) 1–9.
[12] A. Graciaa, Y. Barakat, M. El-Emary, L. Fortney, R.S. Schechter, S. Yiv, W.H. Wade, HLB CMC, and phase behavior as related to hydrophobe branching, J. Colloid Interface Sci. 89 (1982) 209–216.
[13] R. Varadaraj, J. Bock, S. Zushma, N. Brons, Influence of hydrocarbon chain branching on interfacial properties of sodium dodecyl sulfate, Langmuir 8 (1992) 14–17.
[14] E. Alami, G. Beinert, P. Marie, R. Zana, Alkanediyl-α,ω-bis(dimethylalkylammonium bromide) surfactants. 3. Behavior at the air-water interface, Langmuir 9 (1993) 1465–1467.
[15] H. Diamant, D. Andelman, Dimeric surfactants: spacer chain conformation and specific area at the air/water interface, Langmuir 10 (1994) 2910–2916.
[16] M. Rosen, L. Liu:, Surface activity and premicellar aggregation of some novel diquaternary gemini surfactants, J. Am. Oil Chemists Soc. 73 (1996) 885–890.
[17] M.-H. Ese, J. Sjöblom, Influence of secondary and tertiary amines on the stability of stearic acid monolayers, Colloids Surf. A 123–124 (1997) 479–489.
[18] Ø. Brandal, J. Sjöblom, G. Øye, Interfacial Behavior of naphthenic acids and multivalent cations in systems with oil and water. I. A pendant drop study of interactions between n-dodecyl benzoic acid and divalent cations, J. Dispersion Sci. Technol. 25 (2004) 367–374.

Paper 5

Is not included due to copyright

Paper 6

Is not included due to copyright